Utilisation of natural fibrous plaster for out-of-plane lateral resistance of masonry walling

by

Furqan Qamar

A thesis submitted in fulfilment of the requirements for the degree of Doctor of Philosophy in Engineering

University of Warwick, School of Engineering

April 2020

THE UNIVERSITY OF WARWICK

Table of contents

List of tables

List of figures

Acknowledgements

First, I praise ALLAH, Almighty, for providing me the strength and capability to seek knowledge. It is commanded by ALLAH (SWT) in the holy book Quran chapter 20 verse 114 “So high [above all] is Allah, the Sovereign, the Truth. And, [O Muhammad], do not hasten with [recitation of] the Qur’an before its revelation is completed to you, and say, “My Lord, increase me in knowledge”. By this supplication I seek effort to achieve this milestone of my life.

I would like to express my special thanks to Dr. Terrence Thomas (supervisor) for guidance and advice throughout this long journey and without him none of findings would have been possible.
In addition, I would like to thank Eng. Prof. Majid Ali (co-supervisor) Department of Civil Engineering, Capital University of Science and Technology, Islamabad Pakistan for his guidance throughout my PhD studies in every step from design idea to final writing. His visionary directions were quite helpful, particularly for research publications made out of this doctoral work.

I am thankful to colleagues at National Housing and Building Research Agency (NHBRA) Tanzania, to mention just a few, B Chilla and H Hatibu for their support in carrying out the experimental work in Tanzania. Without their help, I could not have completed the experimental work. I am also thankful to the laboratory staff at University of Warwick for their help in completing the experimental work. Thanks to Dr. Shunde Qin who helped and advised me for finite element modelling and on the use of TNO DIANA, especially. I also acknowledge the library staff for their efficient and effective service; provision of literatures within and outside the University at the appropriate time.

Last but not least, I would like to thank my family including respected parents Qamar-uz-Zaman and Sakina Khanum, my beloved wife Nasira Furqan and four lovely daughters Rudaina Furqan, Noor Ul Huda Furqan, Aroosh Fatima and Hafsah Furqan. The encouragement during hard times was very helpful. Without this, I would not have had enough strength to complete this milestone.

Declaration

This declaration confirms that this thesis is original and sole work of the author alone. The thesis does not include any previous material submitted by any other researcher in any form not acknowledged as required by existing regulations.

No material contained in this thesis has been used elsewhere for publication prior the production of this work.

This declaration also officially affirms that this thesis is being submitted for the degree of Doctor of Philosophy of the University of Warwick only and not to any other similar institution of higher learning for the same purposes.

Abstract

Masonry is an ancient form of construction which is used in many countries around the globe, mainly for houses and especially for walls. Worldwide shortage of houses/housing leads to find the new methods/technologies for quick and economical masonry construction. One of these technologies is mortarless masonry walling with interlocking blocks. Masonry walls in general and particularly interlocking walls have least resistance to lateral loads like wind and earthquake. The specific aim of this doctoral research was to develop a technique to enhance the lateral resistance of masonry walling with a focus on interlocking block walls. To achieve this objective use of natural fibres (rice straw and sisal) was considered within cement-based plaster. Wide range of natural fibres exists around the world and the major chemical composition is lignocellulose (cellulose, hemicellulos and lignin) and the quantity of the component varies with the type and has effect on mechanical characteristics.

Characterisation of mechanical properties of interlocking stabilised soil block (ISSB) and fibrous plaster was carried out in small-scale experiment. After indication of improvement in the mechanical properties of cube samples by the addition of natural fibres, 1500 mm high interlocked mortar-free and mortared conventional block columns were built with 8 mm thin and 20 mm thick plaster. Significant improvement of 2.6 times in lateral static stiffness and 3 times in lateral failure load was observed for fibrous as compared with plain-plastered columns. Non-linear finite element models were developed for unplastered, plain-plastered and fibrous plastered interlocked column and validated using the experimental results.

For practical application improvement in the lateral stiffness and strength of 2200 mm high interlocking walls connected with roof truss and timber beam (defined as diaphragm onwards) was also experimentally evaluated. Significant improvement of 142% for total energy absorbed and 55% for toughness index was observed for plain plastered as compared with unplastered wall and further improvement of 144% for total energy absorbed and 47% for toughness index was observed for sisal fibrous plastered walls. Empirical and analytical modelling were developed in light of the experimental work for estimating the resistance of interlocked walling system for poor developing countries. This indicated the benefit of novel method of utilisation of natural fibrous cement-based plaster for lateral capacity of low-cost masonry housing.

Abbreviation and symbols

A_p	Area of plaster (mm^2)
SSB	Stabilised soil block
CTIp	Compressive toughness index of plaster cubes (-)
ISSBs	Interlocked stabilised soil blocks
NLFE	Nonlinear finite element modelling
PEb	Pre-crack absorbed energy for block (J)
TIB	Tanzanian interlocking block
T_p	Thickness of plaster (mm)
w	Width of wall (mm)
C_b	Compressive strength of block (MPa)
Cp	Compressive strength of plaster cubes (MPa)
CE_b	Post-crack energy absorbed for block (J)
CE_p	Post-crack absorbed energy for plaster cubes (J)
CTI_b	Compressive toughness index for block (-)
Df_{11}	Normal linear stiffness modulus (N/mm^3)
Df_{22}	Shear linear stiffness modulus (N/mm^3)
d_w	Density of wall (kg/m^3)
E	Young Modulus (MPa)
E_b	Modulus of elasticity of block (GPa)
E_{fk}	Effective flexural strength factor (-)
E_p	Modulus of elasticity of plaster cubes (GPa)
E_o	Overall energy absorbed (J)
E_1	Pre- crack energy absorbed (J)

E_2	Post crack energy absorbed (J)
f	Frequency (Hz)
f_a	Axial stress (MPa)
f_c	Compressive strength (MPa)
f'_c	Compressive strength of plaster (MPa)
f_d	Dynamic factor (-)
F_{fe}	Effective stress (MPa)
f_m	Wall compressive strength (MPa)
f_t	Tensile strength of plastered walling system (MPa)
F_1	Slip corresponding to peak bond stress (mm)
F_2	Maximum slip (mm)
G	Geometrical stiffness (N/mm)
G_f	Fracture energy (N/mm)
G_{fi}	Interfacial fracture energy (N/mm)
I	Toughness Index (-)
K	Stiffness (N/mm)
K_d	Dynamic Stiffness (N/mm)
K_e	Empirical stiffness (N/mm)
L	Length of wall (mm)
m	Mass of masonry wall (kg)
M_{cr}	Cracking moment (kN-m)
M_D	Design moment (kN-m)
M_n	Out of plane flexural strength (kN-m)
M_R	Design resistance (kN-m)
M*	Applied moment (kN-m)

n	Number of blocks (-)
N_a	Depth to neutral axis for lateral loading (m)
P	Applied lateral load (N)
PEp	Pre-crack absorbed energy for plaster cubes (J)
S	First moment of area (m^3)
S_u	Ultimate slip (mm)
S_{peak}	Slip corresponding to the peak bond stress (mm)
S_1	Peak bond stress (MPa)
S_2	Stress (MPa)
t	Thickness of wall (mm)
TE_b	Total energy absorbed for block (J)
TEp	Total absorbed energy for plaster cubes (J)
Z	Section modulus (mm^3)
μ	Coefficient of friction (-)
δ	Displacement (mm)
ε_d	Design strain (-)
ε_e	Effective strain (-)
α, β	Equivalent stress block parameter (-)
γ_f	Safety factor for loads (-)
γ_m	Material factor (-)
τ_{peak}	The peak bond stress (MPa)
n	Poison's ratio (-)

List of publications

Journal articles

Published**:**

Qamar, F., Thomas, T. & Ali, M. (2018). Use of natural fibrous plaster for improving the out of plane lateral resistance of mortarless interlocked masonry walling. *Construction and Building Materials,* 174 320-329. Impact factor: 4.046

Qamar, F., Thomas, T. & Ali, M. (2019). Assessment of mechanical properties of fibrous mortar and interlocking soil stabilised block (ISSB) for low-cost masonry housing. *Materiales de Construccion,* 69 (336) e201. Impact factor: 1.886

Qamar, F., Thomas, T. & Ali, M. (2019). Improvement in lateral resistance of mortar-free interlocking wall with plaster having natural fibres. *Construction and Building Materials,* 234 117387. Impact factor: 4.046

Peer reviewed periodicals:

Qamar, F., Thomas, T. & Ali, M. (2018). Contribution of Sisal Reinforced Plaster in out of Plane Resistance of Masonry Column. *Key Engineering* Materials ISSN 1662-9795, Vol. 765, pp 343-348. SCIMAGO Impact factor: 0.18

Refereed conference papers:

Qamar, F., Thomas, T. & Ali, M. (2019). Effect of natural fibrous plaster on lateral resistance of mortarless interlocking wall. *5th International Conference on Sustainable Construction Materials and Technologies (SCMT5). Kingston University* London, UK 14 – 17 July. Paper IDSCMT5149.

Qamar, F., Thomas, T. & Ali, M. (2018). Effect of rice straw reinforced plaster in improving out-of-plane resistance of mortar-free interlocking column. *50th Annual New Zealand Society for Earthquake Engineering,* Auckland, New Zealand 13-15 April. Paper ID 23.

Qamar, F., Thomas, T. & Ali, M. (2018) Effect of Sisal Fibrous Mortar in Improving Out Of-Plane Resistance and Damping Ratio of Masonry Column. *Canadian Society for Civil Engineering*, Fredericton Canada, 13-16 June. Paper ID 155.

Qamar, F., Qin, S. and Ali, M. (2018). Estimating seismic resistance of fibrous plastering effect on mortarless interlocked masonry walling with finite element modelling. *Australian Earthquake Engineering Society Conference*, Perth, Australia. 16-18 November. Paper ID 22.

Chapter 1. Introduction

1.1 Prologue

Earth is one of the oldest construction materials and has been used in the construction of low-cost houses for thousands of years (Emami, 2011). It is used in different forms like adobe, compressed earth - masonry blocks, etc. However, basic earth-construction suffers from problems of shrinkage, cracking, low tensile strength, brittleness and poor durability (Bouhicha, 2005). So, despite its low cost, this material is regarded as inferior to most of other walling materials (Millogo, 2014). There is thus a requirement of improvement of its properties (Danso, 2015).

Improvement of soil properties are explored by using two different methods, one by use of energy-intensive binders like cement and lime. However, inclusion of these additives results in an increase in material cost and harm to the environment (Juarez, 2010). The second method by means of mechanical compaction and it consists of adding plant fibres (hereafter called natural fibres) in earth construction (King, 2013). Natural fibres are available in many countries. Their use in improvement of the properties of construction material costs very little as compared with use of cement, mortar and concrete composites (Ali, 2012). "*To exploit the structural potential of any material, it is essential to understand its strengths and weaknesses"*. Most Masonry is weak in tension and, for economic use of material, it is required to overcome this weakness. Many studies have shown that the addition of natural fibres improves the mechanical properties of soil – (Danso, 2015; Curtin, 2006; Mesbah, 2004). These improvements include compressive, tensile, shear and flexural strengths.

Housing is inadequate in number and quality in most developing countries, relative to growth of population. This deficiency explains the need to find the improvements in the construction industry, especially in masonry housing (Kintingu, 2009). Conventional masonry construction is slow, labour-intensive and expensive due to the large number of mortar joints (Amin Al-Fakih, 2018; Anand & Ramamurthy, 2000). Attempts have been made to reduce the size of mortar joint by increasing the size of block/bricks but this also has some limitation on the construction of number of courses per day due to use of bed mortar joint. Further development in eliminating the need for mortar joint has led to the introduction of different forms of interlocked masonry walls (Kohail et al., 2019).

Unreinforced masonry structures (URM) are highly vulnerable to lateral load due to wind or earthquake. In particular, under earthquake loading URM exhibits brittle failure that can lead to complete collapse of a structure. In some studies, (Ali, 2007 & Macabuag, 2012), the dynamic properties of masonry structure are considered and use of natural fibres is suggested to enhance the earthquake resistance of the structure. The addition of fibres in cement-based plaster enhances structural ductility and energy dissipation capacity. The dynamic properties of a material are measured in three main parameters, namely dynamic modulus of elasticity, natural frequency and vibration damping coefficient (Ali, 2007). These three properties are closely interlinked. The dynamic response of a material defines its dynamic modulus. Energy dissipation of the material is a characteristic of damping and natural frequency. It is associated with both the material and the structural design in which it is used. Good vibration damping mitigates the hazards of earthquake, wind or accidental loading and enhances the reliability of walling.

This thesis focuses on the possible use of cheap natural fibres to improve walling in low-cost housing. The main attention is given to *unmortared* masonry, both because omission of mortar reduces cost (typically by ca 30%) and because mortarless masonry (even that containing block-to-block interlocks) has a poor performance – low resistance to lateral forces. However occasional reference is made to mortared blockwork, either as a datum for resistance to lateral forces or to evaluate the effect of natural fibres in mortar. Experimental work has been carried out whose findings are reported in this thesis.

1.2 Research motive and problem statement

In developing countries, especially rural areas, there is an obvious requirement for suitable and robust housing at low cost. There is also a shortage of houses relative to the growth of population (Kintingu, 2009). On the other hand there is a risk of mass destruction of low-cost non-engineered housing due to earthquake (Ali, 2012). Among many examples is that in Kashmir in 2005, which resulted in the loss of 73,000 lives and destruction of more than 600,000 houses. Given these facts, there is a requirement of new techniques for low-cost housing in such areas (Figueiredo,2013). Natural fibre (e.g. rice straw and sisal) is less expensive than conventional steel or plastic fibres and is readily available in many countries. The annual world production of sisal is around

378,000 tons and for straw 607 Million tons, out of which sisal is mainly produced in Tanzania and Brazil whereas rice straw is obtained from USA, China and India (Ramamoorthy et.al, 2015). This drove the author to research new technique for enhancing the strength and stiffness of low-cost housing, in particular the addition of natural fibres to masonry walling. Of particular interest, considered construction is (very cheap) mortarless masonry whose poor performance might be enhanced by use of natural fibres in plaster. Thus the problem may be stated as follows:

Masonry walls are mostly designed to resist compressive loads but these have less resistance to horizontal (out-of-plane) loading due to wind and earthquake. Therefore the structural performance of the masonry wall under these loadings is a primary concern (Gupta, 2014 and Tripura, 2018). In particular, mortarless interlocked masonry walling has least resistance to out-of-plane lateral loading without lateral restraint. This could lead to complete collapse of masonry structure and loss of life.

1.3 Overall goal of research programme and specific goal of this doctoral study

The overall aim of the research programme was to develop new techniques for enhancement of the lateral strength and stiffness of low-cost masonry walling. The simplified experimental work as a single block column was chosen first due to limitation of loading equipment prior to 2200mm high walls with unidirectional loading.

The specific four objectives of this doctoral study were to evaluate:

- the suitability of natural (rice straw and sisal) fibre reinforcement in the *plaster and mortar* to be used in low-cost masonry walling to enhance its strength and stiffness under lateral loading.
- mechanical and dynamic properties of unplastered, plain plastered and fibrous plastered interlocked single-block columns subjected to unidirectional loading (size and height of column is limited due to available loading equipment).
- physical and economic performance of a range of fibre-reinforced masonry columns via numerical modelling calibrated using experimental data.

- the overall performance of fibrous and non-fibrous plastered mortarless masonry walls to develop guidelines of its out-of-plane lateral resistance.

1.4 Scope of doctoral work and study limitations

The scope of this study was as follows:

1. Perform small-scale experimental work using fibrous/non-fibrous plaster cube samples (18 No. samples) and single ISSBs (9 No. samples) to characterise their mechanical properties.
2. Construct 1500-mm high single-block columns (both mortarless 35 No samples and conventionally mortared 12 No. samples) with different plastering variations to evaluate the improvement in lateral resistance due to inclusion of fibre subjected to lateral static point loading.
3. Develop non-linear finite element models (7 No.) for interlocked columns calibrated using the results of experimental work for parametric studies for potential cost- saving by reducing the thickness of masonry blocks.
4. Build 2200 mm high (represent minimum height of single storey low-cost house) three-block interlocked walls (4 No. i.e. unplastered, plain-plastered and two fibrous-plastered) connected by diaphragm to evaluate the lateral resistance of masonry walling, subjected to lateral static point loading.

The study limitations for this doctoral work were as follows:

1. Only two types of natural fibres were readily available for experimentation i.e. sisal and rice straw. But these two covered the whole range from strong to weak fibres, and were therefore considered sufficient for the research; Use of more types of natural fibres was not practically feasible.
2. In the laboratory, lateral static-point loading was applied (to the single-block-wide, 1500 mm high columns and the 2200 mm high three-block-wide walls) instead of using uniformly distributed lateral loads like those occurring naturally during high winds and earthquakes. However, this should not matter in the strength *comparison* of different designs of column and wall: their performance ranking under point loading should be the same as their ranking under distributed loads.

Identification of first-crack loading was limited to spotting the formation of visible cracks (i.e. greater than 0.1 mm wide) in the columns and walls. However, cracks less than 0.1 mm are normally classified as hairline and are not considered indicative of yielding.

3. The loading technique available in the labs, especially that in Tanzania, did not allow application of loading large enough to take all the walls to failure point. For the strongest examples, walls could only be loaded as far as their yield point.
4. The experimental loading assembly that was used could record displacement-v-load characteristics only as far as 'yield' and not beyond. This constraint did not apply to the finite element modelling undertaken. The finite element model could thus be calibrated only up to linear peak load; for behaviour between yield and collapse, an uncalibrated theoretical model had to be employed.

1.5 Brief methodology

In order to achieve the objectives outlined above, a literature review was carried out to identify the type, content and best use of natural fibres in optimising mechanical properties. Two types of natural fibres were selected: rice straw since cheap and widely available, and sisal because it has superior properties to those of other natural fibres. Experimental work was carried out at the National Housing and Building Research Agency (NHBRA) in Tanzania and the University of Warwick's Structures lab. Small-scale experimental work was carried out to characterise the mechanical properties of fibrous plaster cubes and ISSBs. 1500 mm high interlocked block and mortared conventional-block **columns** were built and tested under lateral loading with 8 mm thin and 20 mm thick plastering variations. Fibrous and non-fibrous cement-based plaster was applied to the tension face of these columns.

Finite-element analysis of ISSB columns was carried out using the software TNO DIANA and compared with the results of laboratory testing. The validated model was then extended into a parametric study for block and plaster strength and thickness. 2200 mm high x 900 mm long interlocked **walls** connected by diaphragm were built to evaluate the overall performance of masonry walling. With the knowledge acquired

from the laboratory testing empirical equations to predict the strength and stiffness of fibrous walling were developed.

1.6 Thesis outline

This thesis is divided into seven chapters.

After this Introduction **Chapter 2** presents a literature review of low-cost masonry housing. This provides the background information for the use of mortar-free interlocked stabilised soil blocks (ISSB) walls and of techniques for improving their lateral resistance. The literature review is divided into three main parts covering respectively (i) different types of ISSB used by other researchers (ii) the use of natural fibres in enhancing the lateral resistance of low-cost masonry construction (i.e. fibres placed in ISSB, mortar or plaster) and (iii) improvement of the lateral resistance of walling in low-cost housing. This review identified the important static and dynamic parameters which needed further to be considered.

Chapter 3 characterises the material properties of interlocked stabilised-soil blocks and natural fibrous plaster. Static and dynamic properties, which included first-crack and maximum loading, compressive strength, modulus of elasticity, pre/post cracking energy absorbed, total energy absorbed and toughness index of ISSB and fibrous plaster, were experimentally evaluated.

Chapter 4 focusses on the investigation of lateral stiffness and strength of masonry columns based on the best use of addition of fibres in plaster or mortar. The materials used for the columns were those characterised in chapter 3. Both mortar-free interlocked and mortared columns were built and tested with variation of plastering from unplastered to fibrous plastering. This chapter details the experimental techniques, apparatus setup, mix ratio and application of loading. This chapter also details the outcome of the experimental work and summarise the conclusions.

Chapter 5 details the development of non-linear finite element analysis modelling of the masonry columns tested in chapter 4. This chapter validate the non-linear finite element model with the help of experimental results of chapter 4. After calibration of

models using the experimental results, this chapter details the parametric study of parameters like plaster strength, thickness and block strength on column performance. The results of a cost analysis are also presented in this chapter, based on numerical modelling of walls of various thickness and plastering configurations.

In **Chapter 6** experimental investigation of the performance of fibrous interlocked masonry walling with diaphragm (rather than just column) is presented. This chapter describes the behaviour of such masonry walling under lateral loading. The influence of fibre-reinforcement in plaster on static and dynamic stiffness is also considered. The results of the experimental works are presented in form of load-displacement plots and the comparison graphs. Empirical equations were developed for stiffness based on experimental work. Analytical procedure was developed for estimating the lateral resistance of walling system.

Finally, **Chapter 7** summarise the conclusions made throughout the thesis and makes recommendations for the housing industry and for future research.
This chapter is followed by list of references and annexures. *Annex A* details the classification and properties of different types of natural fibre. It also details the application of natural fibres in the construction industry and highlights the need to improve the durability of natural fibres. *Annex B* gives additional information on plaster cube preparation for material characterisation. *Annex C* shows the preparation process of ISSB and SSB which is used for interlocked and conventional mortared block columns. *Annex D* lists the photographs for preparation of roof truss and set up for dynamic testing for interlocked walls.

Chapter 2. Literature review

Related ISI Impact Factor Journal Papers:

Qamar, F., Thomas, T. & Ali, M. (2018). Use of natural fibrous plaster for improving the out of plane lateral resistance of mortarless interlocked masonry walling. *Construction and Building Materials*, 174 320-329. Impact factor: 4.046

Qamar, F., Thomas, T. & Ali, M. (2019). Assessment of mechanical properties of fibrous mortar and interlocking soil stabilised block (ISSB) for low-cost masonry housing. *Materiales de Construccion*, 69 (336) e201. Impact factor: 1.886

Qamar, F., Thomas, T. & Ali, M. (2019). Improvement in lateral resistance of mortar-free interlocking wall with plaster having natural fibres. *Construction and Building Materials* 234 117387. Impact factor: 4.046

2.1 Background

Having stated in the previous chapter the need for low cost housing, this (literature search) chapter provides the background for the use of mortar-free interlocking stabilised-soil blocks (ISSBs) in walls and techniques for improvement in such walls' lateral resistance. Different types of ISSBs and their mechanical properties are explored in section 2.2. The effect of cementitious composite with natural fibres on the strength of interlocked masonry construction is identified through literature review. The techniques to improve its lateral resistance are explained in section 2.3. The background of finite element modelling for masonry structures is explained in section 2.4. This chapter also outlines in section 2.5 the performance of different walling systems explored by other researchers. In each of the following sections knowledge gaps are identified, defining the scope of this doctoral study. In further chapters these gaps are minimised by conducting research as part of this doctoral study.

2.2 House construction with ISSBs

2.2.1 Masonry typologies and cause of damage

Masonry is the most valuable construction material in the history of human beings other than wood. Masonry has been used in different forms for public and residential buildings in the past several years, from tower of Babylon to the Great Wall of China. The number of masonry buildings still exists around the world, proving that masonry can successfully resist loads and environmental impacts. Different types of masonry can be found around the world depending on various factors which include material used for construction (adobe, stone, brick and block), formation of blocks (fired, pressed, stabilised interlocked), structural system (plain, confined, reinforced), place of construction (rural, urban) and use of building (residential, public) (Tomazevic, 2009).

Masonry structures which are subjected to earthquakes were severely damaged and collapsed. Therefore, masonry has been considered as unsuitable material for the construction in seismic zones. Considering the damage due to earthquakes, adobe and stone-masonry suffered severe damage. However continuous attempts are being made to improve the construction technique for masonry structures. Different type of damages is observed in the masonry structure which include cracks between walls and floors, out of plane collapse of walls, diagonal cracks in structural walls and complete collapse of structure. Some causes of these damages are related to the poor quality of masonry material, heavy earthen roofing, insufficient connections between walls and floors, irregular layout and large openings. The review of damage patterns can help in finding the weak and strong point of structural system. Based on this, failure behaviour of individual element like structural walls can be defined.

2.2.2 Mechanical properties of different types of ISSBs

Due to the increase of population in developing countries, the need for low-cost residential housing has increased considerably around the world (Lee et al., 2017 & Bosiljkov et al., 2015). At the same time the need for a faster construction system has led to the change in conventional approach of masonry construction to interlocking-construction techniques. Interlocking masonry units or blocks can be laid without layers of mortar and so require less labour (Jaafar, 2006, Juarez, 2010 and Martínez,

2019). Interlocking masonry units differ from conventional blocks in that these units can be assembled with geometrical features built into blocks without the need of a mortar layer (Anand, 2000). Interlocking mortarless has a lower material cost and interlocking mechanism resist shear failure. The interlocking blocks available in the industry vary in geometry, material and dimensions. Eurocode 6 provide guidance for the design values of dimensional changes for unreinforced masonry. Against the advantages of removing bedding mortar and reduction in cost, interlocking blocks have some limitations. These include their reduced lateral resistance and requirement for stricter dimensional tolerances. The structural behaviour of an interlocking block wall of a masonry house may differ from that of a conventional masonry wall when subjected to in-plane and out-of-plane loading due to geometrical imperfection (Kintingu, 2009, Fundi, 2018, Dehghan, 2018 and Chewe Ngapeya, 2018).

Masonry walls are required to resist both compressive loading and the horizontal (out-of-plane) loading caused by wind and earthquake. Therefore the structural performance of the interlocking wall under these loadings is of primary concern (Gupta, 2014 and Tripura, 2018). In previous studies many different types of interlocking block, varying in their material, geometry and interlocking mechanism, were used. Different types of mechanical property were explored, as detailed in Table 2.1. In the research work by Ali 2012 coconut fibre reinforced concrete interlocking blocks were used and tested for mechanical properties like modulus of elasticity, compressive and flexural strength. It was found that the addition of 5% fibres was resulted in decreased modulus of elasticity by 6% as compared to plain sample. In research undertaken by Fundi et al. 2018 cement-stabilised soil blocks were used to test the behaviour of small walls (900 mm length and 1200 mm height) under vertical and horizontal loading. The optimisation of the compressive strength of blocks by the addition of cement stabiliser was also determined and it was shown that the minimum 2.5 MPa compressive strength found could be increased to 4.5 MPa at 28 days' curing by the addition of lime in soil and cement. Water absorption of soil blocks was also tested with different stabilisers. It was found that increase of cement content resulted in reduced water absorption. In another study by Anand the compressive strength of interlocking concrete blocks was reported to be 5.42 MPa for a single block (400 mm x 150 mm x 100 mm) and 3.77 MPa for small walls (400 mm x 600 mm x 100 mm).

Shear and tensile strengths of small walls were also reported to be 0.48 MPa and 0.21 MPa respectively. In this study bond strength between block and mortar for conventional masonry was also compared with interlocking block by evaluating flexural strength. It was found that for interlocking blocks failure stress was higher for tension normal to bed joint than for tension parallel to bed joint as in conventional masonry case. In a study by Lee, where interlocking block columns were built and interlocking holes were infilled with mortar and steel reinforcement, the material properties and failure behaviour were studied and a compressive strength of 14.28 MPa was reported for interlocking blocks. In research conducted by Jaafar hollow interlocking blocks were used and a correlation developed between the compressive strength of a single block, 2-block prism and wall panel. The prism and wall panel compressive strengths were respectively, 0.47 and 0.39 times the strength of interlocking block. In all research studies the compressive strength of different types of interlocking block was measured and found to be in the range of 2.5-16.5 MPa. Other mechanical properties like shear strength and compressive toughness were also measured and found to be in the range of 0.48-2.65 MPa and 0.56 MPa, respectively. It became evident from the outcome of a variety of studies that properties of interlocking block vary depending on geometry, material and interlocking mechanism, which could affect the overall strength of masonry wall.

2.2.3 Influence on mechanical properties of cementitious composite with natural fibres

As reported in the literature, interlocking block walls show low lateral resistance to wind and earthquake. Therefore, to enhance lateral resistance different techniques like plain or reinforced grouting, surface bonding and plastering, are considered (Anand, 2000). Use of natural and artificial fibres in cementitious composite are reported for conventional masonry but nothing is reported for interlocked masonry. For conventional masonry use of natural fibres in mortar was considered in a variety of studies and the mechanical properties of specimens with and without fibres were compared, as detailed in Table 2.2. In a study by Pereira mechanical properties like compressive and bending strength and toughness of plain mortar and mortar with sisal fibres were compared. It was observed that there was a 21% decrease in compressive strength with the addition of fibres, but a 60% and 600% increase in bending strength

Table 2.1: Mechanical properties of Interlocking blocks by other researchers

Type of block (Mix ratio)	Compressive Strength (MPa)	Modulus of Elasticity (GPa)	Shear Strength (MPa)	Compressive Toughness (MPa)	Shear Toughness (MPa)	References
Coconut fibre reinforced concrete interlocking block (1:2:2)	16.48	2.34	2.65	0.56	7.59	Ali et al. 2012
Solid interlocked block (1:2:4)	5.42	-	0.48	-	-	Anand et al. 2000
Hollow Interlock block (1:4:1)	15.2	-	-	-	-	Jaafar et al. 2006
Interlocking block (-)	14.28	-	-	-	-	Lee et al. 2017
Cement stabilised soil interlocking block (6% cement in soil)	2.5	-	-	-	-	Fundi et al. 2018

Table 2.2: Mechanical properties of fibre-reinforced cement-based mortar by other researchers

Type of Fibre	Fibre Volume Fraction (%age)	Compressive Strength (MPa)	Modulus of Rupture /Flexural Strength* (MPa)	Toughness Index	Modulus of Elasticity (GPa)	References
Plain (1:1)	0	28	5*	0.45	-	Pereira et al. (2015)
Sisal (1:1)	3%	22	8*	3.28	-	Pereira et al. (2015)
Sisal (1:1)	8%	-	16.8	1.41	6.07	Savastano et al. (2009)
Banana	8%	-	21.8	0.59	6.7	Savastano et al. (2009)
Basalt (1:3)	4%	29	8.9*	-	-	Zych et al. (2012)
Coconut (1:1)	5%	41	10*	-	-	Lertwattanaruk et al. (2015)
Oil palm (1:1)	5%	36	8*	-	-	Lertwattanaruk et al. (2015)
Polypropylene (1:3)	0.5%	21	7.50*	-	7.9	Toihidul Islam et al. (2011)

and toughness respectively. In research by Savastano et al. 2003 and 2009 natural fibres like sisal and banana with cementitious composite were tested under three-point bending. Mechanical properties, including flexural strength, modulus of elasticity and toughness index were obtained and compared with those of non-fibrous composite. It was found that the addition of fibres resulted in 100% improvement in flexural strength and significant enhancement of toughness index. This could be of interest where cement-based components are exposed to lateral loading like wind and earthquake. Basalt-fibre reinforced mortar was tested by Zych, 2012 and Asadi, 2017. A 20% increase in bending strength and 15% reduction in compressive strength were found to be due to the addition of fibres. This finding/ result is consistent with that of Pereira, 2015. In a study by Ali coconut-fibre reinforced concrete cylinders and beamlets were tested for dynamic and mechanical properties and it was found that a fibre content of 5% gave best properties. Lertwattanaruk, 2015 used coconut and oil palm fibre in cementitious composite which was tested for mechanical properties prior to its recommendation for residential housing application. Differing fibre content of 5%, 10% and 15% by mass of cement was used and it was found that increasing the fibre content resulted in lower compressive and flexural strength. In a study by Toihidul Islam impact resistance of masonry units bounded with fibrous mortar was investigated. Mechanical properties including compressive and flexural strength were also evaluated for fibrous cementitious composites. It was found that 0.5% fibre content in the mortar improved impact resistance of a masonry unit, whereas bond strength was reduced with an increase in fibre content from 0 to 0.5%. The outcome of these various studies has indicated that type and content of fibre influence the mechanical properties of cementitious material. The addition of fibres generally increases flexural strength but decreases compressive strength and similar results can be expected for interlocked masonry. Decrease in compressive strength is not a big problem as most walls have more than adequate compressive strength.

2.2.4 Performance of interlocked block masonry wall

In other studies the performance of interlocking block masonry wall was tested and it was found, as expected, that the compressive properties of the wall were directly proportional to the strength of masonry units (Fundi, 2018). The mechanical properties were also improved by the percentage and type of stabiliser used for interlocking

block. The mechanical properties of ISSB determined by other researchers are detailed in Table 2.1. It was found that for ISSB only compressive strength had been measured: other properties like modulus of elasticity, pre/post crack energy absorbed, total energy absorbed and toughness index had not been evaluated. As these latter properties are required for modelling wall performance they need to be measured. Therefore in this study material properties of interlocking soil-stabilised block (ISSB) were explored for their possible use in a typical masonry house.

a. Static and dynamic properties of materials

Different types of masonry materials can be found ranging from traditional masonry to more developed types. Since masonry is non-elastic, non-homogenous and anisotropic material, it is difficult to determine the mechanical properties without carrying out testing of samples. Different types of mechanical properties are explored by different researchers as detailed in Table 2.1. Mostly compressive strength was obtained from the testing and lacking information about other properties. These include first crack loading, maximum loading, compressive strength, modulus of elasticity, pre/post crack energy absorbed, total energy absorbed and toughness index. Compressive strength and modulus of elasticity can be classified as static properties. Whereas energy absorption and toughness index are related to the dynamic properties.

2.3 Best use of natural fibres for lateral resistance of masonry construction

2.3.1 Use of natural fibres in blocks

Masonry has been employed as a major construction technique throughout human history (Emami, 2011). A vast variety of masonry buildings exist around the globe, depending on resources and traditions. Masonry can be expected to continue to be of major importance due to its design ease and economy. However, masonry has some shortcomings, like low resistance to bending, tension and shear forces (Tomazevic, 2009). Moreover, unreinforced masonry (URM) structures have low capacity to resist lateral loading like earthquakes. Under seismic conditions, URM undergo inelastic failure that could lead to a sudden failure of structure (Ehsani, 1996). Much research had been undertaken on the inclusion of strong and durable fibre (such as glass, steel, plastic) in cementitious materials (Park, 1991, Graham et al., 2013, Pereira et al.,

2015). These fibres were used in different sizes and have been tested for different mechanical parameters and are further detailed in annex A Table A4. But using widely available natural fibres in combination with the very lean cementitious mixes (stabilized soil) has rarely been considered. Types and classification of natural fibre are detailed in annex A1, A2 and Figure A2.1.

In masonry economy demands minimal use of cement mortar. In some cases masonry blocks are interlocked instead of being mortared to prevent sliding failure. Masonry walling usually comprises three main components, namely bricks, mortar and plaster. It is important to identify the best technique (i.e. adding fibres to a chosen component) for improving the resistance of masonry to vertical and lateral load. For this various failure types need to be researched.

In a variety of studies experimental works have been carried out ranging from using full-scale walls to masonry prisms/wallets. Several types of failure were observed, depending upon the category of loading, choice of material and geometric form. The following three failure types were leading: friction/sliding, rocking and diagonal shear failure. The shear and tensile strengths of masonry require improvement to avoid these types of failure. In different studies natural fibres have been used in blocks to enhance their mechanical and physical properties. Research findings from a variety of sources are summarised in Table 2.3. The use of fibres in soil blocks has some limitations. Their use is limited to compressed earth or cement-stabilised block as the fibres cannot be used in fired clay bricks. A fibre content of more than 5% resulted in significant reduction of compressive strength due to decrease in density, whereas the inclusion of less than 5% of fibre could increase compressive strength by up to 10% (Juarez, 2010). The optimum volume of fibre in a composite is limited (by workability requirements) to 1.5-2% (Sivaraja, 2010).

Decay of natural fibres could create pores /air voids in blocks, which could result in a decrease in strength over time. In the literature the durability of fibres and measures to improve it were reported to have been explored only over short periods of time, days rather than years. The failure of block/brick was not normally the principal type of failure in a masonry structure (Sandoval, 2011 and Bernat, 2013). It was apparent that the addition of natural fibre to soil blocks/bricks contributed little to the long-term strength and durability of walling.

2.3.2 Use of natural fibres within mortar

Alecci (2013) carried out experimental investigation into different types of brick masonry to find their shear capacity, using diagonal compression and shear triplet tests. The outcome of both tests showed that shear capacity depended solely on the strength of the mortar used. In another study the interaction between mortar and brick was considered a prime factor in long-term strength of masonry construction. The parameters which could affect this interaction were mortar and brick strength and joint thickness (Zhu and Chung, 1997). Zhu and Chung (1997) showed a 150% bond strength increase by adding fibres (0.5% by cement mass) to the mortar. (Park, 1991) found that cement reinforced with 3 mm long carbon fibres (5% in volume) increased the tensile resistance by more than three times, and the bending resistance by just under three times that of fibreless cementitious composite. The effect of including wheat fibres in mortar for one-directional axial compressive and three-point bending load was investigated by Albahttiti and Rasheed (2013).

Various prism and cube models were experimentally tested. Their conclusion was that the addition of fibre resulted in the ultimate load's being enhanced by 15-27% as compared with that of samples without fibre. The addition of natural fibre to cementitious material also increased its toughness. This increase in toughness occurred due to the phenomenon of fibre bridging. The toughness of the composite was reported to be 2-6% more than that of plain cement paste (Savastano et al., 2009; Zhu & Chung, 1997). It was determined that the use of fibres in mortar could increase the vertical load-carrying strength of a mortared masonry structure. In another study by Wang, 2016, a different strength of mortar was used in masonry wall samples and tested for failure load. It was observed that strength of mortar has no influence on mechanical behaviour of masonry walls. Both types of mortar resulted in a very similar failure pattern and failure load. However, in this study we are mainly focussed on low-cost and therefore mortar-less walling. A comparison of different parameters obtained from the literature review is presented in the Figure 2.1. The bar chart in Figure 2.1 compares the fibrous and non-fibrous cement-based mortar. This shows the increase or decrease in different properties due to the addition of different types of fibres within cement-based mortar.

Table 2.3: Natural fibres within soil blocks

Fibre	Contents	Composite	Variables investigated	Main findings	Author
Coir	25, 50 & 75mm; 1%, 2%, 3% & 5% by mass.	Concrete	Mechanical and dynamic properties	50mm fibres @ 5% content gave overall optimum mechanical strengths. Improved dynamic properties: higher damping ratio, lower fundamental frequency and decreased dynamic modulus of elasticity were also found.	Ali, 2012
Straw	10-60mm 0-3.5% by mass	Soil blocks	Shrinkage. Compressive, shear & flexural strength.	10-20% increase in compressive strength. Small decreases in shrinkage, increase in flexural and shear strength.	Bouhicha, 2005
Multiple fibres		Soil blocks	Compressive, tensile and flexural strength	Fibres doubled the strength of soil, Fibre-effectiveness dependent on soil matrix.	Danso, 2015
Lechuguilla	25 & 50mm fibres; 0.25-1.0% by vol.	Concrete blocks (730 x 340x130 mm)	Compressive and splitting tensile strength	10% higher compressive strength for short length fibre, first cracking load capacities enhanced up to 2.65 times.	Juarez, 2010
Grass species		Clay and cementitious mortars	Shrinkage, tensile strength and elastic modulus	Cracking in clay delayed by 5 hours and crack width reduced from 5mm to 0.5mm.	King, 2013
Hibiscus	60-80mm, 0.8% by weight	adobe blocks formed at 2 MPa	Compressive and (3-point) bending test	Shorter fibres more effective than longer ones. Max compressive strength increase was 16%.	Millogo, 2014
Sisal	20mm & 50mm, 0.5% by weight	Compressed earth blocks	Tensile strength	Improved tensile strength and enhanced post cracking behaviour.	Mesbah, 2004
Coir and sugar cane	1.5% by vol.	Concrete	Compressive & splitting tensile strength, mod of rupture	Increase strengths at early curing stage.	Sivaraja, 2010

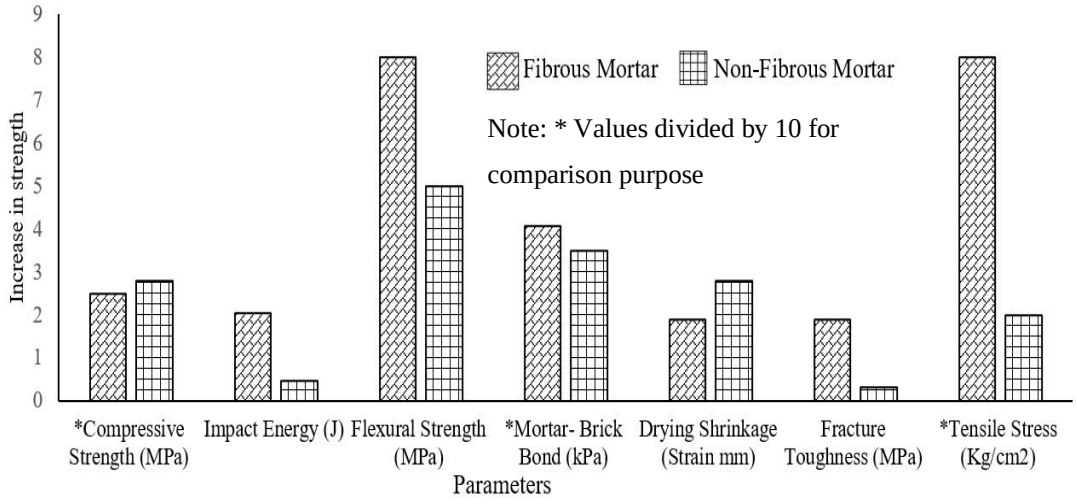

Figure 2.1: Comparison of parameters for fibrous and non-fibrous mortar

2.3.3 Use of natural fibres within plaster

Masonry walls strengthened by fibres in plaster has also been evaluated in many studies. In a study by Menna (2015), plaster walls were strengthened by hemp fibre composite. Shear testing using diagonal compression technique was applied to these walls and compared with unstrengthened walls. A five times increase in shear capacity was observed. This improvement was more than that observed when fibrous mortar was used in masonry. Results from other studies are given in Table 2.4 and the plaster application is shown in Figure 2.2. Different thickness of plastering was used in these studies varying from 5 -30 mm. 5-10 mm are classified as thin plastering and 10-30mm as thick plastering. In all studies significant improvement was observed, following addition of fibre to plaster.

In the studies by Humberto et.al (2020), textile reinforced plaster was applied on hollow clay infill panels and evaluated for out-of-plane loading. Significant improvement was observed for strengthened panels as compared to the panel without textile reinforced plaster. Energy dissipation was obtained 2 times more than the reference panel. In research by Di Bella (2014) three lime-plasters were evaluated. Synthetic fibres (polypropylene) and natural fibres (sisal and kenaf) were used as reinforcement. Comparison of plaster reinforced with artificial and natural fibres was carried out. It was found that the natural fibres could raise tensile capacity and could decrease cracks due to plastic shrinkage more than the artificial fibres. The durability of fibres in cementitious matrix is considered in many studies and detailed in annex A

Table A3. Degradation of plaster material when exposed to freeze/thaw cycles could occur regardless of the type of fibre used. This study lacked the information of comparison of plasters reinforced with and without fibre. Failure type and crack pattern in all strengthened panels were found to differ from those in fibreless 'control' panels. In control panels stair-stepped cracking was noted, while in strengthened panels a uniform crack pattern was found in the direction of diagonal loading. In all studies, addition of fibrous plaster to mortared masonry was found and nothing reported for mortarless masonry.

2.4 Finite element modelling of masonry columns

2.4.1 Modelling techniques for masonry

Masonry is a common term for a composite material made of various separate small elements (units) bonded together by some binding filler (mortar) or interlocked mechanisms for mortarless construction (Giamundo,2014a). Historical masonry structures are, for a number of reasons, normally classified as low-strength and these masonry structures can be broadly divided into following three categories: (Giamundo,2014a).

- Masonry with poor mortar strength
- Masonry with poor unit strength
- Masonry with poor unit and mortar strength

Masonry with poor *mortar* strength refers to structures where the unit/mortar interface governs the formation of cracks and collapse mechanism. Masonry with poor *unit* strength concerns structures where the strength of unit dominates mechanical behaviour. Tuff blocks are prime example of this case. In the third case the strength of mortar and unit are considered comparable and both have a major effect on failure mode. The type of material and bond strength affect the mechanical performance of the overall masonry structure. Masonry walls are considered to be strong in resisting of vertical axial load (Mohamad 2007) but there is often a need to improve their resistance when subjected to lateral load (Khonsari 2018) like wind and earthquake. Evaluation of the safety of masonry structures under seismic loading is a complex problem and both linear and non-linear methods have been used in different studies (Cakti,2016).

Wall strengthened by plaster	Reference	Wall strengthened by plaster	Reference
	Menna et al. (2015)	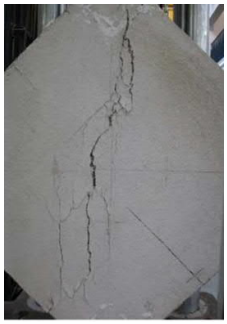	Parisi et al. (2013)
	Balsamo et al. (2011)		Mahmood et al. (2011)
	Kalali et al. (2012)		Gattesco et al. (2015)
	Humberto et.al (2020)		Humberto et.al (2020)

Figure 2.2: Plastered application by other researchers

The finite element method is the most well-known analysis technique for elements subjected to static or dynamic loading. For a numerical model effectively to represent the behaviour of a real structure, both the constitutive model and the input material

properties must be selected carefully. For this study the computational software TNO DIANA was used for the application of the finite element method. For a masonry structure FEM analysis can be performed using various modelling approaches. These include macro-element and micro-modelling approaches (Giamundo,2014a) The most refined approach used by other researchers is micro-modelling (Parisi,2011). Here different mechanical parameters and constitutive laws are used for different component parts. It allows for local failure of the units and of any bonding so they can be modelled separately. In addition it is possible to model the units with or without interfaces. Furthermore, to study structural failure cracking behaviour should be modelled accurately. Two types of cracking model are available to simulate behaviour numerically, which include the discrete crack and smeared crack models. The former introduces the crack to FE models manually by means of a separation between element edges (Scordelis and Ngo, 1967). The smeared crack approach does not track individual cracks but smears their effect over the FE by modifying its mechanical properties, as shown in the Figure 2.3 (Rot 1989, Soto, 2017 and Bejarano-Urrego, 2018).This approach is considered better than its discrete crack counterpart, which requires the mesh configuration to be updated as the cracks develop in the FE model. The smeared crack approach is further divided into two types: fixed smeared-cracking and rotating smeared-cracking approaches. With the former, the orientation of cracks remains fixed, which leads to an unrealistic and distorted crack pattern. With the rotating smeared crack approach, the orientation of the crack follows any change in the direction of principal tensile stresses. This gives results closer to the realistic value accepted by other studies (Qapo et. al 2014 & Dirar et.al 2013).

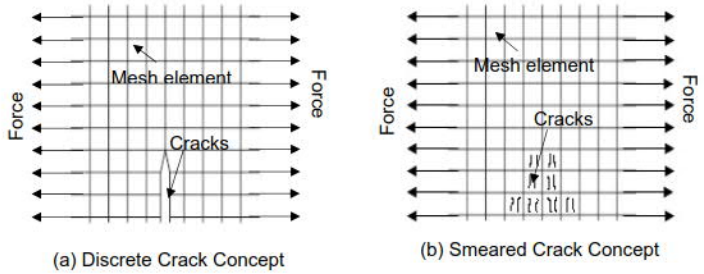

Figure 2.3: Cracking concept (Rots and Blaauwendraad 1989)

Table 2.4: Natural fibres within plaster

Fibre	Contents	Type of masonry	Max shear strength of reinforced plaster, MPa	Max shear strength of plain plaster, MPa	Increase compared to plain plaster panel	Author
Hemp	40mm thick mortar & hemp cord	Solid clay brick	0.95	0.176	5.39	Menna et al. (2015)
Basalt	10% of total weight	Tuff masonry	0.60	0.15	4	Balsamo et al. (2011)
Glass FRP	10mm thick, 10% of total weight	Tuff masonry	0.70	0.20	3.5	Parisi et al. (2013)
Glass and Carbon FRP	Fabric strips	Solid clay brick	0.46	0.14	3.25	Mahmood et al (2011)
Glass FRP	Mesh type 66*66m²	Clay brick	0.627	0.292	2.14	Kalali et al. (2012) & Gattesco et al. (2015)

2.4.2 Masonry FE models developed by other researchers

Non-linear finite element models have been developed in other studies of masonry structures using TNO DIANA. In some cases FE models are used to simulate the behaviour of experimental work. Table 2.5 shows the outcome of the different studies and the details of the parameters explored. The scale of modelling varies from a single block to a masonry wall panel. Modelling was also used to identify the material parameters for a masonry structure in the study by Sarhosis et. al 2014. In Figure 2.4 below, FE models developed in a variety of studies using TNO DIANA are shown.

In light of the outcome of previous studies micro modelling, rotating-smeared-crack finite-element modelling was chosen in this study to predict the lateral failure load of interlocked masonry. The proposed FE modelling was validated by comparing peak load with the experimental lateral failure load, as explained in chapter 5.

Table 2.5: Comparison of numerical and experimental results from the literature

Sample	Type of test	Parameters	Numerical (experimental) outcome	Author
Tuff masonry panel	Diagonal compression	Shear stress	0.39 MPa (0.38 MPa)	Basili, 2016
Adobe wall panel	Diagonal compression	Shear stress	0.15 MPa (0.14 MPa)	Giamundo,2014a
Hollow concrete block	Compression	Peak load	550 kN (600 kN)	Soto Izquierdo,2017
Hollow clay units	Cyclic shear load	Shear capacity	215 kN (222 kN)	Lignola, 2012

Model	Modelling approach	Reference
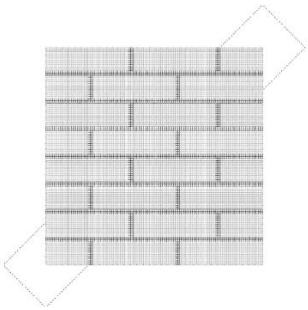	Micro-modelling smeared crack approach representing the tuff and the mortar independently	Lignola et.al 2009
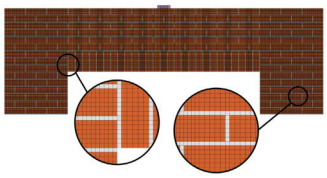	Masonry wall panel using micro -modelling approach with brick and mortar without interface.	Giamundo et.al, 2014a
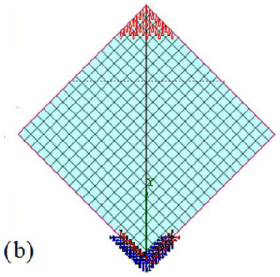 (b)	Macro-modelling approach unreinforced masonry panel for diagonal compression testing.	Basili et.al, 2016
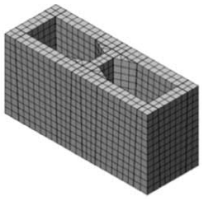	Smeared crack approach for sisal reinforced concrete block.	Soto Izquierdo et.al, 2017

Figure 2.4: FE models developed by other researchers

2.5 Lateral resistance of walling system with diaphragm

2.5.1 Mechanical properties of different walling systems

One of man's primary needs is a place in which to live. This normally comes third after food and clothing (Kintingu, 2009). As noted above, housing is inadequate in quantity and quality in most developing countries, considering the growth of population. This deficiency is the reason for the need to find improvements in the construction industry, especially in masonry housing. Conventional masonry construction is slow, labour intensive and expensive, due to the large number of mortar joints (Amin Al-Fakih, 2018; Anand & Ramamurthy, 2001). Attempts have been made to reduce the size of mortar joint by increasing the size of block/bricks but this limits the construction of many courses per day due to use of a bed mortar joint. Further development in eliminating the need of mortar joint has led to the introduction of different forms of interlocked masonry walls (Kohail et al., 2019). Interlocked masonry construction could introduce more affordable, safe and durable houses around the world (Laursen et al., 2015). It minimises the need for highly skilled labour, reduces construction time and lowers labour cost (Ramamurthy & Anand, 2001). Over the years studies have been carried out with the aim of improving the material properties of interlocking blocks (Asasutjarit *et al.,* 2009; Sturm *et al.,* 2015). These have improved the performance of an interlocked masonry system at material level, but there is still too limited an understanding of structural performance of this system for it to be adopted worldwide (Qu et al., 2015; Vaculik et al., 2014).

The various aspects of structural behaviour of interlocked masonry walling have been evaluated by many researchers. Safiee et al., 2011 investigated the structural behaviour of interlocked block walls under out-of-plane loading. The observed failure mode was mainly large lateral displacements and dry-joint opening approximately at the mid height of walls. It was found, as expected, that the slenderness ratio and pre-compressive load significantly affected the lateral load-carrying capacity of a wall. In this study pre-compressive load was applied through a steel I beam at the top pushed by a hydraulic jack. This assembly of pre-compressive load was the representation of roof truss and beam (diaphragm) in the real situation. The word diaphragm which is representation of timber roof truss and beam. In the rest of thesis instead of timber roof truss and beam, it is taken as diaphragm. Historic masonry structures normally consist

of timber joist and plywood sheathing, which is defined as flexible diaphragm (Ismail, 2016). The main purpose is to redistribute forces to the load bearings walls. By increasing the pre-compressive load the moment capacity of the wall increased proportionally; the out-of-plane load capacity of the wall was increased by decreasing the slenderness ratio. Ngowi, 2003 & Uzoegbo, 2001 carried out research into dry-stacked masonry walls with plaster, subject to out-of-plane loads. Their results indicated that the capacity of dry-stack walling systems to resist lateral load is strongly influenced by the presence of plaster. Lateral resistance can be increased by about 20% but significant reduction in ductility was observed when plastering both sides of the wall. Thanoon et al., 2007 concluded that interlocked walling systems are a possible alternative to conventional mortared-brick masonry as they exhibited better or comparable structural performance under axial and eccentric loading. The failure mode observed by Thanoon et al. 2007 showed better response for interlocking walls under eccentric vertical loading than mortared masonry walls. The typical failure mode was vertical splitting. In the experimental study by Kohail et al., 2019, under in-plane cyclic loading, flexural failure was observed exhibiting a rocking failure mode characterised by formation of an opening at the interface between the wall and its footing. The behaviour of conventional masonry walls under out-of-plane loading has been investigated by many researchers. In studies by Velazquez-Dimas & Ehsani, 2000, an unreinforced masonry wall was retrofitted with glass fibre strips and subjected to out-of-plane loading. Preliminary design recommendations were suggested for selecting the tensile strain in glass-fibre composites and maximum deflection. In the various studies different parameters were investigated to explain the performance/behaviour of interlocked masonry walls. These included lateral resistance, compressive and tensile strength, wall stiffness and ductility. A summary of these studies is detailed in Table 2.6. In studies by Martinez,2019 and Thanoon, 2007 the increase in strength of interlocking walls was related to the increase in compressive strength of their composite units.

2.5.2 Testing of walling systems by other researchers

Walling systems using different types of interlocked blocks were explored in various studies to determine the failure modes under lateral load. This type of loading is

considered critical to masonry structures and requires further exploration (Martínez & Atamturktur, 2019). Different types of the masonry unit have been developed, from simple to interlocking blocks, leading to mortarless (Ismail & Ingham, 2016) construction. The types of the block used in mortarless construction around the world these days include Haenar system, Mecano system (Vargas, 1988), Abang interlocking system, Putra Block (Thanoon et al., 2004), Bamba system and Tanzanian interlock brick (TIB) system (Kintingu, 2009). Most of the blocks are similar to conventional block units except that they carry extra projections that provide an interlocking mechanism (Safiee et al., 2011). Different walling systems based on various types of interlock have been explored by researchers, as shown in Figure 2.5. In each study several parameters were explored and failure mechanisms evaluated. In the study by Safiee et al., 2011, it was found that the mode of failure of walls is controlled by dry-joint opening failure. This failure was due to physical characteristics of wall itself due to absence of mortar between the layers. In the experimental work by Uzoegbo 2001 comparison of interlocked plain and plastered wall was carried out. It was also found that the mode of failure was the opening of joints between the interlocked courses. Plastered walls showed better load capacity, as plaster forms an effective restraint against rotation at the joint. The failure mode observed by Thanoon et al. 2007 showed better response for interlocking walls under eccentric vertical loading than mortared masonry walls. The typical failure mode was vertical splitting. In the experimental study by Kohail et al., 2019, under in-plane cyclic loading, flexural failure was observed exhibiting a rocking failure mode characterised by formation of an opening at the interface between the wall and its footing.

2.5.3 Improvement in lateral resistance by plastered walling system

It has been demonstrated in many studies that the addition of plaster to interlocked masonry walls significantly improves their lateral resistance. Laursen et al. 2015 used plaster coating on a 1100 mm high interlocked wall and it was observed to possess higher strength and significantly higher stiffness than was the case with unplastered walls. Higher stiffness could lead to reduced ductility; therefore further improvement in the plaster was required to improve ductility. The addition of natural fibres in plaster due to their high tensile strength could strengthen the plaster coating and thus enhance its ductility.

Table 2.6: Mechanical properties of different walling system explored by other researchers

Type of Walling system	Type of Test	Lateral Resistance (kN)	Compressive Strength (MPa)	Tensile Strength (MPa)	Wall Stiffness (N/m)	Strength Increment	Ductility Index/Damping ratio (%)	Failure Mode	References
Dry Stacked Blocks Wall	Lateral Load	115	14.62	1.46	-	35%	-	Tensile failure	Martinez et al. (2019)
Interlocking Blocks Shear walls	Lateral cyclic loading/Push Test	84.60	-	-	32.80	-	1.56	Rocking/sliding failure	Kohail et al. (2019)
Putra Interlocked Blocks	Lateral Load	23.89	18.62	2.06	-	-	-	Dry Joint Opening at mid height of wall	Safiee et al. (2011)
Interlocked Hollow Block Panel	Compressive Load	-	5.9 (Wall Panel)	-	-	-	-	Shear stresses at interlocking webs	Jaafar et al. (2006)
Putra Block Interlocking Wall	Eccentric Compressive load	-	5.26 (Wall strength)	-	-	33.53	-	Vertical splitting failure	Thanoon et al. (2007)
URM Walls	Cyclic out of plane loading	20.7	20.0	-	326	-	5.0	Delamination/Tension mode of failure	Velazquez-Dimas et al. (2000)

Wall Specification	Observation	Reference
	Improvement in ultimate lateral load capacity due to increase in block compressive strength was evaluated and also fully and partially grouted walls were compared.	Martinez et al. (2019)
	Behavior of post-tensioned dry-stack interlocking masonry walls under cyclic in-plane loading was investigated. Dry-stack masonry walls behaved like conventional masonry.	Kohail et al. (2019)
	Dry joint opening of interlocking mortar-less wall subject to out-of-plane load was evaluated. The dry joint opening mechanism around mid-height of wall, was dominant.	Safiee et al. (2011)
	Strength correlation between individual block, prism and basic wall panel for load bearing interlocking mortar-less block masonry was established.	Jaafar et al. (2006)
	It was found interlocking wall showed superior response as compared to the conventional mortared wall under eccentric loading.	Thanoon et al. (2007)
	It is recommended that the maximum service load be limited to that corresponding to a strain of 0.004. The majority of the specimens exhibited a fracture ductility index of 3.75–5.0	Velazquez-Dimas et al. (2000)

Figure 2.5: Tested walling system by other researchers

Table 2.7 details the reported chemical and mechanical properties of the rice straw and sisal fibres. Properties of other fibres are detailed in annex A Table A1. It can be

observed that sisal fibre has a much higher tensile strength than rice straw. Therefore, a better contribution was expected by the addition of sisal fibres for lateral resistance. Similar findings were found from the other studies for fibres with high tensile strengths (Menna et al. 2015 and Balsamo et al. 2011)

Table 2.7: Chemical and mechanical properties of rice straw and sisal fibres

Fibres	Chemical Properties				Mechanical properties		Reference
	Cellulose (wt. %)	Lignin (wt.%)	Hemicellulose (wt.%)	Wax (wt.%)	Tensile strength (MPa)	Elastic Modulus (GPa)	
Rice Straw	41-57	8-19	33	8-38	74.6	3.3	Ramamoorthy (2015)
Sisal	67–78	8-11	10-14	2	468-640	9.4-22	

2.6 Summary

It became evident from the outcome of different studies that the properties of interlocking blocks vary greatly depending on their geometry, material and interlocking mechanism. This could affect the overall strength of masonry walls. There was, however, no study found relating the mechanical properties of interlocking blocks to the overall performance of a masonry structure. Therefore it is important to assess the mechanical properties for ISSB. For fibrous cementitious matrices as a plaster (reinforced coating), some evidence of mechanical properties like compressive strength, flexural strength and toughness index is available, but the majority of the studies are related to artificial fibres possessing high tensile strengths. Therefore the mechanical properties of natural fibre sisal, rice straw and treated rice straw cementitious matrix needed experimentally to be evaluated in this study.

It is evident from the studies mentioned in section 2.3 that the use of fibres in plaster is a better technique for enhancing the strength of masonry structure than adding fibre to either blocks or mortar. Moreover, the addition of fibre to plaster is easier than its addition to blocks or mortar. However, the lack of durability of natural fibres when repeatedly wetted may exclude their inclusion in *external* renders.

Evaluation of masonry performance under lateral loads is a complex problem. The finite element method is a well-known analysis technique for elements subjected to

static and dynamic loading. However, for a numerical model effectively to represent the behaviour of real structure, use of realistic material properties plays an important role. Therefore the development of the FE model needed to be carried out for ISSB unplastered, plain plastered and fibrous plastered columns.

In light of the review of studies mentioned in section 2.5 it can be observed that various innovative interlocking masonry systems have been considered around the globe. The understanding of the structural performance of these systems is too limited for their adoption worldwide. Therefore in this study research needed to be extended to evaluate the performance of the fibrous plastered interlocked walling system for out-of-plane lateral resistance.

Evaluation of mechanical properties of ISSB and fibrous plaster is required to evaluate the overall performance of a masonry interlocking wall as explored from the literature. It is indicated through literature review that fibres in the plaster of a masonry wall are the best place in which to enhance lateral resistance. Therefore evaluation of out-of-plane resistance due to inclusion of natural fibres in plaster is required. Finite element modelling is the best technique to analyse the element subjected to static and dynamic loading. Given the different properties of ISSB and fibrous plaster development of the FE model needed to be carried out. Extensive literature was also found which details improvement in the material performance of interlocked walls. However, very limited literature was found on the behaviour of fibrous plastered interlocked walls for out-of-plane lateral load.

Chapter 3. Material characterisation of fibrous plaster and ISSB for masonry housing

Related ISI Impact Factor Journal Paper:

Qamar, F., Thomas, T. & Ali, M. (2019). Assessment of mechanical properties of fibrous mortar and interlocking soil stabilised block (ISSB) for low-cost masonry housing. *Materiales de Construccion,* 69 (336) e201. Impact factor: 1.886

3.1 Background

Evaluation of mechanical properties of ISSB and fibrous plaster are required to evaluate the overall performance of masonry wall as explored from the literature. Two fibres of particular interest are considered, one because they are very cheap (rice straw and 'treated' rice straw) and second (sisal) because it is known to have superior properties and is representative of other deliberately cultivated natural fibres. In every case, the fibres are assumed to be embedded in a cementitious matrix (sand-cement) to improve the mechanical properties of that matrix. In this chapter, the material properties of cementitious materials, strengthened with the fibres listed above with 2% and 5% content by mass of cement are examined and their characterisation as reported in the literature is extended through small-scale experiments. Because the lowest-cost form of cementitious walling employs mortarless, interlocking stabilised-soil masonry (ISSB) rather than conventional mortared, sand-cement masonry, ISSB material itself without fibres is also characterised in this chapter. As for author knowledge, there is no study found where mechanical properties of interlocking blocks were related to the overall performance of a masonry structure. The mechanical properties considered were both static and dynamic, including:

- First crack loading and maximum loading
- Compressive strength
- Modulus of elasticity
- Pre/post crack energy absorbed
- Total energy absorbed
- Toughness index

In addition, attention has been given to observing 'modes of failure' – e.g. crushing, spalling and cracking. Also, surface morphology of two fibres were compared using Bruker 3D optical microscope. The microscopic observation of tested fibrous cementitious material sample was also carried out to study the bond between the fibres and matrix (explained in section 3.3). Empirical relations were also developed for the compressive strength and modulus of elasticity of the ISSB, plain and fibrous cementitious material with the help of experimental data of this work and are presented in section 3.4.

This chapter follows the normal pattern of scoping, experimental design, presentation of (data) findings and discussion of those findings' implications.

3.1.1 Value of exploring material properties before exploring wall properties

Interlocking walls are already being used in many developing countries due to their lower cost than mortared walls. In different studies, the performance of interlocking block masonry wall has been tested and it has been shown that the compressive strength of the wall was directly proportional to the strength of masonry units (Fundi, 2018). It has also been found that other properties like modulus of elasticity, energy absorption and toughness index are also required to evaluate the wall performance for lateral load. As per author knowledge, these later properties were not measured. Therefore, in this chapter, the material properties of interlocking stabilised-soil block are explored. The length and contents of fibres have also an impact on the mechanical properties of cementitious matrix. Different fibre lengths and contents are used in different studies. It was found that below 5% use of natural fibres would be economical and would cost fraction of total cost of composite (Paramasivam et.al, 1984). It is also suggested in the literature to use 1.5-2% of the contents of the fibres due to workability requirements and 20 mm - 50 mm long fibres for optimum properties (Sivaraja, 2010). In this study, both strong (sisal) and weak (rice straw) fibres based on their tensile strength were used. The mechanical properties (as detailed earlier) of sisal, rice-straw and treated rice-straw in a cementitious matrix were experimentally evaluated.

The outcome of the properties of ISSB and fibrous cementitious matrix will dictate its use for walling of a typical masonry house as shown in the Figure 3.1. Figure 3.1 shows the elevation and section of a proposed masonry house. This house is a typical single storey house mostly constructed in poor developing countries. It consists of

timber beam and roof truss between the two connected walls. The load is transferred from one wall to another through roof truss. The connection of the walls with roof truss is important for transfer of loads.Walls of single ISSB width require projection outside wall at regular intervals for their stability. A timber roof truss is anchored to walls with steel ties. The structure is mortar-free and lateral resistance is to be ensured by ISSB assembly (single ISSB width wall having projections at regular interval) and plastering. The outcome of the mechanical properties of the ISSB and fibrous plastering material will lead to its use for masonry columns and walls in the following chapters.

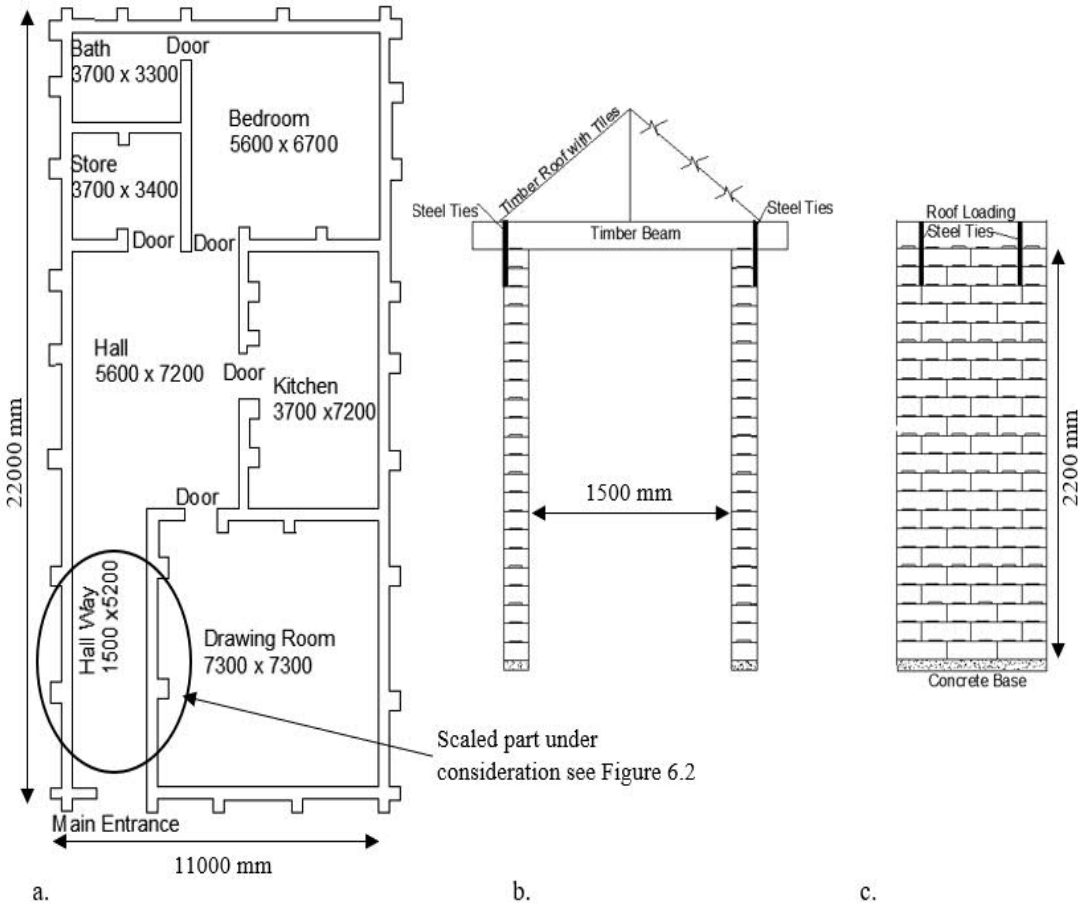

Figure 3.1: Schematic diagram of proposed technique for house construction a. Plan, b. Section and c. Elevation

3.1.2 Choice of two particular fibrous materials

A wide range of natural fibres exists around the world with different physical and mechanical properties. The variation in properties are linked with factors which include environment, type, method of fibre extraction. Tensile strength of fibres is considered to play an important role to enhance the overall performance of cementitious composite. Therefore, in this study, two types of fibres, possessing low and high tensile strengths, were considered. The chosen fibres were rice straw (low tensile strength) and sisal (high tensile strength). In addition, low-tensile-strength rice-straw fibres were treated mechanically to evaluate the effect of such treatment on their strength.

3.1.3 Gaps in the literature that justify the further measurements

The type of walling chosen for research into means of enhancing performance was, ISSB masonry strengthened by fibrous plaster. Wall performance therefore depends on the mechanical properties of these components. The mechanical properties of ISSB and fibrous plaster reported by other researchers are detailed in Table 2.1 and Table 2.2. It was found that for ISSB only compressive strength had been measured: other properties like modulus of elasticity, pre/post crack energy absorbed and toughness index had not been evaluated. These latter properties are required for studying wall performance using finite element modelling. Therefore, it is important to characterize the properties of material for ISSB. In this chapter, three configurations of ISSBs were considered which include single block, 1*2 blocks and 2*2 blocks. This would help in relating the effect on mechanical properties with different configurations.

On the other hand, for fibrous cementitious matrix, some evidence of impact on mechanical properties like compressive strength, flexural strength and toughness index exists, but this is only for natural and artificial fibres possessing high tensile strengths. In this study, both strong (sisal) and weak (rice straw) fibres based on their tensile strength were used. 2% and 5% of fibre contents with 50 mm in length were used. These contents of fibres was considered to produce optimised properties of cementitious mix as reported in the literature. Due to different fibre types, content and length it was required to characterise the properties of cementitious fibrous matrix. This will help in evaluating the performance of columns and walls detailed in the following chapters.

3.2 Experimental programme

3.2.1 Materials and composition

In the preparation of interlocking stabilised-soil blocks, soil and ordinary Portland cement were used. Soil was outsourced from Boko quarries Dar es Salam and it was obtained at a depth of 1m below the earth surface in order to eliminate the addition of humus materials. The cement was sourced from Twiga cement factory Dar es Salam. Chemical and physical properties as adopted from the manufacturer are shown in Table 3.1 and 3.2.

Table 3.1: Chemical properties of cement used

Material	Composition (%)					
	SiO_2	$Al2O_3$	$Fe2O_3$	CaO	MgO	Na_2O
Portland Cement	17.55	4.70	1.77	64.74	1.23	0.37

Table 3.2: Physical properties of cement used

Properties	Value
Porosity %	12.21
Density (g/cm3)	2.11
Water Absorption %	5.96

Same cement was used for the preparation of plain and fibrous plaster cubes. Three types of natural fibres were used which include sisal, rice-straw and treated rice-straw as shown in figure 3.2. The length of the fibre used was about 50 mm. The width of rice straw was about 7 mm and diameter of sisal fibres was reported as 100±30 µmm (Zhang, 2018 and Naveen, 2019). Water absorption %age by mass was reported for sisal as 110-240% and 290-400% for rice straw (Agopyan et al., 2005). These were obtained locally from Kibaha district Dar es Salam. For treated rice straw, fibres were washed using portable water and then boiled for half an hour. After half an hour boiled water was drained and fibres were washed again and then left to get sun dry before using in plaster cubes. For plaster cubes preparation, river sand was also used and obtained from Kibaha district Dar es Salam. The properties of sand as obtained from supplier are detailed in the Table 3.3.

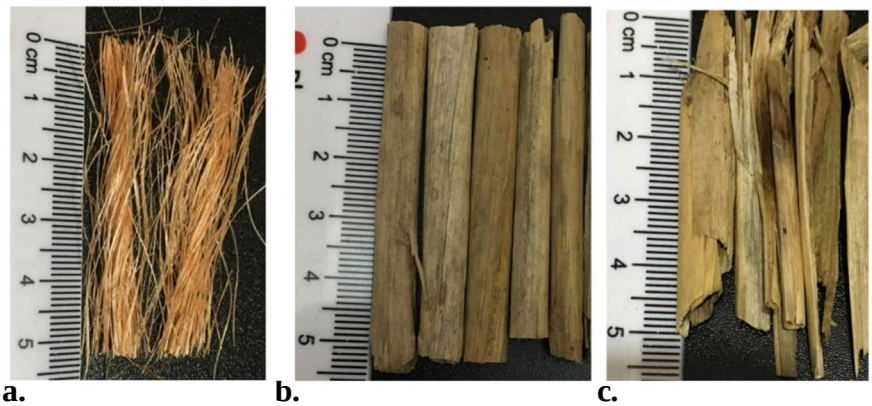

a. **b.** **c.**

Figure 3.2: Fibres used, a. Sisal fibre, b. Rice straw, and c. Treated rice straw

Table 3.3: Properties of sand used

Properties	Value
Fineness Modulus	2.14
Dry Unit Weight (kN/m^3)	14.89
Density (g/cm^3)	2.51
Absorption %	1.77
Moisture	7.08

3.2.2 Specimen preparation and mix ratio

a. Plain and fibrous plaster cubes

The mix proportions for plain and fibrous plaster cubes are listed in the Table 3.4. Further details of cubes preparation are included in Annex B. Cement and sand were dry mixed and water added to make a workable mix. For fibrous plaster cubes, fibres were added to dry mix of cement, sand and water added later to make it workable mix. 2% and 5% (by weight of cement) fibre contents were used. Plaster mixes for fibrous and non-fibrous samples were casted into cubes of dimensions 100 mm * 100 mm. In order to ensure consistency in test conditions, the cubes were casted from the same batch of plaster. The specimens were left in their moulds at room temperature and humidity to be demoulded after 7 days at which time they were stored under ambient temperature and humidity for at least 28 days before testing.

b. ISSB

ISSB were available in the NHBRA which were moulded using manually pressed machine and were producing blocks of dimensions 300 mm (length) * 150 mm (width) * 100 mm (height). The soil cement ratio for blocks were 12: 1. Locally available soil

was used to produce ISSB. Sand size particle-size distribution tests was performed previously by Kintingu 2009, showing a uniform medium sand with only 5% fines passing sieve 0.075. The normally recommended maximum ratio of free water to cement is 0.8. However, this did not work for manual brick pressing. It was increased to 1.4, which was found to be sufficient for easy moulding and handling. The blocks were cured for 28 days, covered by wet-sacking and plastic sheet for the whole period. Similar procedure and mix ratio were used for CSSB produced in UK laboratory.

Table 3.4: Mix proportion and labelling of mortar specimens

Combinations	Sample Symbol	Mix Proportion Cement: Sand	W/C ratio	Fibre content*
Plain Plaster Cubes	A	1:3	0.50	-
2% Rice Straw Plaster Cubes	B	1:3	0.67	2%
2% Sisal Plaster Cubes	C	1:3	0.67	2%
5% Rice Straw Plaster Cubes	D	1:3	0.67	5%
5% Sisal Plaster Cubes	E	1:3	0.67	5%
2% Treated Rice Straw Cubes	F	1:3	0.67	2%

3.2.3 Testing

The cubes and blocks were tested as per standards BS EN 1015-11 and BS EN 1052-1 in a universal testing machine and were instrumented as shown in Figures 3.3 and 3.4, respectively, to derive the stress-strain response. For blocks three different configurations which include single block, 1x2 blocks and 2x2 blocks were used as tested in other studies by Jaffar, 2006 & Ali, 2012 to develop the correlation between single block and prism with the performance of wall. In order to record the displacement of samples corresponding to the applied loading, steel plates are used. This kept the loading surface plane and parallel and the dial gauge was attached to this smooth surface. Generally, three samples of each case sufficed to get an average. The mechanical properties which include compressive strength, pre and post crack energy absorbed, total energy absorbed, modulus of elasticity and toughness index were observed. Surface morphology of sisal, rice straw and treated rice straw were compared using a Bruker 3D optical microscope to evaluate the surface roughness of fibres. The microscopic observation of tested plaster samples was carried out to study the bond between the fibres and plaster. Empirical relations were also developed

between compressive strength and modulus of elasticity with the help of experimental data, for the interlocking block, plain and fibrous plaster.

Figure 3.3: Typical test set up for plaster cubes

a. **b.** **c.**

Figure 3.4: Test set up of ISSB blocks, a. Single block, b. 1x2 blocks, and c. 2x2 blocks

3.3 Mechanical properties

3.3.1 Compressive properties of plaster cubes

a. Compressive behaviour of plaster cubes

The compressive stress-strain curves are shown in Figure 3.5 (a-f) for each sample of fibrous and non-fibrous plaster cubes. In all cases, samples with fibres could carry higher stress and strain than plain plaster sample resulting in enhanced ductility after first crack due to the presence of fibres with higher tensile strength. In the Figures 3.5c and 3.5e, which is representing 2% and 5% sisal fibres samples, very high stiffness and ductility is observed as compared to all other samples. This is due to high tensile strength of sisal fibres and their presence in the mix bridges the cracks and resist more deformation.

Figure 3.6 (a-f) shows the fractured surfaces of tested samples. Figure 3.6a represents the tested plain plaster sample and crushing failure of the sample is observed leading

to the spalling. Figure 3.6b and 3.6d with 2% and 5% rice straw shows buldging effect due to the presence of fibres and provides the ability of taking more load. Figure 3.6c and 3.6e with 2% and 5% sisal fibres shows the bridging effect due to their high tensile strength and shows the ability to delay the cracks progression and increased failure load. In the case of fibrous samples, as shown in figure 3.6d, the intentionally broken sample establish that de-bonding of fibres was observed other than breaking of fibres. The reason for this more debonding and less fibre fracture can be due to higher tensile strength of fibres and lower bond strength.

b. Compressive strength, compressive pre-crack/post crack, absorbed energies and compressive toughness index of plaster cubes

The compressive strength was taken as the peak value of stress from stress strain curve. The area below the stress-strain curve up to the stress of first crack was defined as pre-crack absorbed energy $(PE)_p$. The area below the stress-strain curve from the first crack stress to maximum load was considered as post crack energy absorbed $(CE)_p$. The total area below the stress-strain curve from initial load to maximum load was categorized as total energy absorbed $(TE)_p$. The ratio of total energy absorbed to first crack energy absorbed was taken as compressive toughness index $(CTI)_p$. Table 3.5 shows the averaged values of first crack load, maximum load, compressive strength, PE_p, CE_p, TE_p and CTI_p of samples A to F. The increase or decrease from datum sample A of all properties are detailed in Table 3.6. The result showed improvement in first crack and maximum load by addition of 2% and 5% sisal fibres as compared to plain sample. In comparison to compressive strength of plain sample to 2% sisal fibre sample, increment was observed whereas in all other cases, reduction in compressive strength for fibrous samples was noted as compared to that of plain plaster sample. This was in line with the finding of many studies (Pereira 2015 and Zia 2017) where addition of fibres resulted in reduction of compressive strength, mainly due to decrease in the density of sample. The CE_p of all samples A to F showed significant improvement as compared to that of plain plaster sample. The PE_p of sisal fibre samples had indicated increment as compared to plain plaster sample, whereas all other samples showed decrease. The TE_m of samples A to F showed improvement for all fibrous samples, which was the indication of fibre bridging which helped in limiting the size of cracks and provided enhanced resistance against stresses after the

initiation of cracks. From Table 3.6, it became evident that the 2% sisal fibre samples had shown increment ranging from 3% to 242% for all properties.

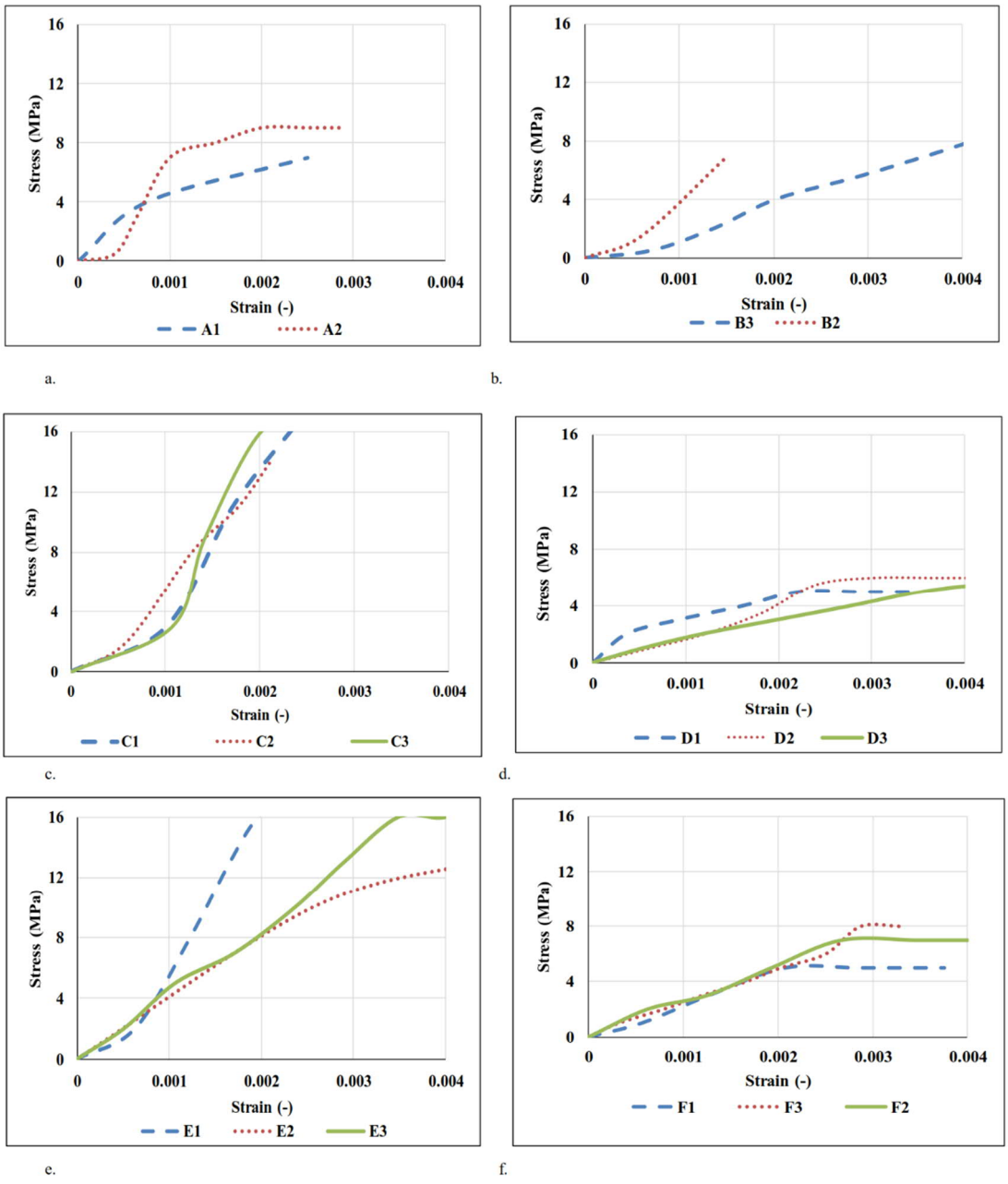

Figure 3.5: Stress strain curves for a. Plain plaster, b. 2% Rice straw reinforced plaster, c. 2% Sisal fibre reinforced plaster, d. 5% Rice straw reinforced plaster, e. 5% Sisal fibre reinforced plaster, and f. 2% Treated rice straw reinforced plaster

The comparison of compressive strength of plain and fibrous plaster samples can be observed in Figure 3.7. The reduction of 2.1 times, 3.16 times and 2.71 times was noted for 2% rice straw, 5% rice straw and 2% treated rice straw, respectively, as compared to plain samples. However, 6% increment was found by the addition of 2% sisal fibre from plain plaster sample, whereas 5% reduction in compressive strength was observed for 5% sisal fibre plaster sample.

This showed that the content and type of fibre had an impact on the compressive strength of properties and lowering the content of fibres could increase the compressive strength.

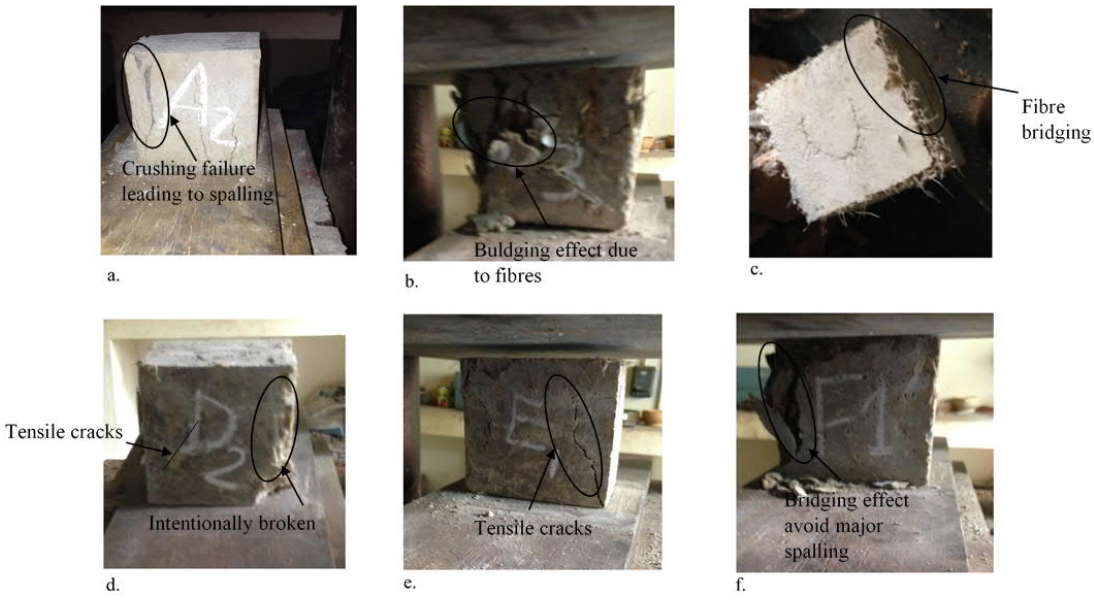

Figure 3.6: Fractured surfaces, a. Plain plaster, b. 2% Rice straw reinforced plaster, c. 2% Sisal fibre reinforced plaster, d. 5% Rice straw reinforced plaster, e. 5% Sisal fibre reinforced plaster, and f. 2% Treated rice straw reinforced plaster

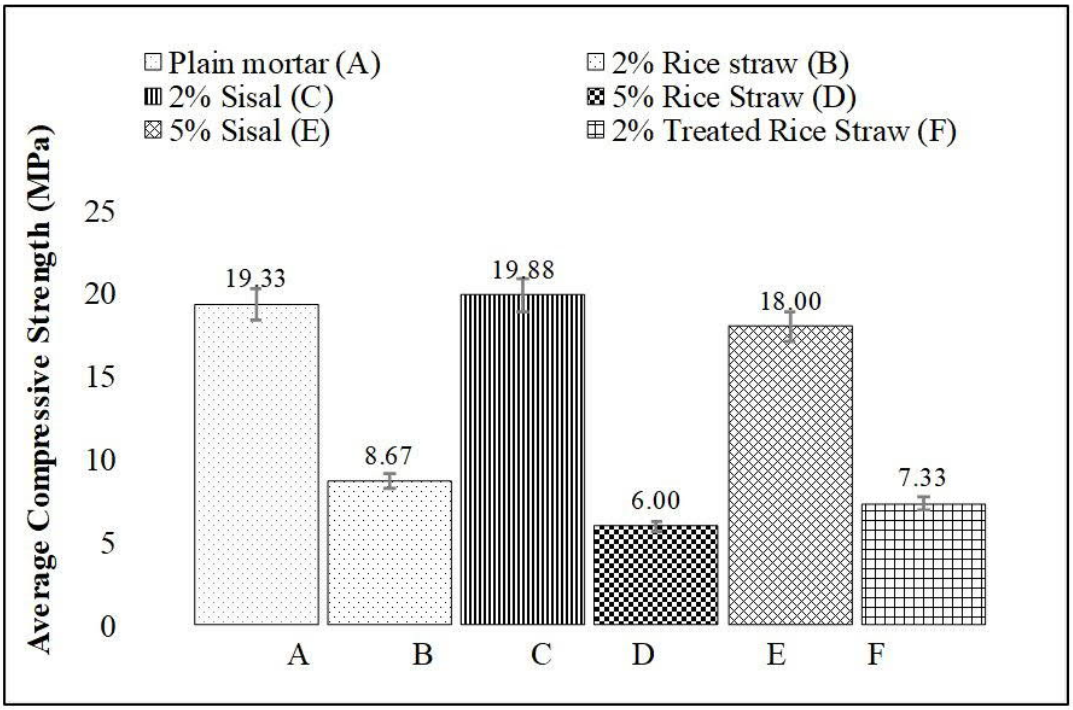

Figure 3.7: Comparison of compressive properties of fibre reinforced plaster

a. Modulus of elasticity of plaster cubes

Modulus of elasticity E_p was calculated as ratio of stress change to strain change within elastic limits. The averaged E_p of samples A to F are given in Table 3.5. In Table 3.6, the E_p for plain plaster considered as datum and increase or decrease was reported for all other fibrous samples. It can be observed that 2% sisal fibre samples showed increment to plain sample which could be attributed to high tensile strength and lower fibre contents. Whereas for all other fibrous samples decrease in E_p was observed.

3.3.2 Compressive properties of ISSB

a. Compressive behaviour of ISSB

The compressive stress-strain curves are shown in Figure 3.8(a-c) for each sample of single block, 1*2 blocks and 2*2 blocks. Single-block samples showed higher ultimate stress and strain as compared to other two sets of blocks. The reduction in stress-strain of the 1*2 blocks and 2*2 blocks compared to the single block might have been due to interlocking interaction between the different block units.

Figure 3.9(a-c) shows the fractured mechanism of tested samples. Figure 3.9a represents the fracture surface of single block sample and shear/vertical cracks can be observed in the region of interlocking. This is due to stress peak in the region of interlocking where resistance area is found to be lower than the rest of the block.

Table 3.5: Average compressive properties of fibre reinforced

Specimen	First crack load (kN)	Max load (kN)	Compressive Strength Cp (MPa)	Failure Mode	Pre-crack energy absorbed PEp (J)*10^3	Post-crack energy absorbed Cep (J)*10^3	Total energy absorbed TEp (J)*10^3	Compressive toughness index CTIp (-)	Modulus of Elasticity Ep (GPa)
A	90.5±44	193.0±44	19.3±5	Crushing	0.017±0.02	0.0035±0.005	0.021± 0.02	1.21±0.82	2.99±0.41
B	52.5±24	90.0±24	9±1.15	Buldging	0.014±0.01	0.0043±0.004	0.018±0.01	1.30±0.76	2.05±0.30
C	106.7±52	198.0±52	19.8±3.8	Bridging	0.03±0.02	0.012±0.01	0.041±0.04	1.41±0.70	7.17±0.20
D	34.7±12	60.0±12	6±0	Tensile	0.016±0.01	0.004±0.003	0.02±0.01	1.23±0.81	1.13±0.17
E	95.0±32	180.0±32	18±2	Tensile	0.03±0.02	0.009±0.008	0.036±0.003	1.31±0.74	2.23±1.01
F	39.7±17	73.0±17	7.3±1.15	Bridging	0.005±0.008	0.005±0.004	0.011±0.012	1.57±0.67	1.79±0.75

Note: Sample size = 3

a.

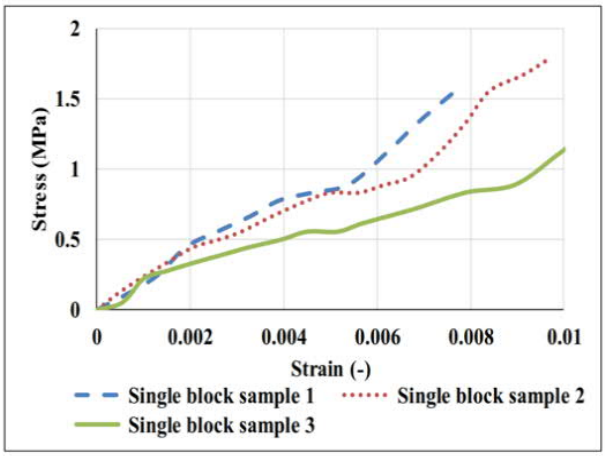

b.

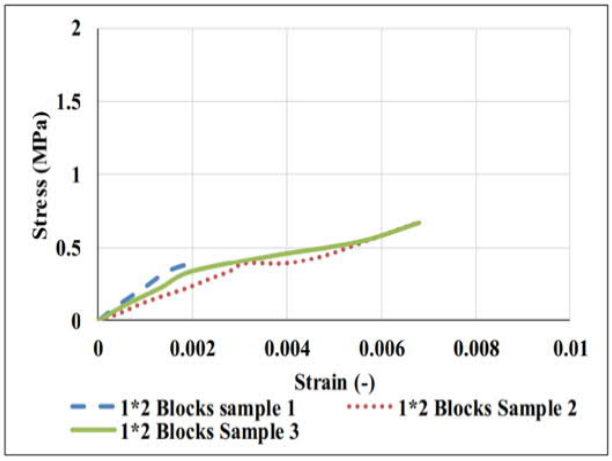

c.

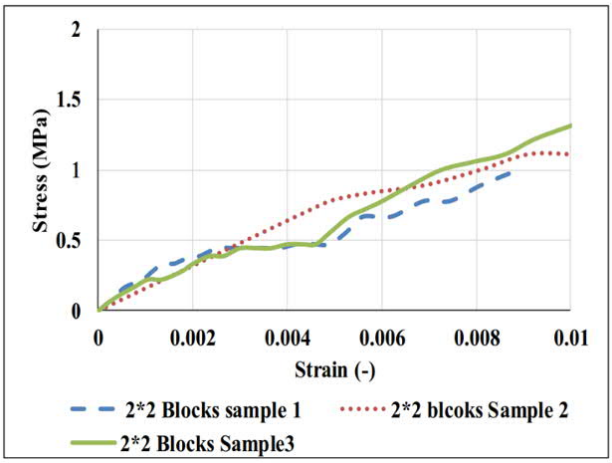

Figure 3.8: Stress strain of ISSB blocks, a. Single block, b. 1x2 blocks, and c. 2x2 blocks

Figure 3.9b and 3.9c showed the failure of 1*2 blocks and 2*2 blocks which indicates cracks development at an inclined angle and not on the joints. This led to blocks failed through crushing by opening of small gaps on individual blocks and finally initiation of cracks without opening up of joints. This could be due to the efficiency of interlocking mechanism of the blocks.

Figure 3.9: Fractured surfaces in blocks: a. Single block, b. 1x2 blocks, and c. 2x2 blocks

b. Compressive strength, compressive pre-crack/post crack, absorbed energies and compressive toughness index of ISSB

The compressive strength was taken as the peak value of stress from stress-strain curve of ISSB. The area below the stress-strain curve up to the stress of first crack was defined as the pre-crack absorbed energy $(PE)_b$. The area below the stress-strain curve from the first crack stress to maximum load was considered as the post crack energy absorbed $(CE)_b$. The total area below the stress-strain curve from initial load to maximum load was categorized as the total energy absorbed $(TE)_b$. The ratio of total energy absorbed and first crack energy absorbed was taken as the compressive toughness index $(CTI)_b$. Table 3.7 shows the values of first crack load, maximum load, compressive strength, PE_b, CE_b, TE_b and CTI_b of samples for single block, 1*2 blocks and 2*2 blocks. The values for first crack and maximum loads were increased by 3-4 times as the number of blocks increased due to better load distribution area. The compressive strengths of single block, 1*2 blocks and 2*2 blocks samples were noted as 1.53 MPa, 0.83 MPa, and 0.92 MPa, respectively. In comparison to compressive strength of single block to 1*2 blocks and 2*2 blocks a reduction of 45% and 39%, respectively, was noted. This decrease could be due to slenderness effect of the samples with more than one block. This also compared well with the fact that as the sample height increased the compressive strength reduced, which was also reported by other researcher (Jaafar, 2006). The comparison of average compressive strength of each sample can be observed in Figure 3.10.

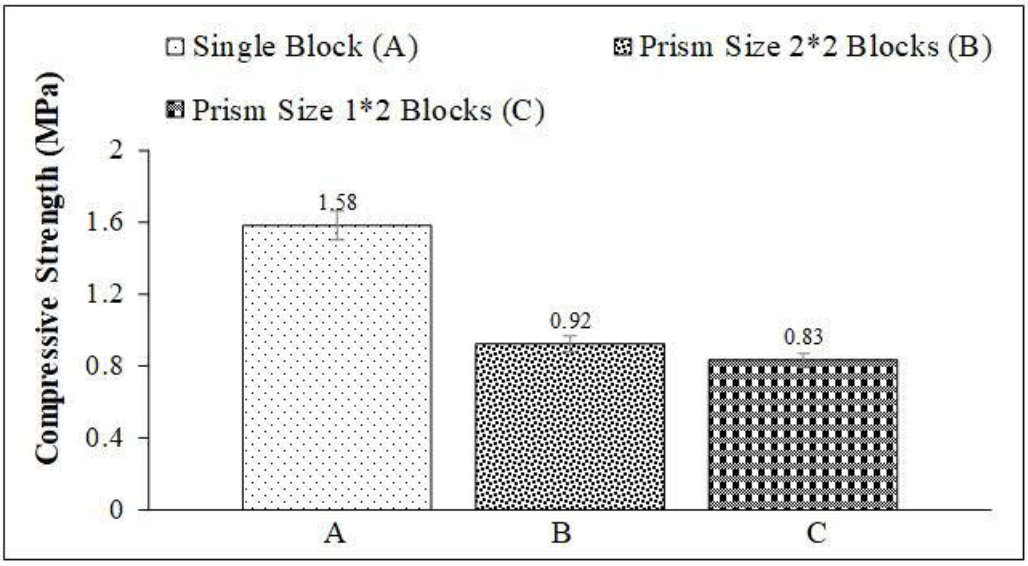

Figure 3.10: Comparison of compressive strength of blocks

The CE_b of three specimen configurations (single block, 1*2 blocks and 2*2 blocks) showed significant improvement of 66% for 1*2 blocks specimen over the single block and no difference was observed for 2*2 blocks specimen. This increment for 1*2 blocks specimen was due to efficiency of interlocking interface between two blocks. The PE_b of three specimens had indicated 54% and 18% reduction in post crack energy absorbed for 1*2 and 2*2 blocks specimens, respectively, as compared to single block. This showed that interlocking mechanism did not perform well after the crack propagation. Similar outcome was observed for the values for TE_b and CTI_b which showed the reduction of 64% for TE_b as compared to single block and reduction of 13% for CTI_b as compared to single block. This proved that the interlocking mechanism did not perform efficiently after the propagation of cracks and required to include another component like plaster to improve the post crack behaviour.

c. Modulus of elasticity of ISSB

Modulus of elasticity (E_b) was calculated as the ratio of stress change to strain change. The E_b is detailed for each specimen in Table 3.7. It was found that the value of E_b for single block sample was 0.201 GPa and for 1*2 blocks and 2*2 blocks specimens, it was calculated as 0.209 GPa and 0.234 GPa, respectively. This showed 4% and 16% increase from single block specimen, which was the indication of interlocking mechanism capacity of taking more deformation as compared to single block

specimen. The values of modulus of elasticity are very close to the values obtained from expression for modulus of elasticity proposed by Kennedy 2013.

3.3.3 Microscopic analysis

a. Surface images of fibres

Natural fibres have different chemical composition depending on variation in cultivation techniques and different soil and environment. Pre-treatment of fibres like washing with tap water and boiling in water does effect on the properties of fibres. Morphological changes of the fibres were investigated using Bruker 3D optical microscope. Figure 3.11 (a-c) shows the surface images of sisal, rice straw and treated rice straw.

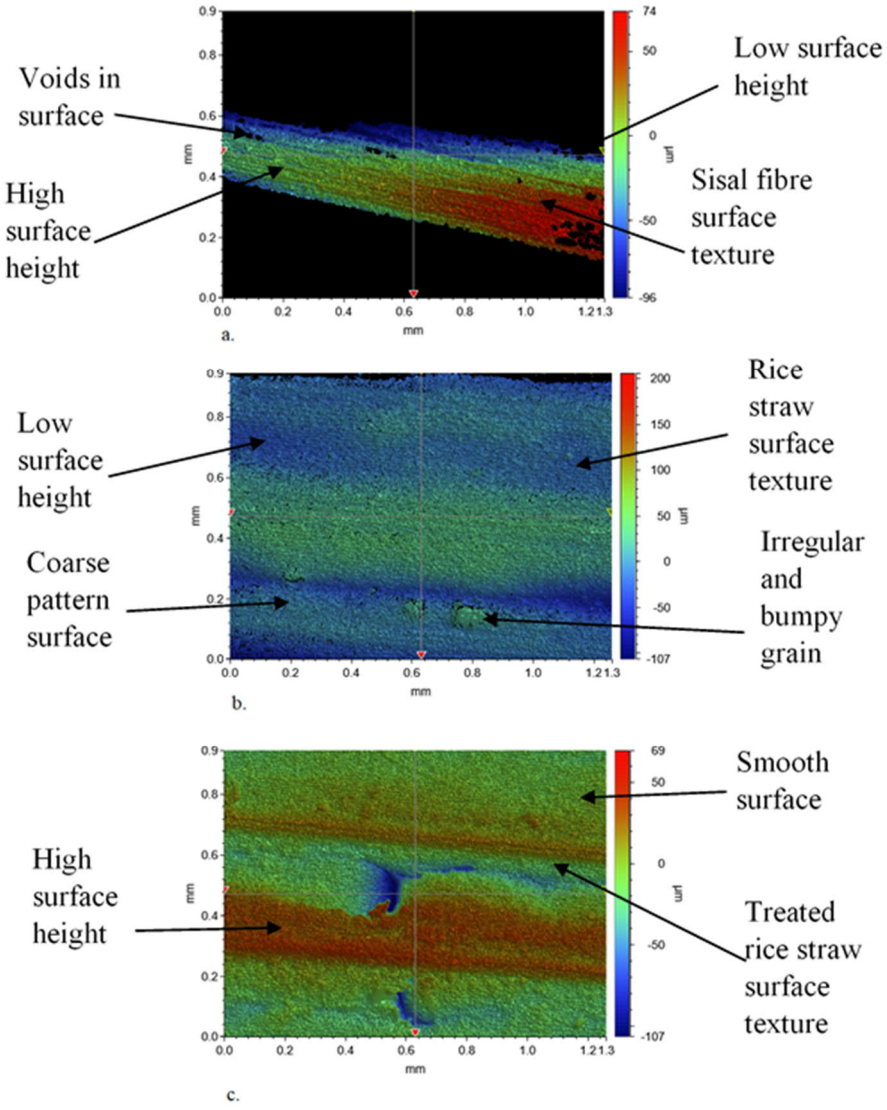

Figure 3.11: Surface contour of fibres, a. Sisal fibre surface roughness, b. Rice straw surface roughness, and c. Treated rice straw surface roughness

Table 3.6: Comparison of compressive properties of fibre reinforced plaster cubes

Specimen	First crack load (kN)	Max load (kN)	Compressive Strength (MPa)	Pre-crack energy absorbed (J)*10^3	Post-crack energy absorbed (J)*10^3	Total energy absorbed (J)*10^3	Compressive toughness index (-)	Modulus of Elasticity (GPa)
A (Datum)	90.5±44	193.0±44	19.3±5	0.017±0.02	0.0035±0.005	0.021± 0.02	1.21±0.82	2.99±0.41
B	-41%	-43%	-53%	-17%	+23%	-14%	+7%	-31%
C	+17%	+8%	+3%	+76%	+242%	+95%	+16%	+139%
D	-61%	-65%	-68%	-5%	+14%	-4%	+2%	-62%
E	+5%	-4%	-6%	+76%	+157%	+71%	+8%	-25%
F	-56%	-59%	-62%	-70%	+42%	-47%	+29%	-40%

Note: (+) increase; (-) Decrease

Table 3.7: Compressive properties of ISSB

Specimen	First crack load (kN)	Max load (kN)	Top contact area (mm^2)	Bottom contact area (mm^2)	Top stress (MPa)	Bottom stress (MPa)	Compressive strength (MPa)	Pre-crack energy absorbed (J)*10^3	Post-crack energy absorbed (J)*103	Total energy absorbed (J)*103	Compressive toughness index (-)	Modulus of Elasticity (GPa)
1 Block	11.7±4.8	20±4.8	15000	45000	2.50±0.6	1.58±0.24	1.58±0.24	0.006±0.001	0.0011±0.0001	0.0071±0.0013	1.30±0.95	0.201±0.04
1*2 Block	34.8±16	72.5±16	15000	45000	4.73±0.7	0.83±0.16	0.83±0.16	0.002±0.001	0.0005±0.0003	0.0025±0.0014	1.18±0.78	0.209±0.05
2*2 Block	51.1±17.7	105±17.7	30000	90000	2.77±0.1	0.92±0.04	0.92±0.04	0.006±0.001	0.0009±0.0001	0.007±0.001	1.14±0.93	0.234±0.04

Note: Sample size = 3

It was observed that treated rice straw has smooth surface as compared to sisal and untreated rice straw which resulted in poor bond between plaster and treated fibre. This was evident from the lowest strength of treated rice straw sample as compared to all other samples. It was also noted from figure 3.11a and 3.11b that surface profile for sisal was higher than rice straw, giving high value of surface roughness, which could be one of the important factors in developing good bond between fibres and cementitious material.

b. Surface images of fibrous and plain plaster cube samples

Figure 3.12 (a-d) showed the microscopic images of plain and fibrous plaster cube samples. These samples were produced from the cube samples after carrying out the compression testing. In Figure 3.12a, micro cracks were observed in the cement paste. In figure 3.12b, sample of sisal fibre plaster cube showed the embedment of sisal fibre within cement paste without any gaps or voids indicating a proper bond of fibre within cement matrix. This resulted in better mechanical properties for sisal fibrous cubes as compared to other samples. Figure 3.12c and 3.12d showed the untreated and treated rice straw samples, respectively, which indicated the presence of micro cracks and voids in the cement paste and loose bond with rice straw. This poor bond and void resulted in reduced post crack performance and toughness.

3.4 Theoretical framework

Relationship between static and dynamic properties and low-cost house performance

In low-cost masonry housing main-component walling is mostly employed to resist compressive and lateral load (Guerreiro,2018; Marcari, 2007 and Dizhur, 2014). Therefore the structural performance of the wall under these loadings is of prime importance. This depends on the characteristics and mechanical properties of the materials used, which include compressive strength, modulus of elasticity, pre/post/total energy absorption capacity (PE and CE, respectively) and toughness (CTI). Therefore it is important to explore the best mechanical properties of material to enhance the performance of walling and in essence overall performance of masonry house. In this study mechanical properties of plain and fibrous plaster cube samples

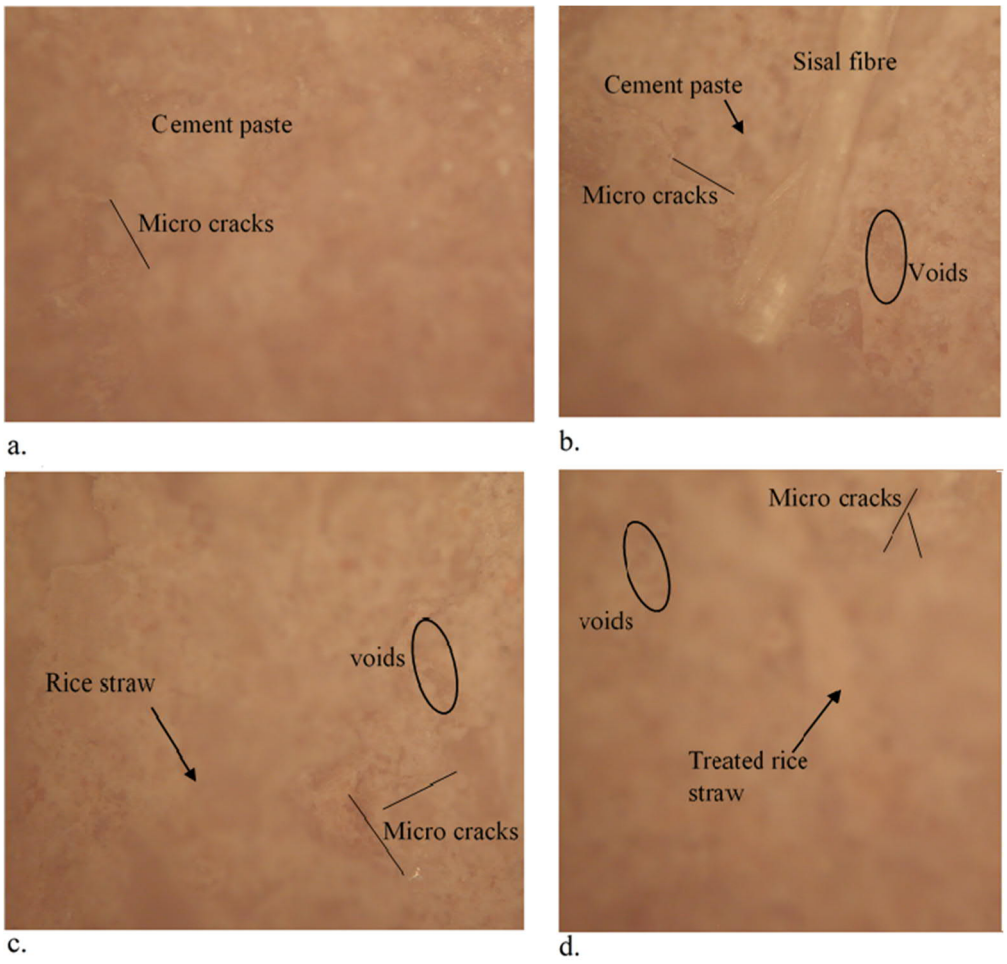

Figure 3.12: Microscopic images from plaster cubes, a. Plain plaster surface texture, b. Sisal fibre embedment in plaster, c. Rice straw embedment in plaster, and d. Treated rice straw embedment in plaster

and ISSBs were examined. The addition of 2% sisal fibre cube samples showed the most promising results, indicating a 3% increment in compressive strength, 76% increment in PE_p, 2.21 times increase in CE_p, 95% increase in TE_p and 17% increase in CTI_p as compared with the plain plaster cube samples. For ISSB there was a 45% and 39% reduction in compressive strength for 1*2 and 2*2 blocks respectively, as compared with single block. In other mechanical properties like CE_b a 66% improvement was observed. The values of PE_b, TE_b and CTI_b for 1*2 and 2*2 blocks were reduced by 54%,64% and 13% respectively, as compared with those of single block. This shows that the use of plaster with 2% sisal fibre for interlocking structure is likely to give optimised mechanical properties and hence improve the overall performance of masonry structure.

Empirical equations

a. Empirical relation between modulus of elasticity and compressive strength of plaster cubes

The following empirical equations were developed (Figure 3.13) with the help of averaged experimental data. These equations are based on limited data (only three values) in order to check the trend of variation due to addition of different content of fibre. These are established by means of best fit curve (R^2 ranging from 0.90 to 1.0) with the simplification of coefficients and exponents of input variables numerically to predict the modulus of elasticity (E) in GPa and in these equations value of x is always greater than zero:

$$E = 0.3 * C^{0.8*K} \quad [1]$$

$$E = (4 + K) * Y * C^2 - 160 * Z * C + 1492 \quad [2]$$

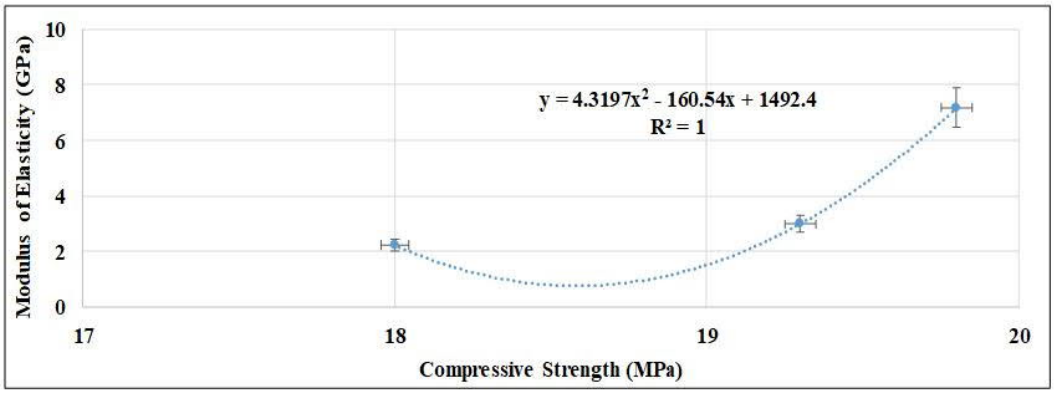

a.

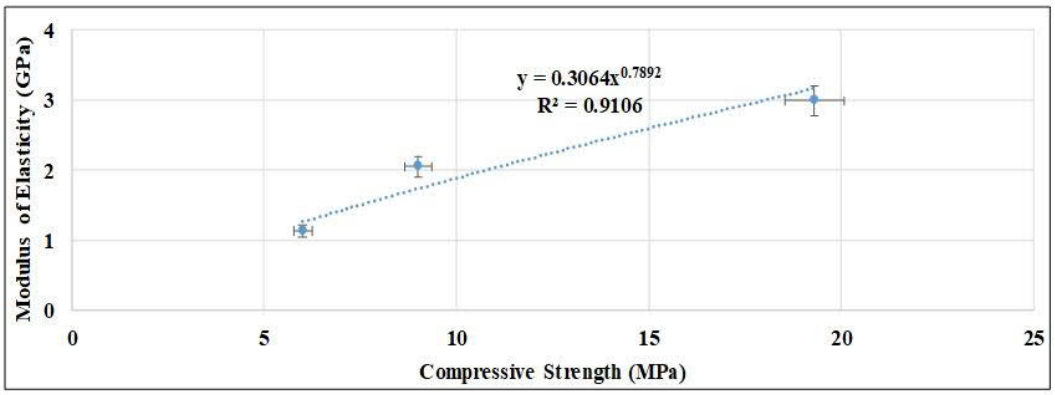

b.

Figure 3.13: Development of empirical equation relating modulus of elasticity to compressive strength, a. Sisal reinforced plaster, b. Rice straw reinforced plaster

where C is compressive strength in MPa and K = 1, 1.1 and 0.95 for plain, 2% rice straw and 5% rice straw specimen respectively in equation 1. For equation 2, K (GPa) = 0.293, 0.294 and 0.291 for plain, 2% sisal and 5% sisal fibre reinforced mortar, respectively, Y ($1/MPa^2$) =1 and Z (GPa/MPa) = 1. It may be noted that for each value an average of three readings is taken. In the case of sisal-reinforced plaster a convex quadratic increase is observed, whereas in rice- reinforced plaster a powered linear increase is found.

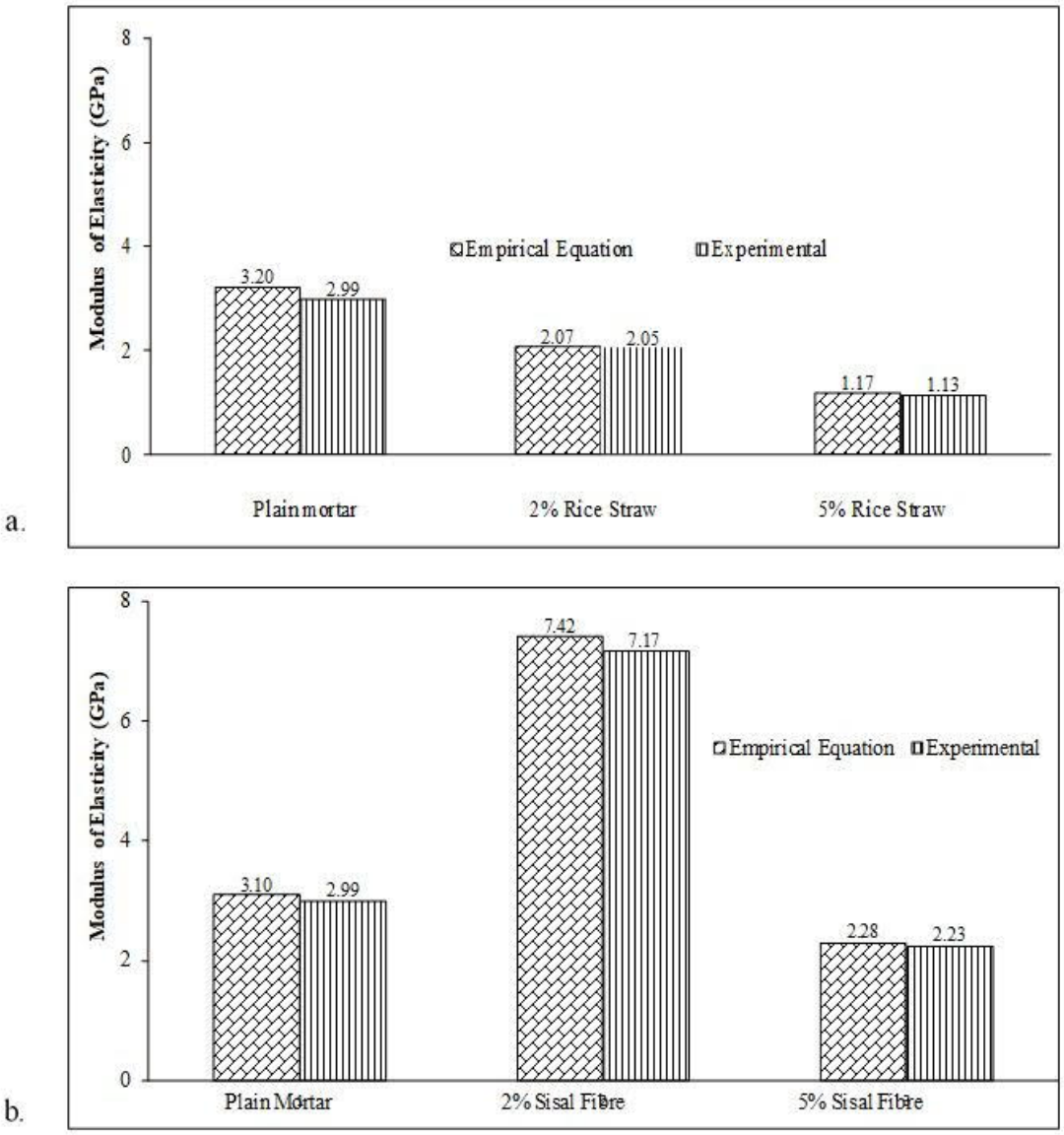

Figure 3.14: Comparison of modulus of elasticity with experimental and empirical values for plain and fibrous plaster a. Equation 1 b. Equation 2

Table 3.8 details the experimental and empirical values of modulus of elasticity (GPa). It can be seen that a correlation holds between compressive strength and modulus of elasticity and these being directly proportional. This direct relationship is attributed to the capacity to take greater load, which is increased due to the presence of fibre of high tensile strength and the bridging phenomenon. It can therefore be stated that an increase in compressive strength results in higher value of modulus of elasticity. Figure 3.14 compares the experimental and numerical values of modulus of elasticity in plain and fibrous samples. It can be seen that the values of E obtained from equations 1 and 2 are very close to the experimental values. There is good agreement between empirical and experimental values. The percentage errors are 3.7%, 1.2-3.6% and 2.4%-3.5% for plain, rice-straw and sisal plaster samples respectively.

Table 3.8: Experimental and theoretical values of modulus of elasticity for plain and fibrous plaster

Specimen	Compressive Strength C_p (MPa)	Modulus of Elasticity E_p (GPa)		
		Empirical Equation	Experimental	Error (%age)
Plain Mortar	19.3	3.10	2.99	3.7%
2% Rice Straw Reinforced Plaster	9	2.07	2.05	1.2%
5% Rice Straw Reinforced Plaster	6	1.17	1.13	3.6%
2% Sisal Fibre Reinforced Plaster	19.8	7.42	7.17	3.5%
5% Sisal Fibre Reinforced Plaster	18	2.28	2.23	2.4%

Note: 1. $E = 0.3 * C^{0.8*K}$; Where K = 1, 1.1 & 0.95 for plain, % rice straw and 5% rice straw specimen, respectively.2. $E = (4 + K) * Y * C^2 - 160 * Z * C + 1492$; Where K (GPa) = 0.293, 0.294 & 0.291 for plain, 2% sisal and 5% sisal specimen, respectively, Y ($1/MPa^2$) =1 and Z (GPa/MPa) = 1 for all cases.

b. Empirical relation between modulus of elasticity and compressive strength of ISSB

The following empirical equation is developed (Figure 3.15) with the help of averaged experimental data. This equation is based on nine samples of blocks representing three no. of samples for single block, 1*2 and 2*2 blocks respectively. This is established by means of best fit curve (R^2= 1.0) with the simplification of coefficients and

exponents of input variables numerically to predict the modulus of elasticity (E) in GPa:

$$E = -0.4 * K * Z * C^2 + Z * C - 0.4 \quad [3]$$

where C is compressive strength in MPa and K (1/MPa) = 0.98, 0.65, 0.60 and Z (GPa/MPa) = 1, 0.95, 0.9 for single block, 1*2 and 2*2 blocks respectively. As far as the behaviour of blocks is concerned, empirical modelling reveals that there is concave variation among single blocks, 1*2 blocks and 2*2 blocks.

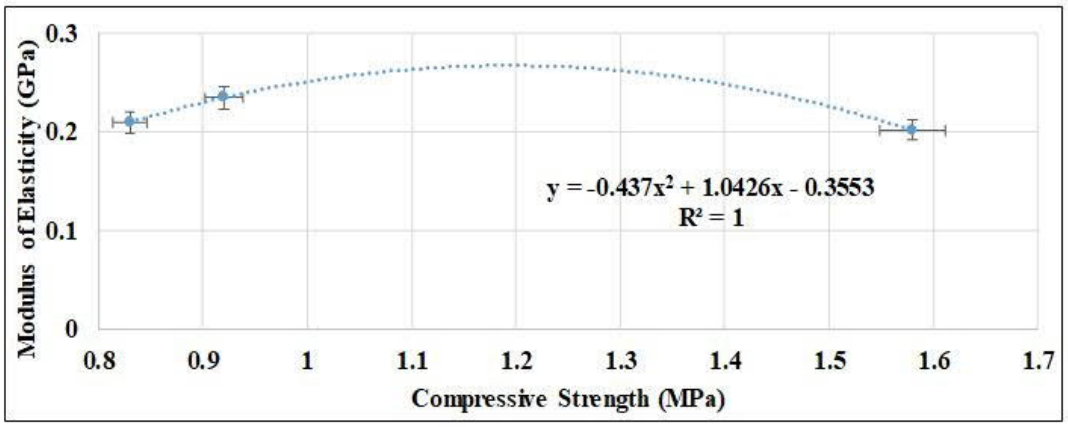

Figure 3.15: Development of empirical equation for modulus of elasticity of blocks

Table 3.9 details the experimental and empirical values of modulus of elasticity (GPa) of ISSB. It can be seen that compressive strength and modulus of elasticity of ISSB are correlative and are inversely proportional. This inverse proportionality is due to the different configuration of blocks. The reduction in compressive strength and increase in modulus of elasticity of other configurations as compared with single block is due to block interface joint which leads to large displacements. Therefore it can be stated that a decrease in compressive strength results in a higher value of modulus of elasticity. Figure 3.16 compares the experimental and numerical values of modulus of elasticity for single block, 1*2 and 2*2 blocks. It can be seen that the values of E obtained from equation 3 are very close to the experimental values. The percentage error is 0.7% - 6.6% for different block configurations.

Table 3.9: Experimental and theoretical values of modulus of elasticity for ISSBs

Sample Symbol	Compressive Strength C_b (MPa)	Modulus of Elasticity E_b (GPa)		
		Empirical Equation	Experimental	Error (%age)
Single Block	1.58	0.20	0.20	0.7%
1*2 Block	0.83	0.22	0.21	4.0%
2*2 Block	0.92	0.25	0.23	6.6%

Note: 1. $E = -0.4 * K * Z * C^2 + Z * C - 0.4$; Where K (1/MPa) = 0.98, 0.65, 0.60 and Z (GPa/MPa) = 1, 0.95, 0.9 for single block, 1*2 block and 2*2 block, respectively.

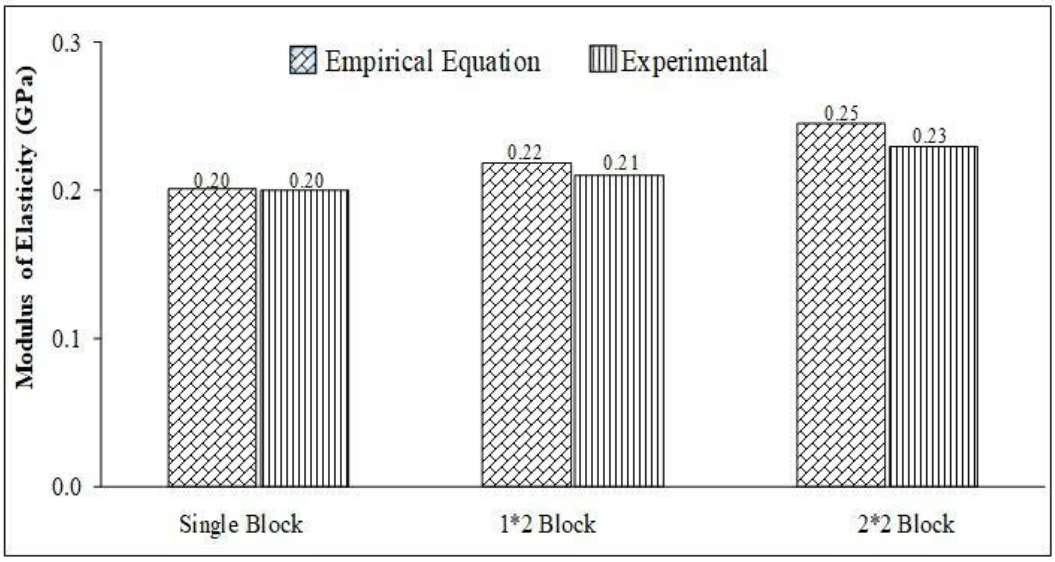

Figure 3.16: Comparison of modulus of elasticity with experimental and empirical (equation 3) values for blocks

3.5 Summary

The mechanical properties (compressive strength, modulus of elasticity, pre and post crack energy absorbed and toughness index) of interlocking stabilised-soil blocks and fibrous/non-fibrous plaster were experimentally investigated to determine how best to enhance the performance of proposed interlocked fibrous plastered (i.e. reinforced coating) low-cost housing. The following conclusions are drawn:

1. A knowledge gap identified from the literature review regarding the mechanical properties (compressive strength, modulus of elasticity, pre/post crack energy absorbed and toughness) of ISSB and fibrous plaster which are prime parameters of enhancing resistance to lateral load like wind and earthquake for a masonry structure.

2. Surface contours of sisal fibres showed a smooth surface, whereas rice-straw fibres exhibited a rough and irregular bumpy surface indication the presence of impurities.
3. The failure modes of the fibrous cubes were characterised by a bridging, buldging effect and tensile cracks due to the presence of natural fibre, as compared with crushing failure of plain samples. 2% and 5% sisal fibre samples showed very high stiffness at first-crack load and ductility at ultimate load, as compared with all other samples.
4. Mechanical properties with 2% sisal-fibre plaster specimens resulted in an increase of 17%, 8%, 3%, 76%, 221%, 17% and 139% of first-crack load, maximum load, PE_p, CE_p, TE_p, CTI_p and $E_{p,}$ respectively, as compared with that of plain mortar specimen.
5. The compressive strength of 2% rice-straw, 5% rice-straw and 2% treated rice-straw reinforced mortar resulted in a reduction of 210%, 316% and 271% respectively. A 6% increment was found with the addition of 2% sisal fibre from a plain mortar sample and a 5% reduction in compressive strength was observed in a 5% sisal-fibre mortar sample
6. Microscopic images of sisal-fibre plaster cube showed the embedment of sisal fibre in cement paste without any gap or void, indicating a proper bond of fibre in cement matrix. This resulted in better mechanical properties in sisal- fibrous cubes than in other samples. Untreated and treated rice-straw samples indicated the presence of micro cracks and voids in the cement paste and loose bond with rice straw. This poor bond and void resulted in reduced pre/post crack performance and toughness.
7. The failure modes of the ISSBs were characterised either by failure perpendicular to bed joint or shear cracks and spalling of block. The compressive stress- strain curves for each sample of single block showed higher stress and strain than did the other two sets of blocks. The reduction in stress-strain of the 1*2 and 2*2 blocks as compared with the single block might have been due to interlocking interaction between the different block units.
8. The mechanical properties of 1*2 blocks were compared with single block and 1.97 times, 2.62 times and 4% increase was found in first crack, maximum

load and modulus of elasticity respectively. Values of compressive strength, PE_b, TE_b and CTI_b were reduced by 47%, 67%, 64% and 9% respectively.

9. With 2*2 blocks 3.36 times, 4.25 times and 16% increase was found in first crack, maximum load and modulus of elasticity respectively. Values of compressive strength, PE_b, TE_b and CTI_b were reduced by 41%, 1%, 1.5% and 12% respectively, as compared with those of single ISSB.
10. Empirical relations were developed with the help of experimental data for prediction of modulus of elasticity for fibrous/ plain plaster samples and interlocking stabilised-soil blocks. The experimental and empirical values were found close enough, with a maximum error of 6.6% in ISSBs and 3.7% in plaster cube samples.

In light of the findings and observed behaviour, the addition of 2% sisal fibre and rice straw in plaster (i.e. reinforced coating) of interlocked masonry walling is likely to be effective in improving the performance including the lateral resistance of low-cost masonry house. However for treated rice straw not much increase in mechanical properties was observed, therefore treated rice straw will not be considered further in this study. Further investigation is required to evaluate the performance of ISSB column and wall with fibre- reinforced plaster when subjected to lateral load. This will be further explored in Chapter 4 and 6, respectively. The material properties for ISSB and fibrous cementitious matrix obtained in this chapter will be utilised for finite element modelling in Chapter 5.

Chapter 4. Behaviour of fibre-reinforced single-block masonry columns under lateral load

Related ISI Impact Factor Journal Paper:

Qamar, F., Thomas, T. & Ali, M. (2018). Use of natural fibrous plaster for improving the out of plane lateral resistance of mortarless interlocked masonry walling. *Construction and Building Materials,* 174 320-329. Impact factor: 4.046

Related SCIMAGO Impact Factor Periodical Paper:

Qamar, F., Thomas, T. & Ali, M. (2018). Contribution of Sisal Reinforced Plaster in out of Plane Resistance of Masonry Column. *Key Engineering* Materials, Vol. 765, pp 343-348.

Related Conference Papers:

Qamar, F., Thomas, T. & Ali, M. (2018). Effect of rice straw reinforced plaster in improving out-of-plane resistance of mortar-free interlocking column. *50th Annual New Zealand Society for Earthquake Engineering,* Auckland, New Zealand 13-15 April. Paper ID 23.

Qamar, F., Thomas, T. & Ali, M. (2018). Effect of Sisal Fibrous Mortar in Improving Out Of-Plane Resistance and Damping Ratio of Masonry Column. *Canadian Society for Civil Engineering,* Fredericton Canada, 13-16 June. Paper ID 155.

4.1 Background

As has been identified previously in chapter 2 from literature review that natural fibres can be utilised within plaster and mortar to increase the mechanical properties of masonry structure. In this chapter, the lateral strength and stiffness of masonry single-block columns was experimentally evaluated by adding the natural fibres (sisal and rice straw) within either 20 mm thick or 8 mm thin plaster. Two types of single-block column with different plastering variations were tested. One ISSBs columns tested at National Housing and Building Research Agency (NHBRA) in Dar es Salam and secondly SSBs columns with 8 mm thin sisal plaster *and mortar* at Warwick University UK. Sisal fibres have high tensile strength and can be classified as strong fibres whereas rice straw can be categorised as a weak fibre. Both strong and weak fibres, at 2% (as shortlisted from Chapter 3) by weight of cement, were utilised within plasters of 20 mm and 8 mm thickness. The evaluation of mechanical properties like

lateral stiffness, lateral strength, energy absorption and toughness index of ISSB and SSB columns were carried out. To evaluate the contribution of plaster and natural fibres, an unplastered single-block column was taken as reference.

4.2 Experimental work

4.2.1 Material used and mix ratio

Ordinary Portland cement, locally-obtained river sand and tap water were used for the plaster mix. Sisal and rice straw fibres were cut into 5cm lengths for fibrous plaster. Interlocking stabilised-soil blocks (ISSBs) and stabilised soil blocks (SSB) were used to create columns in Tanzania and in UK respectively. Further details of block preparation and column preparation are included in Annex C. The mechanical properties of the material used for plastering are detailed in chapter 3.

For both plain plaster and for fibrous plasters, the design mix comprised a 1:3 ratio for cement: sand. 0.67 ratio for water-cement was used for plain plaster. However, more water was required in fibrous plasters to make them workable. 2% fibres by weight of cement were added into the fibrous plaster samples. Figure 4.1 shows images of the materials used, of mix preparation and of the different phases of specimen preparation. Figure 4.1a shows cement, sand, sisal fibres and rice straw. Commercially accessible sisal fibres and rice straw were gathered. Rice straw was available as waste. Tensile strengths of sisal and rice straw are reported to be 468-640 MPa and 75 MPa (Ramamoorthy et.al, 2015) which is considered comparable to and representative of the material used for this experimental work. The compressive strength of the ISSBs was tested as described in chapter 3. Manual mixing was used for preparing both the plain and the fibrous plaster. Figure 4.1b shows images of mix preparation and a slump test for Tanzanian experimental work. First, cement and sand were mixed and then water was added to make a workable mix. For fibrous plaster, first sand and cement were mixed together, then a layer of fibres was spread over and dry mixed. Finally, water was added slowly to make a workable mix. A slump test was done for each plain and fibrous mix. The slump values for rice straw fibrous plaster was only 40 mm, but the mix was workable despite this low slump. The slump values for all other samples were between 90-140 mm.

For interlocking stabilised-soil blocks (ISSB) and stabilised soil blocks (SSB), the mix design ratio for soil and cement was 12:1. Figure 4.1c shows different phases of specimen preparation, i.e. erection of column and plastering.

a.

b.

c.

Figure 4.1: Different stages of experimental work; a. materials used (cement, sand, sisal fibre and rice-straw; b. mix preparation and slump test; and c. column erection and plastering

4.2.2 Column preparation and labelling

ISSBs (Figure 4.2) of size 300 mm x 150 mm x 100 mm were used. These stabilised-soil blocks were produced in a manual press and included vertical holes and an interlocking mechanism. Special care was taken to construct stable columns. Five

columns, 300 mm x 150 mm x 1500 mm high, for each plaster specification were built and tested under a lateral load. Various plaster constitutions, A to G, were employed in the experiments and coded as shown in Table 4.1. Column type A was unplastered, column types B to G were plastered only on the tension face.

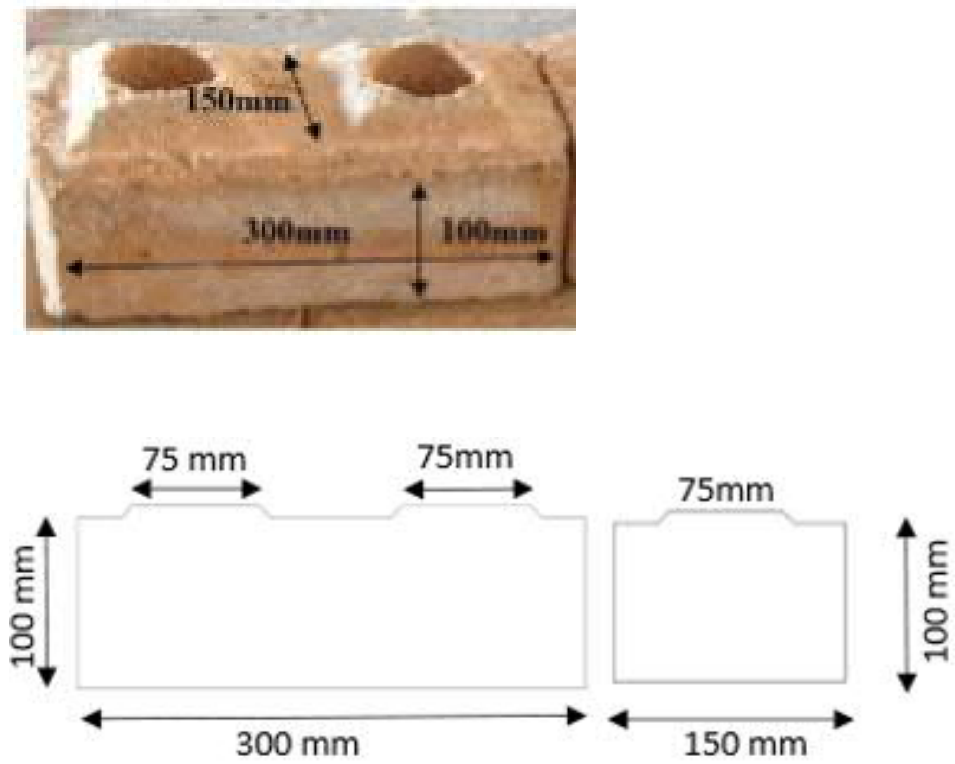

Figure 4.2: ISSB with dimensions

Columns of SSB blocks (Figure 4.3) of size 300 mm x 150 mm x 100 mm and lacking any interlock were built: three columns, 1500 mm high, for each case, and tested under a lateral load. Samples H to L were employed in the experiments and coded as shown in Table 4.2.

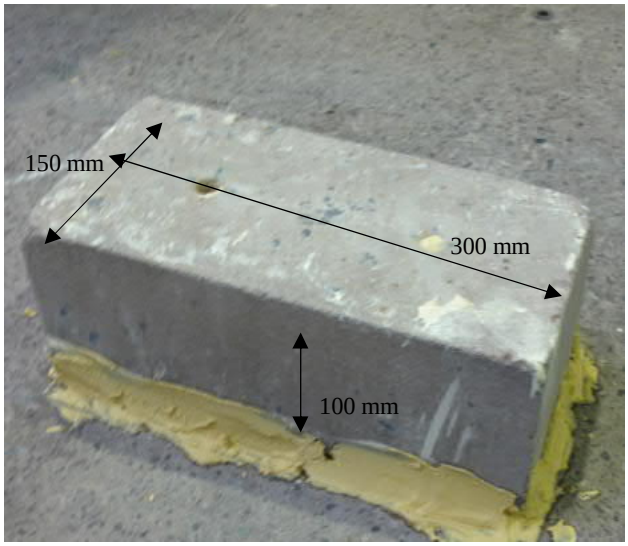

Figure 4.3: SSB Block with dimensions

Table 4.1: Plaster specifications for ISSB columns

Combinations	Sample Symbol	No of Samples
Unplastered U	A - (U)	5
Plastered P 8mm No Fibre	F - (P,8,N)	4
Plastered P 20mm No Fibre	E - (P,20,N)	4
Plastered P Sisal-fibre S 8mm thick	B - (P,S,8)	5
Plastered P Sisal-fibre S 20mm thick	G - (P,S,20)	5
Plastered P Rice-fibre R 8mm thick	C - (P,R,8)	5
Plastered P Rice-fibre R 20mm thick	D - (P,R,20)	5

Table 4.2: Plaster specifications for SSB columns

Combinations (3 No. Samples each)		Sample Symbol
Non-fibrous mortar M;	Unplastered U	H – (M,U)
Fibrous mortar MF;	Unplastered U	J – (MF,U)
Non-fibrous mortar M;	Plastered P No Fibre N	K – (M,P,8,N)
Fibrous- mortar column MF;	Plastered P Sisal-fibre S 8 mm	L – (MF,P,8,S)

4.2.3 Experiment setup and loading for NHBRA samples

Figure 4.4 shows the test setup in Dar es Salaam. In small increments, lateral load was applied via a weight-and-pulley system at a height of 1000 mm, as shown in Figure 4.4b. The self-weight of the blocks above 1000 mm was considered as compression force for the lateral load testing. Column was erected and checked for out of plumbness and considered bottom of column level with top of column, where displacement is measured. A non-digital theodolite and plain scale with spirit level was used to obtain the displacements at the top of column. Loading was set initially to that, giving a displacement of 1 to 2 mm. Loading was later increased, generally in steps of 35 N, to find the start of cracking and the collapse load. The first block of column was embedded in the lean concrete on a strong concrete floor and considered to be rigid enough as a fixed support.

a.

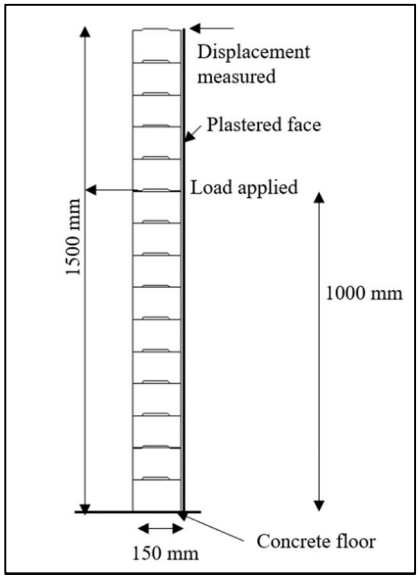

b.

Figure 4.4: Bespoke system for lateral load application for ISSB column; a. schematic diagram and b. test setup

4.2.4 Experiment setup and loading for Warwick samples

A similar set up was employed for testing SSB columns at Warwick as at NHBRA and is shown in Figure 4.5, however a dial gauge was used instead of a theodolite to record the displacement at the top of columns.

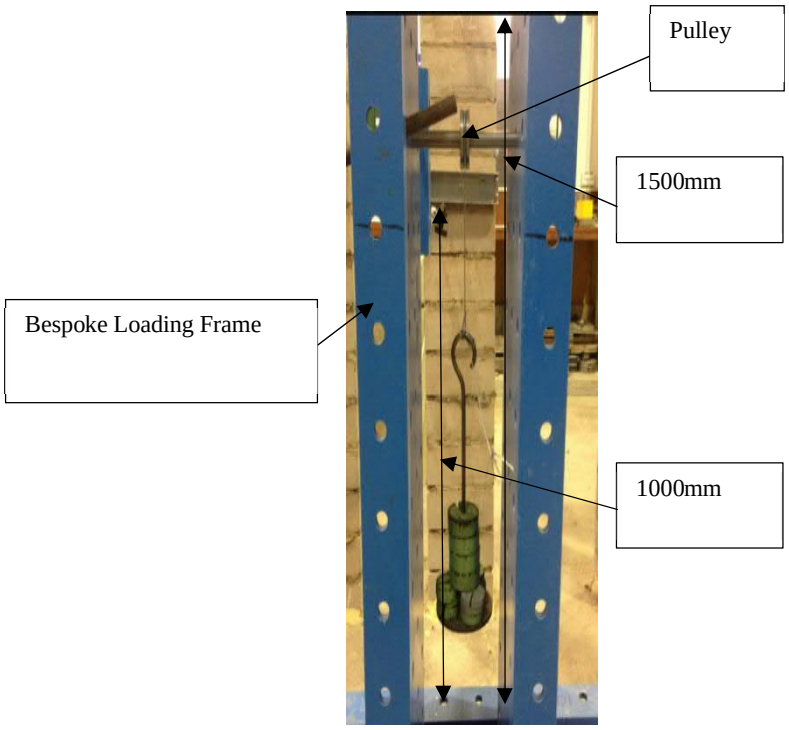

Figure 4.5: Test setup (i.e. bespoke system for lateral load application for SSB column)

4.3 Column behaviour

4.3.1 Load displacement curves for interlocked block columns

The load displacement plot for each column is shown in Figure 4.6(a to g). In all cases sample size was 5 except for the plain-plastered columns for which only 4 were tested, as the 5th got damaged before testing. *Unplastered columns*, A1 to A5, see Fig 4.6a: four out of five columns showed a similar response. It can be observed that the displacement is 3-6 mm for a very small failure load of 10-20 N, showing very low stiffness and brittle/sudden failure. This behavior was expected for the un-mortared structure as the column was resisting over-turning just because of its self-weight. However there was a high resistance to lateral shear failure because of the interlocking mechanism.

Plain-plastered columns of both 8 mm and 20 mm thickness did enhance the stiffness and load carrying capacity as detailed in Figure 4.6(b-c), respectively

representing samples E1-E4 and F1-F4. The loads were increased to 29-67 N and 53-97 N, respectively, but the specimen failures were still brittle. The displacements in both cases were around 4 mm. All columns with 8 mm thick plaster showed the same load-displacement trend. The columns with 20 mm thick plaster showed similar behaviour to the 8 mm thick plaster columns, with little variation in stiffness.

Sisal fibrous plaster having 8 mm and 20 mm thickness (Figure 4.6(d-e), samples B1-B5 and G1-G5): showed a remarkable increase in their stiffness and load. The maximum loads increased to 165-319 N and 216-408 N, respectively, and the displacements at failure were 4.5-12 mm and 5-13 mm, respectively. Columns with 8 mm thick sisal fibre-reinforced plaster showed two slope behaviours with little variation in load-displacement curve particularly in the second-slope section. The columns with 20 mm reinforced plaster showed a similar two-slope behaviour.

Rice straw plaster having 8 mm and 20 mm thicknesses (samples C1-C5 and D1-D5). Figure 4.6(f-g), showed an increase in stiffness over that of the plain-plastered and unplastered samples but exhibited a less ductile behaviour than the sisal plaster samples. The maximum loads were 169-307 N and 174-338 N, respectively, and the failure displacements were around 3-6.5 mm and 3.5-5 mm, respectively. Columns with 8 mm and 20 mm thick rice straw reinforced plaster both showed single slope behaviours. But the latter were stiffer. The columns with sisal fibres were more ductile with onset of cracking prior to failure. The displacement was about 13 mm before failure, whereas for all other cases the displacement was about 6-8 mm.

Figure 4.6 shows individual results for all 5 x 7 columns. Figure 4.7 shows averaged results for each of the 7 plastering variants. The averaged load-displacement curves of 8 mm and 20 mm plastered columns are detailed in Figure 4.7a and 4.7b, respectively, along with that of unplastered column for comparison. Since an average of five samples is taken for each curve, therefore the behaviour of load displacement can be regarded as robust. It can be observed that all plastered columns have more or less same trend with the exemption that there is extended averaged load displacement curve in fibre reinforced plastered columns. As expected, columns with 20 mm thick plaster are stiffer than those with 8 mm thick plaster. The failure of the fibrous columns was more ductile as compared to columns without plastering or with only plain plastering. It can also be observed a step like behaviour for fibre reinforced column

samples which indicate an increase in peak load without no or very little displacement. This is an indication where fibres contribution is started after first crack load.

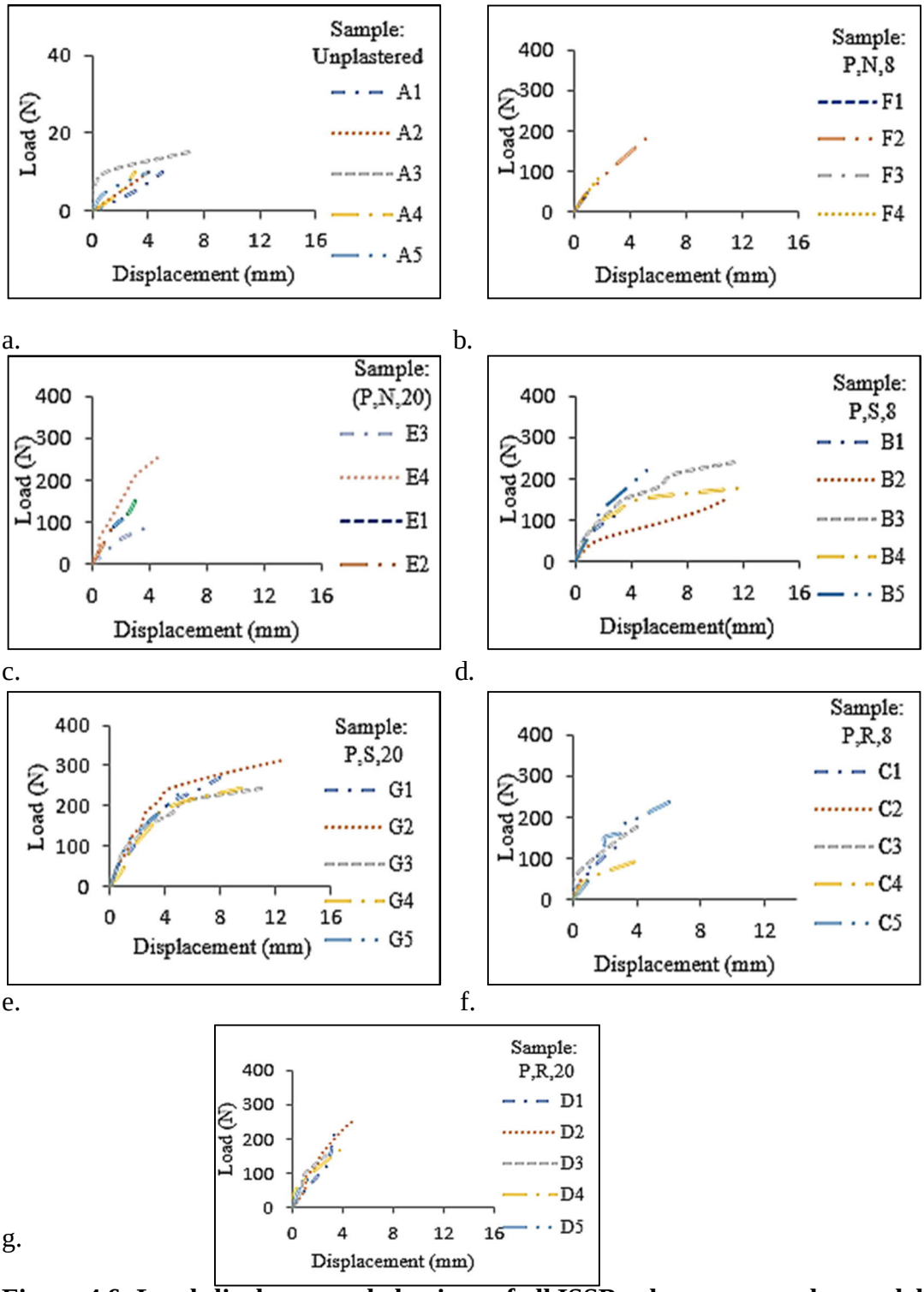

Figure 4.6: Load-displacement behaviour of all ISSB columns; a. unplastered, b. 8 mm thick plain plastered, c. 20 mm thick plain plastered, d. 8 mm thick sisal plastered, e. 20 mm thick sisal plastered, f. 8 mm thick rice plastered, and g. 20 mm thick rice plastered.

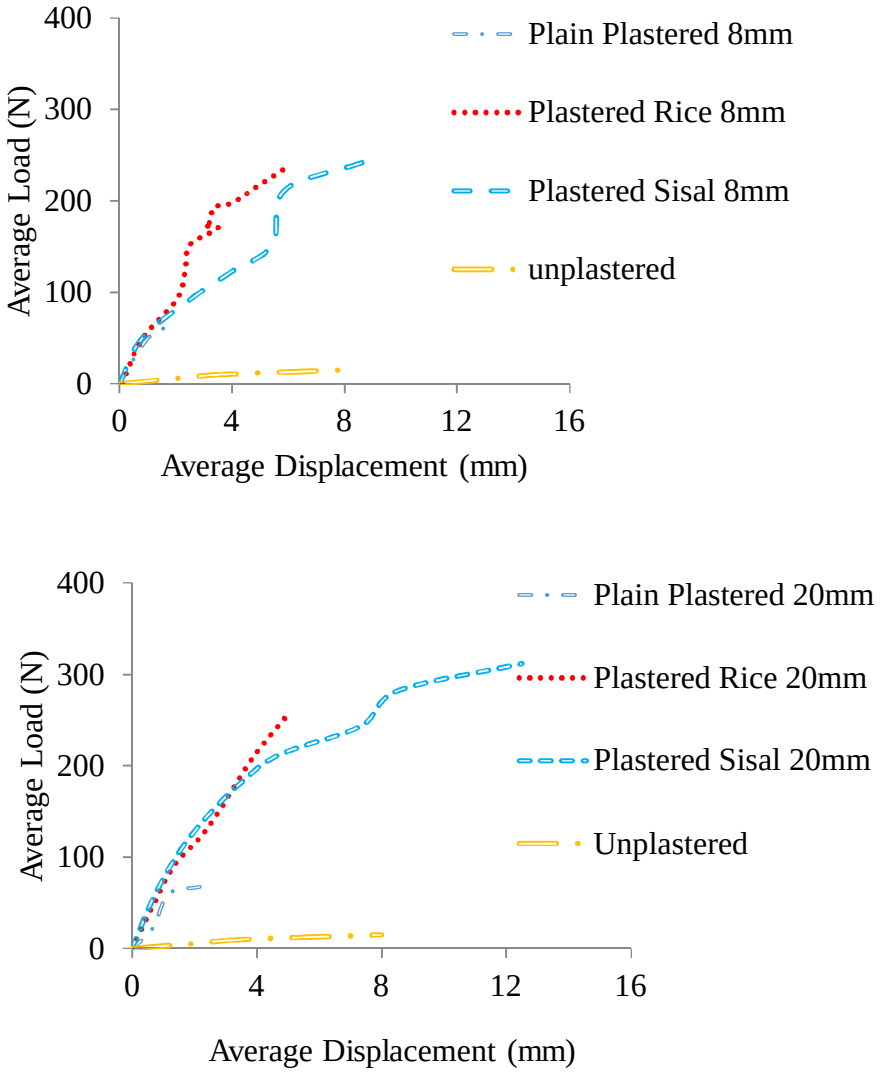

Figure 4.7: Averaged load-displacement plots for all ISSB column sets.

Figure 4.8 explains the failure loads for the seven plastering variations. The increase in failure load from unplastered to 8mm and 20mm thick plain plaster is from 15±5N to 48±19N and 75±22N, respectively. These demonstrate about 3 and 5 times increase in lateral strength due to application of plaster. The increase in failure load from unplastered and 8mm thick plain plaster to 8 mm thick sisal fibre reinforced plaster is 15±5N and 48±19N, respectively, to 242±77N. These are improvement factors of about 16 and 5 times, respectively. The increase in failure load from unplastered and 20mm thick plain plaster to 20 mm thick sisal fibre reinforced plaster is 15±5N and 75±22N, respectively, to 312±96N. These are about 21 and 4 times increase in strength due to applied lateral load, respectively. The increase in failure load from unplastered

and 8mm thick plain plaster to 8mm thick rice straw reinforced plaster is 15±5N and 48±19N, respectively, to 238±69N. These are about 16 and 5 times increase in strength, respectively. The increase in failure load from unplastered and 20mm thick plain plaster to 20mm thick rice straw reinforced plaster is 15±5N and 75±22N, respectively, to 256±82N. These are about 17 and 3½ times increase in strength, respectively. It may be observed that the 8mm thick plaster reinforced with either sisal fibres or rice straw has almost the same effect i.e. about 16 and 5 times increase with respect to that of unplastered and 8 mm thick plain plaster, respectively. One the other hand, 20 mm thick plaster reinforced with fibres has increased the failure load up to about 17-21 and 3½-4 times with respect to that of unplastered and 20 mm thick plain plaster, respectively. Conclusively, 20 mm thick sisal fibre reinforced plaster has given the highest increase i.e. about 21 and 4 times with respect to that of unplastered and 20 mm thick plain plaster, respectively.

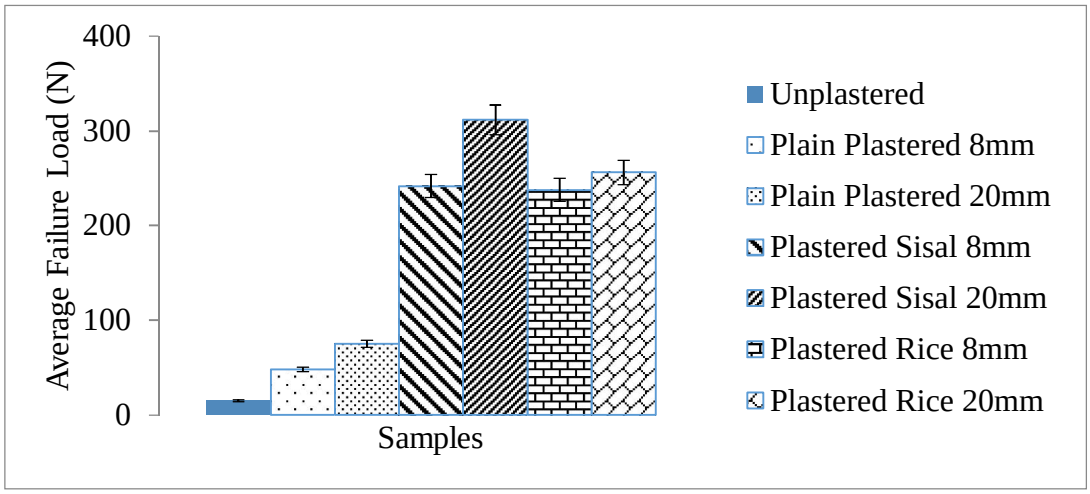

Figure 4.8: Comparison of averaged failure load of ISSB columns

Figure 4.9 shows typical crack propagation from first-crack load to maximum crack load for plain plastered, sisal fibre and rice-straw reinforced plastered samples. The first crack in the 8 mm thick plain, sisal fibre reinforced and rice-straw reinforced plastered columns is observed at 25N, 212N and 122N, and these are 52%, 88% and 51%, respectively, of their corresponding peak loads. Whereas, for 20 mm plastered columns it is observed at an average load of 68N, 212N, and 152N, and these are 91%, 68% and 59%, respectively, of their peak loads. This behaviour suggests that the fibres addition enables the columns to take more load after the observation of first crack. This is more prominent for 20 mm thick sisal fibre and rice straw reinforced plastered

columns. The increase in thickness of plaster from 8 mm to 20 mm also increased the inertia which is also a reason for getting higher load for 20 mm thick plaster columns. Even the appearance of first crack in fibre reinforced plastered columns is at much higher load as compared to the respective plain plastered columns. The cracks observed in the fibrous plastered columns are more, when compared to plain plastered columns. The cracks in the fibrous columns get wider and more visible at the ultimate load, whereas plain plastered columns get failure instead of further development of cracks. Fibres contributed to the bridging phenomenon and higher failure load due to cracks at closely spaced. In case of plain plastered columns, 23N and 7N additional load was taken by 8 mm and 20 mm thickness, respectively, from first crack to ultimate failure. For sisal fibre reinforced plastered columns, 30N and 100N additional load was taken by 8 mm and 20 mm thickness, respectively, from first crack to ultimate failure. For rice straw reinforced plastered columns, 116N and 104N additional load was taken by 8 mm and 20 mm thickness, respectively, from first crack to ultimate failure. Also, there is a notable enhanced lateral stiffness and strength (failure load) of fibre reinforced plastered masonry columns as compared to unplastered and plain plastered columns. Figure 4.10 shows the bridging effect of sisal fibres and rice straw in fibre reinforced plastered columns. It may be noted that the multiple cracks are connected by sisal fibres. Whereas, two separate pieces are being bridged by rice straw. This bridging mechanism has enabled fibre reinforced plastered to take additional load and to enhance the lateral stiffness. The bond of fibres with plaster and interfacial bond with block has increased the load carrying capacity.

4.3.2 Mechanical parameters of interlocked block columns

Table 4.3 details the mechanical parameters of all samples which include elastic stiffness, pre- crack and post crack energy absorbed and toughness index. Elastic stiffness is calculated as the slope of graph to the point when first crack occurs. Pre-crack (E_1) and post crack energy (E_2) absorbed are found by evaluating the under-slope areas up to first-crack load and from first crack to ultimate load, respectively. Their summation is taken as overall energy (E_o) absorbed and the ratio of overall energy to pre-crack energy is taken as toughness index. Table 4.4 details the increase or decrease of the mechanical parameters for all samples as compared to reference unplastered sample. It is evident from test data that the value for elastic stiffness of

8mm and 20 mm thick plain and fibrous plastered samples is increased from 4 to 26 times as compared to unplastered samples.

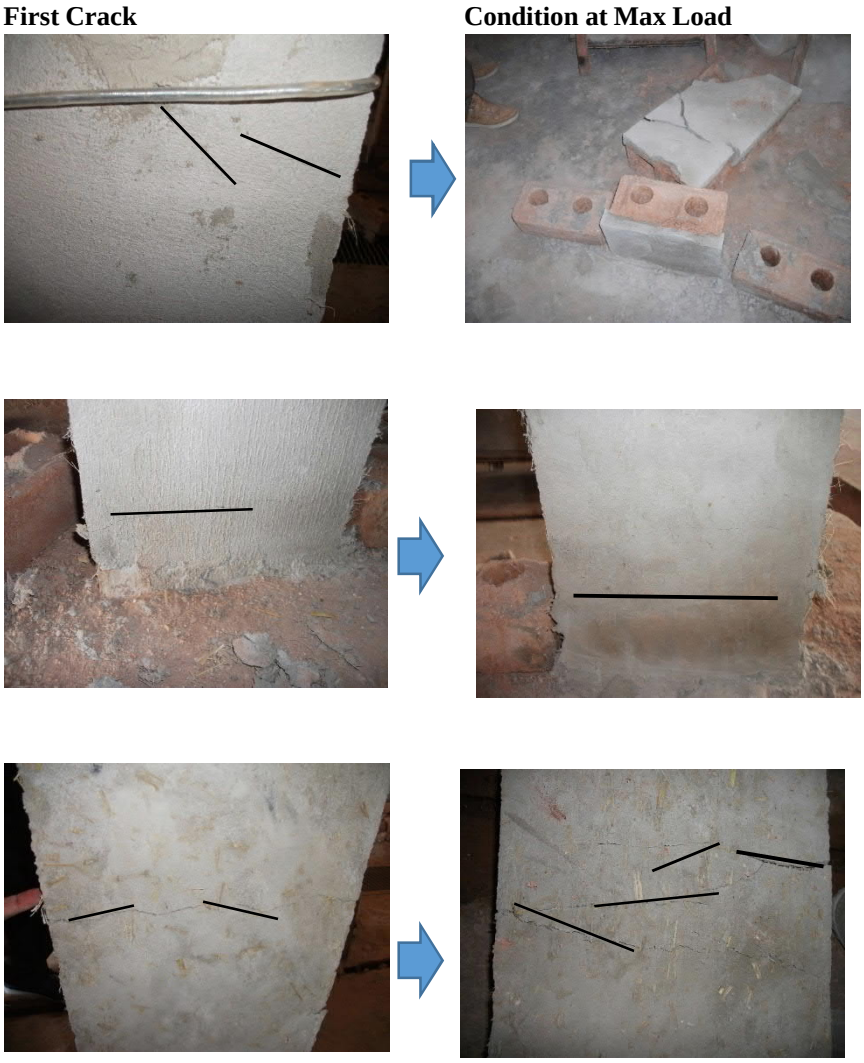

Figure 4.9: Crack propagation from first crack to maximum load to ISSB columns

Figure 4.10: Bridging effect to ISSB columns: a. sisal fibres and b. rice straws

It can be observed that there is a notable increase in elastic stiffness from un-plastered to plain-plastered columns. Whereas, further increase is observed by addition of fibres and this increase is more evident for 20 mm thick fibrous plastered. The pre-crack absorbed energy values shows improvement up to 20 times and most prominent for sisal fibrous plastered samples. It is observed that the post-crack absorbed energy shows enhancement up to 10 times and most notable for sisal fibrous plastered samples. Similarly, significant improvement is observed for total energy absorbed for sisal fibrous and rice-straw plastered samples. This shows that the fibres enhance the capabilities of column to absorb post crack energy. The value of 1.0 for toughness index of unplastered and 8 mm thick plain plastered column represents the brittle/sudden failure. The high value of 2.59 for sisal fibrous plastered column represents ductile behaviour due to phenomenon of fibre bridging. This indicates that fibrous plastered column has the ability of taking some load even after the first crack. The large standard deviation values show that there is a vast dissimilarity in the fibres properties for a specific type. The reason for this dissimilarity can be the variability in different fibres aspect ratio.

Table 4.3: Mechanical parameters for ISSB columns

Specimen	First crack load (N)	Max load (N)	Elastic Stiffness (N/mm)	E_1 (N-mm)	E_2 (N-mm)	E_o (N-mm)	Toughness Index (I)
A (U =DATUM	15±5	15±5	2±1	33±25	0	32±25	1±1
F (P, N,8)	25±38	48±19	10±19	94±3	116±0	134±67	1.42±0.00
E (P, N,20)	68±25	75±22	31±18	130±41	62±7	192±48	1.48±1.17
B (P, S,8)	212±69	242±77	36±17	704±125	1051±26	1756±106	2.49±0.85
G (P, S,20)	212±69	312±96	45±25	648±71	1029±80	1677±107	2.59±1.51
C (P, R,8)	122±54	238±69	52±23	336±90	366±70	702±149	2.09±1.66
D (P, R,20)	152±53	256±82	54±25	278±85	410±112	689±96	2.47±1.14

Table 4.4: Increase or decrease of mechanical parameters from those of unplastered datum for ISSB columns

Specimen	First crack load (N)	Max load (N)	Elastic Stiffness (N/mm)	E_1 (N-mm)	E_2 (N-mm)	E_o (N-mm)	Toughness Index (I)
F (P, N,8)	+66.7%	+220%	+400%	+184%	+116%	+318%	+42%
E (P, N,20)	+353%	+400%	+1400%	+294%	+62%	+500%	+48%
B (P, S,8)	+1313%	+1513%	+1700%	+2033%	+1051%	+5387%	+149%
G (P, S,20)	+1313%	+1980%	+2150%	+1863%	+1029%	+5140%	+159%
C (P, R,8)	+713%	+1486%	+2500%	+918%	+366%	+2093%	+109%
D (P, R,20)	+913%	+1600%	+2600%	+742%	+410%	+2053%	+147%

4.3.3 Load displacement curves for mortared block columns

The result of each sample is detailed in the form of a load-displacement plot as detailed in Figure 4.11(a-d). Figure 4.11(a) shows the load displacement plots for unplastered columns with non-fibrous mortar. The behaviour of three columns H1, H2 and H3 were similar showing a displacement of 12-14 mm for a load of 70-80 N. In all cases there was not any sign of cracking and failure was considered as brittle. Figure 4.11(b) shows the unplastered samples reinforced with sisal fibres within mortar. There was no variation in the behaviour of samples J1, J2 and J3. The samples showed similar stiffness as compared to non-fibrous samples. The maximum load increased to 90 N for sample J2 as compared to samples H1, H2 and H3 but the columns behaviour was still brittle/sudden without showing any signs of cracking. Adding of fibres within mortar enhanced the load carrying capacity as detailed in Figure 4.11(b). The loads were increased to 90 N, but the specimen failures were still brittle. The displacements in both cases were around 14-16 mm. Figure 4.11(c) shows the plain plastered samples with non-fibrous mortar. All samples K1, K2 and K3 showed similar behaviour with improved stiffness as compared to the samples H and J. These samples showed less displacement in the range of 4-6 mm but the maximum load was still in the same range as for samples H and J. Figure 4.11(d) shows the fibrous mortar and fibrous plastered samples. These samples showed similar initial stiffness as to all other samples but showed enhanced maximum load of 92 N as compared to all other samples. The failure

mode for the samples L1, L2 and L3 was ductile showing sign of cracks, due to the addition of fibres within plaster.

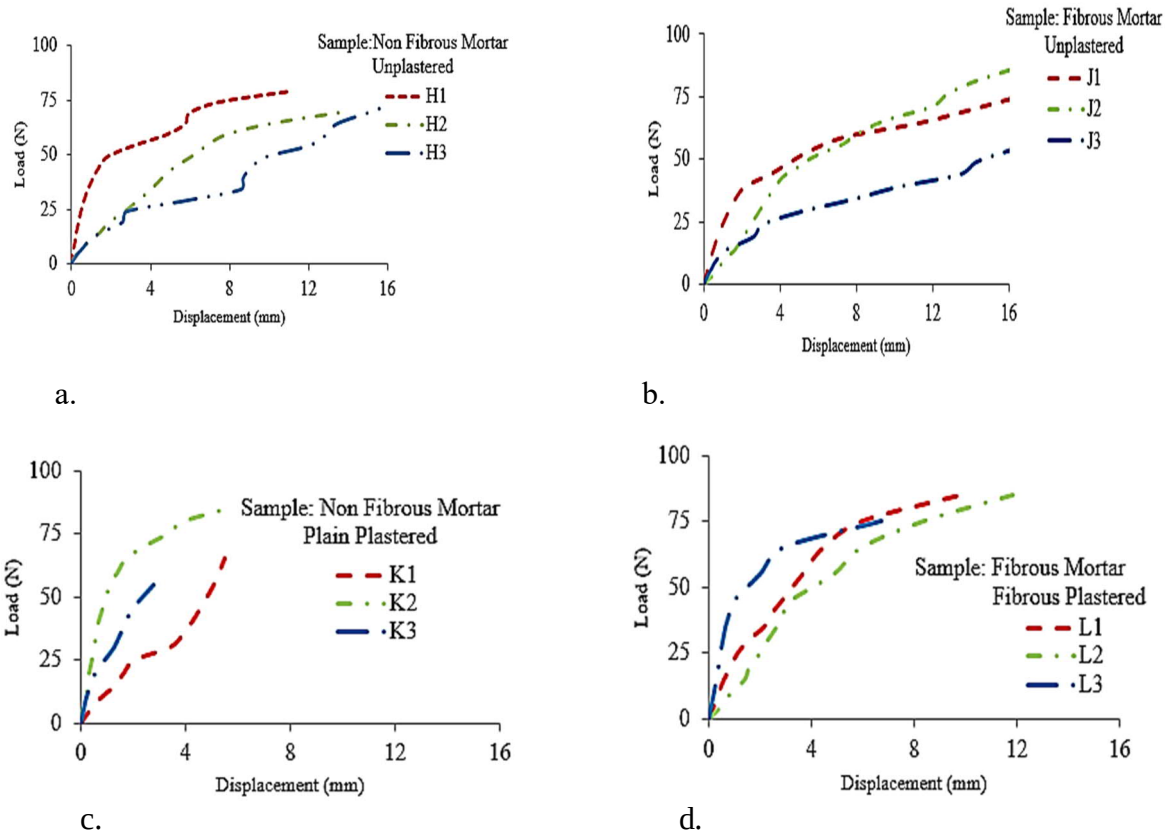

Figure 4.11: Load displacement curves; a. non-fibrous mortar unplastered SSB column, b. fibrous mortar unplastered SSB column, c. non-fibrous mortar plain plastered SSB column, d. fibrous mortar fibrous plastered SSB column

Figure 4.12 shows the average failure loads for the four variations of fibrous and non-fibrous mortar with fibrous and non-fibrous plastering. The failure load variation within unplastered non-fibrous mortar column and unplastered fibrous mortar column was not significant and was ranged from 73-79 N which indicated addition of fibres within mortar was not adding any benefit to the behaviour of columns. Whereas the samples with plain and fibrous plastered showed increase in failure load from 75 N to 92 N. In all cases samples with fibrous plastered and fibrous mortar indicated 22% increase in the failure load. Which showed benefit of adding fibres within plaster. It was also noted that increase in failure load for SSB column with fibrous plastered was not that significant as compared to ISSB column which showed 21 and 4 times increase from unplastered and plain samples to fibrous plastered samples.

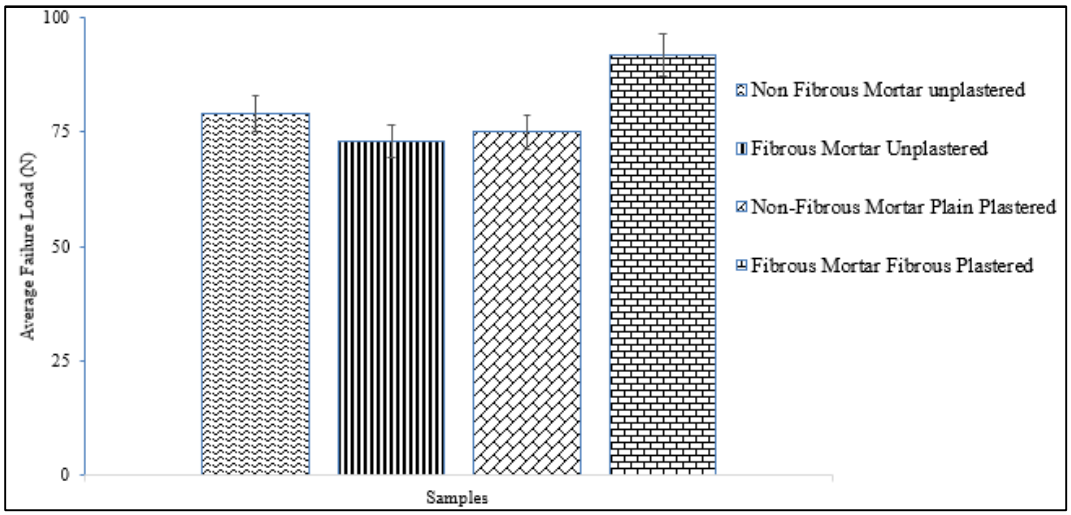

Figure 4.12: Average failure load of SSB columns

4.3.4 Contribution to Mechanical Properties for mortared block columns

Table 4.5 details the mechanical parameters of all samples which include first crack load, failure load, first crack stiffness, pre- crack and post crack energy absorbed and toughness. First crack stiffness is calculated as the slope of load-displacement curve up to first crack load. Pre-crack and post crack energy absorbed are found by evaluating the areas up to first crack load and from first crack to ultimate load, respectively. Their summation is taken as total energy absorbed and the ratio of total energy to pre-crack energy is taken as toughness. It is evident from test data that the value for first crack stiffness for non-fibrous to fibrous mortar column is increased from 15±4 to 17±0.7 which is about 12% increase from non-fibrous to fibrous mortar column. It can be observed that there is marginal increase in first crack stiffness is achieved by the addition of sisal fibres within mortar of column. The samples with plain and fibrous plastered showed minor improvement in first crack stiffness showing value of 18±5 which is about 20% increase from unplastered plain mortar samples. The pre-crack absorbed energy for fibrous mortared column is increased to 816±202 from 776±178 non-fibrous mortared column value which represent only 5% increase in pre-crack energy absorbed from non-fibrous to fibrous mortared column. It is observed that the post crack energy for non-fibrous and fibrous mortared columns gives a value of 0 showing brittle/sudden failure. The value of 1.0 for toughness of non-fibrous and fibrous mortared column represents the brittle/sudden failure. The samples with plain and fibrous plastered showed 72% increase in pre-crack energy

absorbed which showing the benefit of addition of fibres within plaster. These samples also showed post crack energy absorbed of 76±42 and 319±66, respectively, which is 3 times increase from plain to fibrous plastered samples. The plain and fibrous plastered sample showed value of toughness index 1.59±1.5 and 2.42±1, respectively, indicating 52% increase by the addition of fibres within plaster and also representing the ductile failure as compared to the unplastered samples.

Table 4.5: Mechanical parameters for SSB columns

Specimen	First crack load (N)	Max load (N)	Elastic Stiffness (N/mm)	E_1 (J)/10^3	E_2 (J)/10^3	E_o (J)/10^3	Toughness Index (I)
H – (M, U)	79±7	79±7	15±4	776±178	0	776±178	1±0.00
J – (MF, U)	73±15	73±15	17±0.7	816±202	0	816±202	1±0.00
K – (M, P,8, N)	57±16	75±8	18±5	129.5±77	76±42	206±118	1.59±1.5
L – (MF, P,8, S)	68±5	92±5	15±5	224±111	319±66	543±110	2.42±1

4.4 Practical aspects

Table 4.6 details the elastic stiffness of 1500 mm high continuous column. Interlocking column is considered to be built by 300 mm x 150 mm x100 mm ISSBs. The area of interlocking holes is also deducted from the calculation of stiffness. Whereas SSB column stiffness is considered as equivalent to continuous column. Stiffness is defined as slope of the load and displacement curve and is calculated using the following formulae: $k = \frac{P}{\delta}$.The formula for maximum deflection when load is applied at a distance "a" from the fixed end of cantilever length "l" $\delta \max = \frac{Pa^2(3l-a)}{6EI}$ therefore,$k = 6EI/a^2(3l - a)$.The elastic stiffness of the continuous interlock column is calculated as 1437 N/mm by assuming modulus of elasticity of 1x10^4 N/mm². The value of modulus of elasticity varies with the strength of the block used. Different values are found for masonry blocks in the literature ranging from 0.70 GPa – 13 GPa in different studies (Valluzzi 2014, De Felice 2016 and Kennedy 2013). As conventional masonry testing was not a part of the scope of this work therefore 1x10^4

N/mm² value of modulus of elasticity was chosen based on the literature for comparison purpose. The comparison of elastic stiffness of test samples with continuous column stiffness is explained in Table 4.7. For all samples, elastic stiffness is considered for comparison. Elastic stiffness for unplastered ISSB column gives a value of 2, whereas, for 8 mm thick plain, sisal fibre and rice straw reinforced ISSB columns 10, 36 and 52, respectively. The values of elastic stiffness for 20 mm thick plain, sisal fibre and rice straw reinforced ISSB columns are 31, 45 and 54, respectively. The comparison of experimental stiffness of the columns with the calculated stiffness of continuous column shows that unplastered ISSB column has only 0.1% equivalent stiffness. The columns with 8 mm thick plain, sisal fibres and rice straw plastered ISSB columns have 1%, 3% and 4% equivalent stiffness. Whereas, the columns with 20 mm thick plain, sisal fibres and rice straw plastered ISSB columns have 2%, 3% and 4% equivalent stiffness. Whereas, this shows that for all fibrous plastered ISSB column, stiffness is higher than unplastered and plain plastered. This indicates the significance of using fibrous columns, which is beneficial not only for post crack situation but also for enhancing the elastic stiffness.

Elastic stiffness of unplastered SSB column gives a value of 15, whereas for 8mm thick plain and sisal fibrous plastered SSB columns 18 and 15, respectively. The comparison of experimental stiffness of the SSB columns with the calculated stiffness of continuous column shows 1% equivalent stiffness for all columns. This has indicated that no increase in stiffness is achieved by addition of plain or fibrous plaster within SSB columns.

Table 4.6 Elastic stiffness of column

Parameter	a (mm)	b (mm)	d (mm)	I ($bd^3/12$) (mm^4)	Length (mm)	E (MPa)	k (N/mm)
Continuous Column	1000	300	150	8.40E+07	1500	1.00E+4	1446
Holes	1000	50	50	5.21E+05	1500	1.00E+4	9
Column with Holes	1000	-	-	8.39E+07	1500	1.00E+4	1437

Table 4.7: Comparison of elastic stiffness with continuous column

Column Type	Stiffness for 8mm (N/mm)	Stiffness for 20mm (N/mm)	Stiffness normalized to that of a continuous column (%age)	
			8mm plaster	20mm plaster
Unplastered ISSB	2	2	0.1%	0.1%
Plain Plastered ISSB	10	31	1%	2%
Plastered with Sisal ISSB	36	45	3%	3%
Plastered with Rice ISSB	52	54	4%	4%
Unplastered SSB	15	-	1%	-
Plain Plastered SSB	18	-	1%	-
Sisal plastered SSB	15	-	1%	-

4.5 Summary

Experimental work was carried out to evaluate the improvement in mechanical parameters of masonry columns by the addition of natural fibres in the plaster or mortar or both. Sisal fibres and rice straw were used. Five samples were tested under out-of-plane lateral loading for each plastering variation for ISSB in NHBRA Dar es Salam and three samples were tested under out of plane lateral loading for fibrous and non-fibrous variation for SSB columns in Warwick University UK. The conclusions are as follows:

1. As expected, unplastered ISSB columns had least stiffness. Plastering increased lateral elastic stiffness by up to 15 times. The elastic stiffness of fibrous-plaster ISSB columns, as compared to plain plastered ones, improved by 400% and by 74% when increasing plaster thickness from 8 mm to 20 mm.
2. The lateral failure load for unplastered to 20 mm thick sisal fibrous plastered ISSB columns was increased by 20 times, whereas three times increase was observed from 20 mm thick plain to 20 mm thick sisal fibrous plastered columns.
3. The lateral failure load for unplastered to 8 mm thick sisal fibrous plastered column was increased by 15 times, whereas four times increase was observed from 8 mm thick plain to 8 mm thick sisal fibrous plastered columns.

4. The increase in thickness of plaster from 8 mm to 20 mm enhanced failure load as 56%, 28% and 7%, respectively, for plain, sisal fibrous and rice straw reinforced plastered ISSB columns.
5. The total absorbed energy from unplastered to plain plastered was increased to five times and there was further seven times increase from plain to fibrous plastered.
6. The behaviour of sisal-fibrous ISSB columns was more ductile with onset of cracking well before collapse. Its toughness index was increased up to 159% and 75% than unplastered and 20 mm thick plain plastered ISSB columns, respectively.
7. Addition of sisal fibres within mortar of SSB column showed similar behaviour as compared to non-fibrous mortar SSB columns, indicating no benefit of addition of fibres within mortar.

It becomes evident that the addition of fibres like sisal fibres and rice straw within plaster contributes to the lateral stiffness of ISSB columns, which results in significantly enhanced strength and ductility. It is also clarified that the addition of fibres within mortar of masonry columns does not add any benefit in the resistance of lateral load and stiffness, which is also in line with the outcome of the chapter 2 literature review. Therefore, the use of SSB and addition of fibres within mortar will not be considered further in this doctoral study. The outcome of this chapter has identified that the lateral resistance of interlocked walls could be enhanced by the addition of plain and fibrous plaster. It was also found that increasing the thickness of plaster from 8 mm to 20 mm for ISSB columns did not enhance the lateral resistance significantly.

Chapter 5. Finite element analysis of single ISSB column under lateral load

Related Conference Papers:

Qamar, F., Qin, S. and Ali, M. (2018). Estimating seismic resistance of fibrous plastering effect on mortarless interlocked masonry walling with finite element modelling. *Australian Earthquake Engineering Society 2018 Conference*, Nov 16-18, Perth, W.A.

5.1 Background

Numerical evaluation of experimental work related to ISSB columns explained in chapter 4 are presented in this chapter. The objective of this numerical work is to develop Non-Linear Finite Element (NLFE) models to explore the likely failure mechanism (e.g. bond failure) which is compatible with the experimental findings and to do parametric studies more cheaply than constructing many walls. To achieve this milestone, the NLFE analysis and the validation of the proposed finite element (FE) models are required. The methodology of modelling unplastered single ISSB columns, and fibrous and non-fibrous plastered ISSB columns, is discussed in section 5.2. The material properties for block, plaster and interface and solution methods are explained. The material model used is also described. The type and application of lateral loading and constraint conditions are defined. The validation of the proposed FE models is presented in section 5.3. The results of experimental work are used to validate the NLFE models. Lateral failure load, load-displacement curves and crack patterns are compared with the experimental results. Section 5.4 explains the sensitivity analysis of different parameters like mesh size for block and tensile strength of block and plaster on the outcome of FE results. The effect of mesh size is considered by exploring coarse, medium and fine sizes. The effect of variation in tensile strength of block and plaster are explored based on the findings from the previous studies. Parametric studies involving variation in block and plaster compressive strength and plaster thickness were undertaken. Cost analysis was also carried out, based on finite-element sensitivity analysis, to find the equivalent thickness of fibrous plastered column having similar or better lateral resistance to the unplastered column. Section 5.5 presents the key findings from the numerical simulation and gives recommendation for further work which is explained in Chapter 6.

5.2 Modelling methodology

5.2.1 Geometry

The geometry of the experimental tests was reproduced by modelling blocks and interlocked mechanism with interface elements between them as shown in Figure 5.1. Seven models were produced as detailed in the Table 5.1.

Table 5.1: Labelling of TNO DIANA Models

Combinations	Model Symbol
Block only unplastered	M1 - (U)
8 mm thick Plain-plastered column	M2 - (P,8,N)
20 mm thick Plain-plastered column	M3- (P,20,N)
8 mm thick rice-straw plastered column	M4 - (P,R,8)
20 mm thick rice-straw plastered column	M5 – (P,R,20)
8 mm thick sisal-plastered column	M6 - (P,S,8)
20 mm thick sisal-plastered column	M7 - (P,S,20)

The block size was 300 mm x 150 mm x 100 mm with a gap of 10 mm representing the interlock between the blocks. 15 blocks were modelled representing a 1590 mm high column. The selection of element types and of material cracking and plasticity models has already been successfully employed in other studies (Lignola, 2009 & Basili,2016) and are applied in this study. A regular and dense discretisation was used based on the CQ16M eight-node quadrilateral isoparametric plane stress elements which was successfully used by other studies (Lignola, 2009, Lignola 2012). Table 5.2 details the no of elements used for different models. In TNO DIANA these elements are represented by eight node brick elements with three translational degrees of freedom at each node. Mesh arrangement with an average dimension of 30 mm, 25 mm and 37.5 mm in x, y and z direction, respectively, have been used for meshing the blocks. For the plaster 30 mm, 25 mm and 4 mm in x, y and z direction respectively, as per previous studies (Lignola, 2009, Lignola 2012 & Basili,2016). Figure 5.2 shows the adopted mesh size of the proposed FE models. Different meshing sizes were examined as explained in the section 5.4.1 and the selected mesh size gave a good agreement between the output of finite-element models and experimental results for unplastered column.

5.2.2 Material and interface properties

a. Block properties

Compressive strength f_c and Young's modulus E were derived from uniaxial compression tests of block samples as explained in Chapter 3. The tensile strength of a masonry unit is difficult to obtain from any direct relationship to its compressive strength. This is because of variation in the shapes, material and method of manufacturing of masonry blocks.

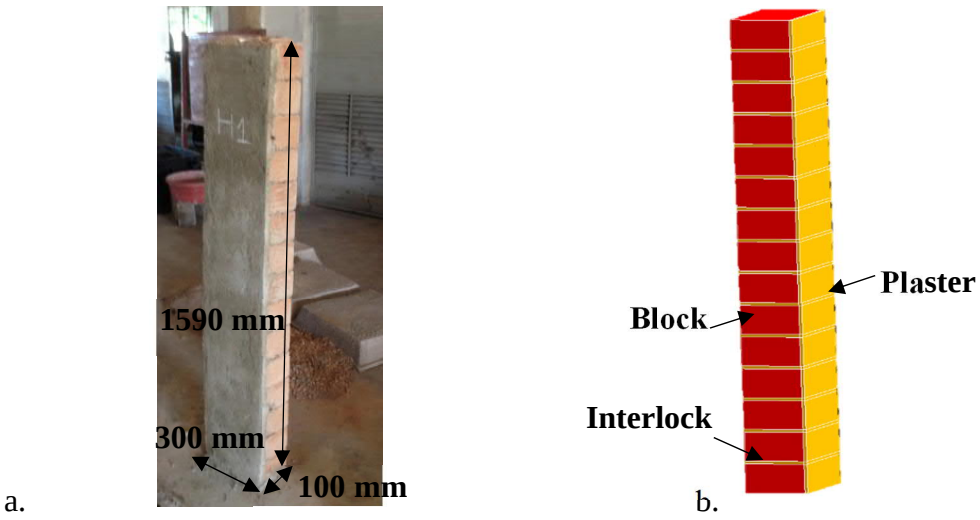

Figure 5.1: Geometry of interlocked masonry column a. Experimental view b. TNO DIANA view

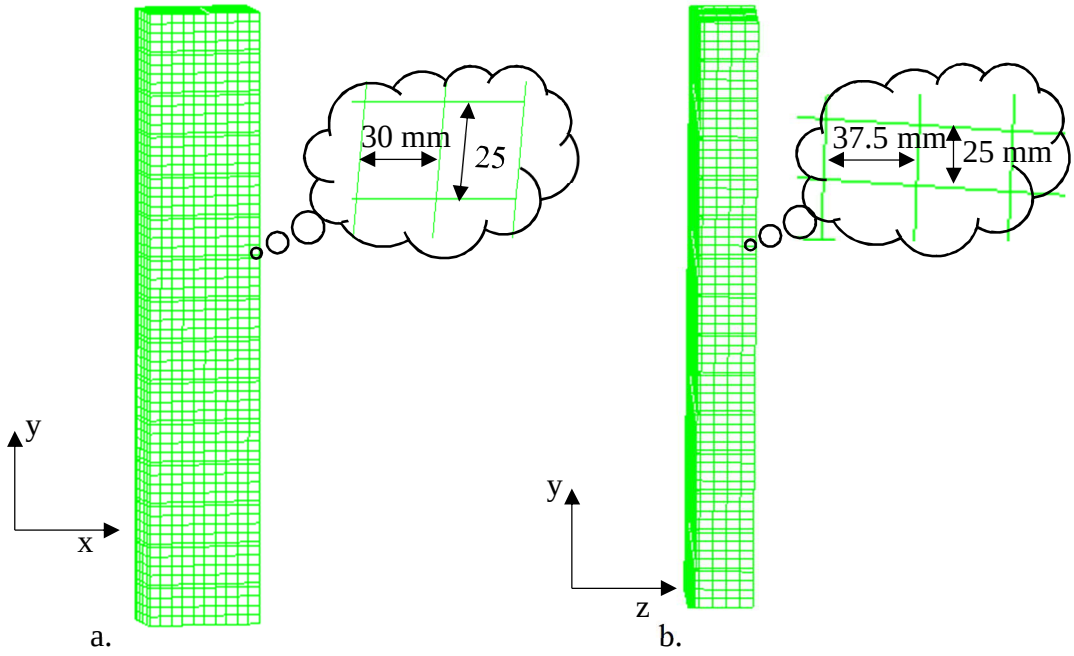

Figure 5.2: TNO DIANA analysis, adopted mesh a. X-View b. Z-View

An extensive testing was carried out by Schubert (1988a) for the tensile strength of clay units and proposed a ratio between the tensile and compressive strength which ranges from 0.30 to 0.10. A 0.10 ratio between tensile and compressive strength was used in this study to best match the experimental findings.

Table 5.2: Number of elements for the TNO DIANA models based on mesh sizes

Model	Block elements No.	Block Interface elements No.	Plaster Interface elements No.	Plaster elements No.
M1 - (U)	2400	520	-	-
M2 - (P,8,N)	2400	520	640	1480
M3- (P,20,N)	2400	520	640	3700
M4 - (P,R,8)	2400	520	640	1480
M5 – (P,R,20)	2400	520	640	3700
M6 - (P,S,8)	2400	520	640	1480
M7 - (P,S,20)	2400	520	640	3700

For block material properties, constitutive models proposed by another researcher (Lignola 2012) were used which were based on a smeared-crack approach, assuming exponential strain softening in tension and plasticity in compression. Parabolic curve formulation both based on tensile and compressive fracture energy as shown in the Figure 5.3.

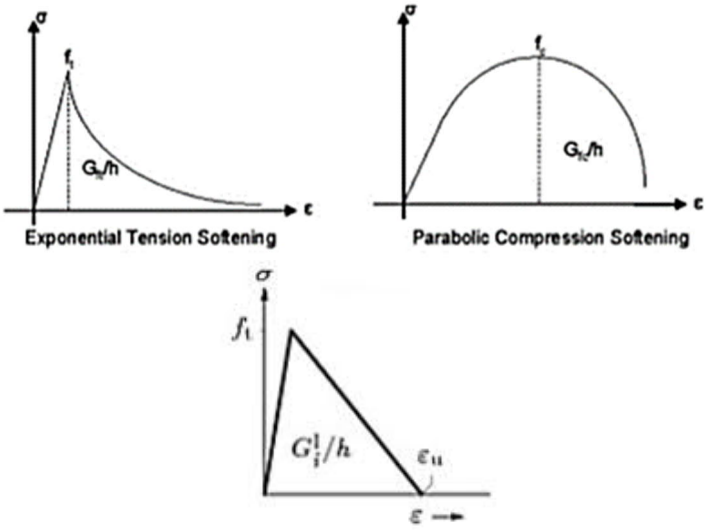

Figure 5.3: Material model used in TNO DIANA (Lignola, 2012)

The validation of models with the experiment values, as demonstrated in Section 5.3, was obtained by using a Poisson's ratio of 0.15. The same Poisson's ratio was also used by several researchers, such as (Prota et al.2006) & Lignola 2009). The fracture energy G_f was related to compressive strength by Equation 5.1 as was used and proposed by different researchers (Phillips and Binsheng (1993). Dirar et al. (2012)).

$$G_f = (43.2 + 1.13 f_{cu}) * 10^3 \qquad \text{Equation 5.1}$$

G_f = Fracture Energy (N/mm)

f_{cu} = Compressive strength of blocks (MPa)

Table 5.3: Block properties used in the models

Material	Modulus of Elasticity E (MPa)	Poison's Ratio n	Compressive strength f_c (MPa)	*Tensile Strength f_t (MPa)	Fracture energy G_f (N/mm)
Block	201	0.15	0.83	0.080	0.0441

*taken as $0.1*f_c$

b. Block Interface Properties

The interlocked mechanism of ISSB was modelled using 8-node bond slip interface elements between the blocks. Both friction-based and perfect bond models were studied and it was found that a friction-based model gave a better match with experimental findings. A friction-based model is based on the resistance being proportional to the self-weight of the block. In the friction-based model as shown in the Figure 5.4, a yield shear-stress is calculated at each course of the blocks in the wall depending on their weight. A value for the coefficient of friction was obtained by using hit and trial method. Maximum slip F2 assumed as 150 mm based on the width of the block. The following Equation 5.2 is used to calculate the interface properties at each layer of the blocks. The values of block interlocked interface properties are shown in the Table 5.4.

$$peak\ bond\ stress = \mu * n * W_b / a_b \qquad \text{Equation 5.2}$$

Where;

μ = coefficient of friction

n = number of blocks

w_b = Weight of block

a_b = Area of block

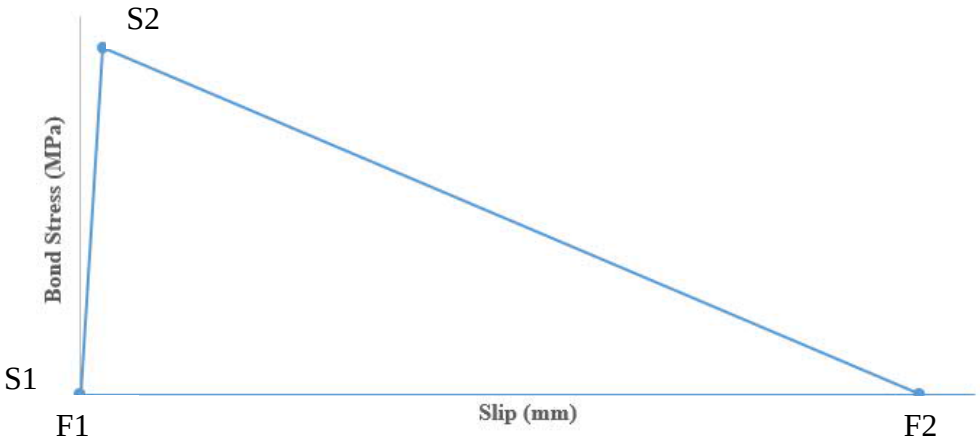

Figure 5.4: Friction based bond slip model for the interface between block and plaster

Table 5.4: Block interlocked interface properties used in the models

Model	Df_{11} (N/mm^3)	Df_{22} (N/mm^3)	μ	S_1 (MPa)	F_1 (mm)	S_2 (MPa)	F_2 (mm)
M1 - (U)	0.02	0.20	0.1	0	0	3.488E-07	150
M2 - (P,8,N)	0.02	0.20	0.1	0	0	0.0001744	150
M3- (P,20,N)	0.01	0.1	0.1	0	0	0.0001744	150
M4 - (P,R,8)	0.0021	0.021	0.1	0	0	0.0001744	150
M5 – (P,R,20)	0.0015	0.015	0.1	0	0	0.0001744	150
M6 - (P,S,8)	0.0021	0.021	0.1	0	0	0.0001744	150
M7 - (P,S,20)	0.00035	0.0035	0.1	0	0	0.0001744	150

Note: where Df_{11}= normal linear stiffness modulus; Df_{22} = shear linear stiffness modulus; μ = coefficient of friction; S_1 = Peak bond stress; F_1= slip corresponding to peak bond stress; S2 = yield stress; F2=Maximum slip.

c. Plaster Properties

Compressive strength f_c and Young's modulus E were derived from uniaxial compression tests of plaster cube samples as explained in chapter 3. The same

constitutive model was used for the plaster as explained above in the block properties section. The values of the material properties used in this study are detailed in the Table 5.5.

Table 5.5: Material properties for plaster used in TNO DIANA

Material	Modulus of Elasticity E (MPa)	Poison's Ratio n	Compressive strength f_c (MPa)	Tensile Strength f_t (MPa)	Fracture energy G_f (N/mm)
Plain Plaster	2990	0.15	19.33	1.933	0.065
Rice Straw Plaster	2483	0.15	8.67	0.867	0.053
Sisal Plaster	7175	0.15	19.88	1.988	0.657

*taken as 0.1*f_c

d. Properties of the interface between block and plaster

Plaster to block interface was modelled with 8-node bond-slip interface elements. In this model it was considered that bond failure occurs within a thin layer of block adjacent to the interface of plaster-to-block, because the plaster is usually stronger than the block. The bond-slip models, which were developed by Sato and Vecchio (2003) were used in this study and values are detailed in the Table 5.6. Hence, the bond-slip model displays the overall behaviour of the block-to-plaster interface, rather than the plaster or block material. Proposed bond-slip model by Sato and Vecchio (2003):

$$\tau_{peak} = (54f'_c)^{0.19}$$

$$S_{peak} = 0.057\sqrt{G_{fi}}$$

$$S_u = \frac{2G_{fi}}{\tau_{peak}}$$

$$G_{fi} = (\frac{\tau_{peak}}{6.6})^2$$

where:

τ_{peak} The peak bond stress (N/mm^2).

f'_c Compressive strength of plaster (N/mm^2).

S_{peak} Slip corresponding to the peak bond stress (mm).

S_u Ultimate slip (mm)

G_{fi} Interfacial fracture energy (N/mm)

The above equations based on bond-slip model consider bond stress-slip linear relation up to the peak bond stress. The separation of block and plaster interface starts if the slip exceed the limiting value, the slip value related to the peak bond stress. This process is based on linear softening behaviour as shown in Figure 5.3. In this research, this model was adopted as it gave a better agreement between the FE predictions and the experimental result, as validated in Section 5.5.

Table 5.6: Plaster and block interface properties used in the models

Model	Df_{11} (N/mm^3)	Df_{22} (N/mm^3)	τ_{peak} (N/mm^2)	S_{peak} (mm)	S_u (mm)	G_{fi} (N/mm)
M1 - (U)	-	-	-	-	-	-
M2 - (P,8,N)	157.8	1577.9	3.590	0.164	0.031	0.295
M3- (P,20,N)	157.8	1577.9	3.590	0.164	0.031	0.295
M4 - (P,R,8)	157.8	1577.9	3.082	0.141	2.66E-02	0.218
M5 – (P,R,20)	157.8	1577.9	3.082	0.141	2.66E-02	0.218
M6 - (P,S,8)	157.8	1577.9	3.609	0.165	0.031	0.299
M7 - (P,S,20)	157.8	1577.9	3.609	0.165	0.031	0.299

5.2.3 Loading applied

Out-of-plane loading was applied in this analysis corresponding to unit displacement applied at the nodes corresponding to 1000mm height of masonry column as per experimental work. A displacement loading method was used for the modelling as this can predict the post-failure behaviour of the columns (in a way not possible in the laboratory). This method was also successfully used by the other researchers (Lignola 2012 & Bejarano-Urrego 2018).

5.2.4 Constraint condition

The bases of the columns were considered fixed and represented by fixed constraint in the model. For experimental work, plain concrete was used at the base of the columns as shown in the Figure 5.5.

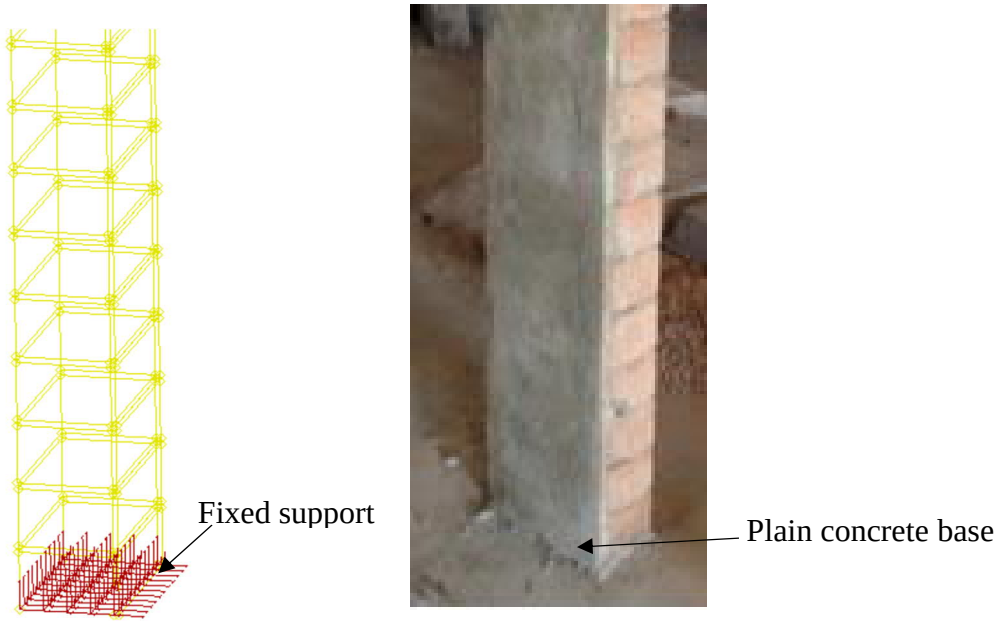

Figure 5.5: Constraint condition for the columns in the model and experimental work

5.2.5 Solution method

To attain convergence in the analysis of failure load, an incremental iterative process was adopted by increasing displacement by 0.1 mm for 20 steps. The Secant iteration method was used, to achieve balance at each step. Similar procedures were adopted by Qapo et al. (2014). Based on Hee and Jefferson (2008) and Dirar et al. (2013), a displacement norm value of 0.05,0.2 and 0.9 for block, plain plaster and fibrous plaster models respectively was adopted to specify convergence. A maximum of 1000,000 iterations was allowed at each step before termination of the analysis in case of non-convergence. This approach proved successful, as convergence was achieved at every load step for the block only, plain-plastered and fibrous- plastered FE models. The output reports showed that convergence was met at each load analysis step. The values used are presented in the Table 5.7 below.

Table 5.7: Mesh sizes and Solver for the TNO DIANA Models

Model	Size (step) mm	Tolerance mm	Non-Linear Analysis method	Max No of Iterations	Convergence critical mm
M1 - (U)	0.1(20)	1.00E-6	Secant	1000000	0.05
M2 - (P,8,N)	0.1(20)	1.00E-6	Secant	1000000	0.2
M3- (P,20,N)	0.1(20)	1.00E-6	Secant	1000000	0.2
M4 - (P,R,8)	0.1(20)	1.00E-6	Secant	1000000	0.9
M5 – (P,R,20)	0.1(20)	1.00E-6	Secant	1000000	0.9
M6 - (P,S,8)	0.1(20)	1.00E-6	Secant	1000000	0.9
M7 - (P,S,20)	0.1(20)	1.00E-6	Secant	1000000	0.9

5.3 Validation/Experimental verification

In this section, the results of comparison between the finite element model output and the experimental work are presented. The comparative study was undertaken to determine the validity of the finite element models in predicting the nonlinear behaviour of the unplastered, plain plastered and fibrous-plastered columns. Failure load, maximum displacement, stiffness and cracking patterns are compared in Sections 5.3.1 to 5.3.3, respectively. The results of the comparative study between FE models and experimental works are presented with the help of graphs and tables.

5.3.1 Maximum load

The experimental results of failure load F_{exp} and the FE predicted values F_{Diana} for all specimens are presented in the Table 5.8. The FE predicted value is the maximum force which can be calculated as sum of the reactions at the point of application of loading. The FE prediction values were in good agreement with the experimental results for all cases within 13% difference. The proposed FE models for all cases underestimates failure load with a maximum mean experimental/FE ratio of 1.07 for plain plastered model. The rotating crack model assumes that cracking always occurs within principal planes, and it has not considered internal shear contribution across the crack plane. Therefore, it was expected to obtain a lower value of failure load from FE models than the experimental value. The only exception was found for the 8-mm rice straw plastered model where the experimental/FE ratio was 0.98. The reason for this

is due to assumed values of block interface properties due to lack of experimental data. Figure 5.6. shows the comparison of the results for both experimental and FE analysis.

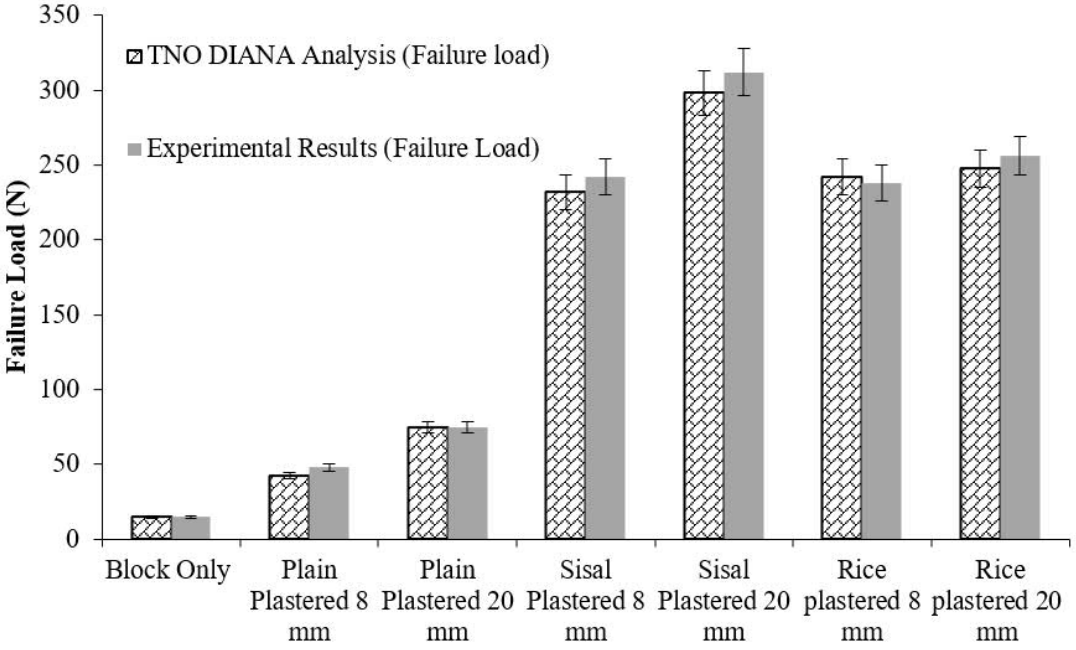

Figure 5.6: Failure load comparison between TNO DIANA model and experimental results

Table 5.8: Comparison of experimental and numerical results

Model	Experimental lateral peak/failure load (F_{exp}) (N)	TNO DIANA lateral Peak/failure load (F_{DIANA}) (N)	Ratio F_{exp}/F_{DIANA}	Average
M1 - (U)	15	14.8	1.01	1.01
M2 - (P,8,N)	48	42.2	1.13	1.07
M3- (P,20,N)	75	74.57	1.00	
M4 - (P,R,8)	238	242.5	0.98	1.00
M5 – (P,R,20)	256	247.9	1.03	
M6 - (P,S,8)	242	232.2	1.04	1.04
M7 - (P,S,20)	312	289.3	1.04	

5.3.2 Load -displacement curves

Figure 5.7(a-g) shows load displacement curves for the results of experimental and FE analysis. Results of seven different FE models listed in Table 5.1 were compared with

the corresponding experimental results. For unplastered columns, the FE results showed good agreement with the experimental load-displacement graph, showing similar peak load and stiffness. The difference between peak load values for FE and experimental results is within 13%. The load-displacement curves can be divided into two stages i.e. loading up to first-crack and further loading up to failure. Comparing the first stage, it was observed that stiffness of the FE model was higher than the experimental work in general for fibrous plaster columns. The more difference in the stiffness behaviour is due to smeared crack modelling technique adopted for FE models. Minor cracks are normally formed during the setting time of plaster and known as shrinkage cracks. An increase in the applied lateral load spreads these minor cracks and steadily forms a bigger more visible crack. However, the FE model was based on using the smeared crack method, which means that cracks due to shrinkage were not captured. Therefore, the stiffness of the FE models was higher than the experimental tests in the first stage of crack formation for fibrous plaster columns. Comparing the displacement of the experimental results and FE predicted values, it can be seen that FE models accurately projected the displacement in general for all cases. Post peak-load behaviour was not compared with FE models as there was not enough data available from the experimental results.

5.3.3 Crack pattern

FE applications has the capacity to show the development of cracks which is considered as one of the merits of using such applications. Figure 5.8 shows the comparison between experimental and FE models crack patterns at failure for unplastered, plain plastered and fibrous plastered samples. The FE models crack pattern is presented by the crack contour plots. It can be seen that the FE model adequately projected the failure cracks of unplastered sample, which showed the stress concentration with red contours at the base and the opening of interlock at tension face, as shown in the experimental results. Similarly, for plain and fibrous samples, FE predicted the cracks within block and plaster interface showing resemblance to the experimental results. The difference between the plain plastered and fibrous-plastered samples can be observed with showing fewer cracks in the plain plastered FE model as shown in the Figure 5.8b. Whereas, the fibrous-plastered sample showed more cracks as is visible in the Figure 5.8c. This ties in well with the outcome of the

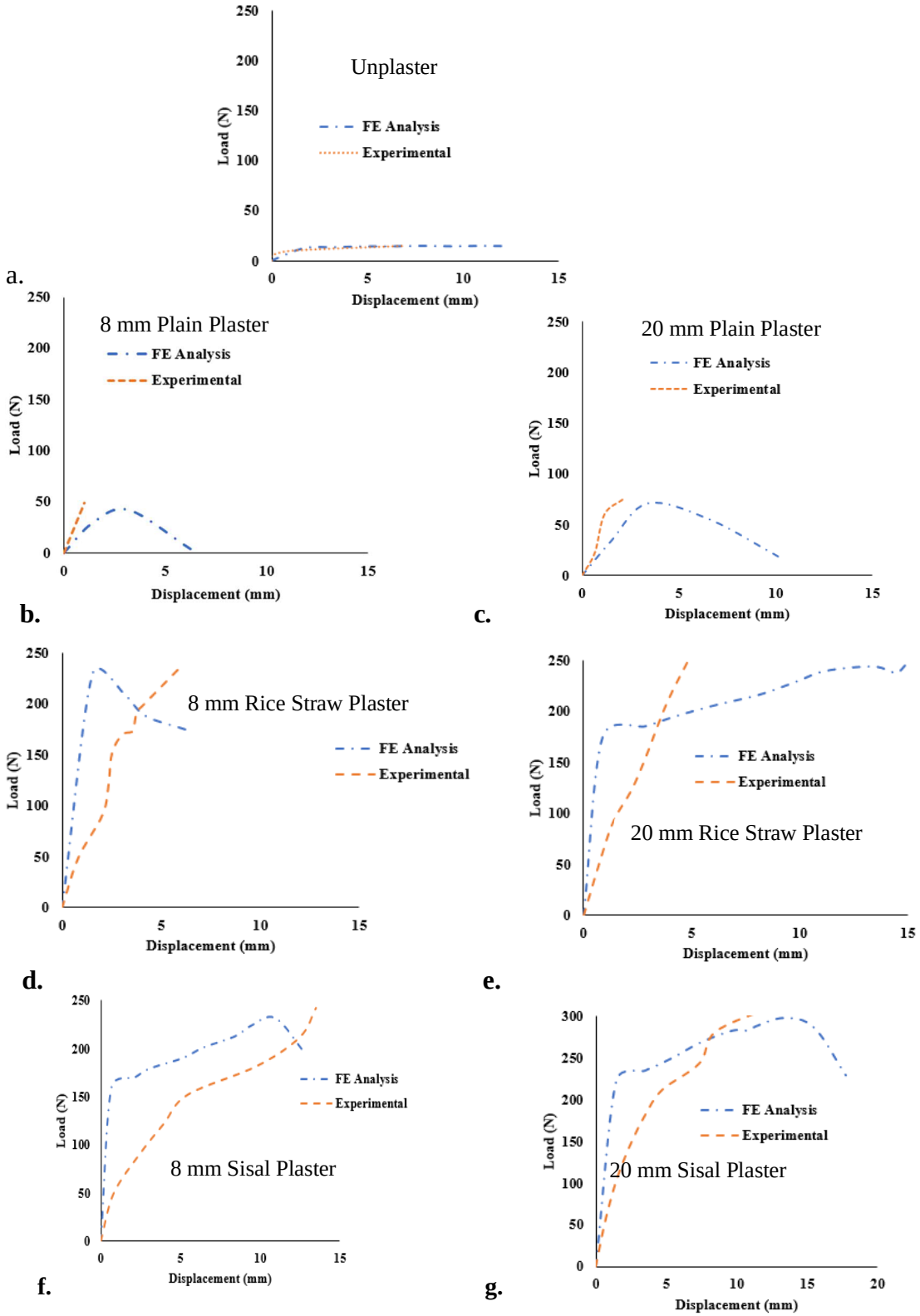

Figure 5.7: Comparison of Load-displacement graphs between TNO DIANA and experimental results a. block only, b. plain plastered 8 mm, c. plain plastered 20 mm, d. rice straw reinforced plaster 8 mm, e. rice straw reinforced 20 mm, f, sisal plastered 8 mm and g. sisal plastered 20 mm

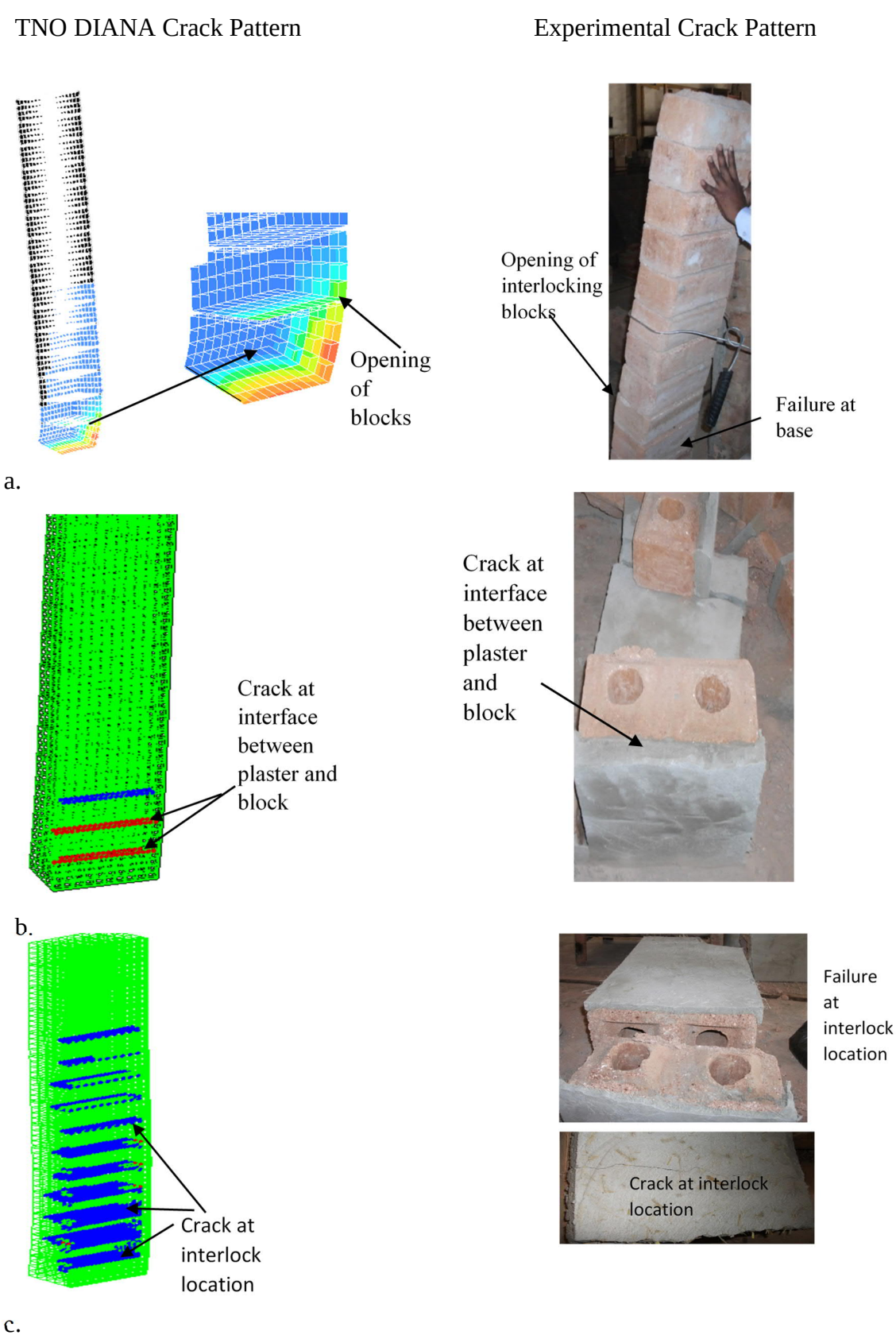

Figure 5.8: Crack pattern comparison experimental and TNO DIANA a. unplastered; b. plain plastered; c. fibrous plastered

experimental work as fibrous plastered samples showed more ductility due to the presence of the fibres. This resulted in the ductile failure of the fibrous plastered samples as compared to the brittle failure for all other samples It can also be observed that failure of plain and fibrous plastered samples occurred due to cracking in the interface between the block and plaster rather than within the block. Similar behaviour was noted in FE models where cracks were initiated within the interface between block and plaster.

5.4 Sensitivity analysis and parametric study

In this section are performed sensitivity analyses for the parameters of the FE model: these include the block mesh size and the block and plaster tensile strengths. Both of these were found critical in predicting the results from FE as compared to experimental value. Mesh size is a modelling variable which influences the FE results, therefore a sensitivity analysis was carried out to find the most suitable mesh size as explained in the section 5.4.1. Tensile strength comes from material testing. However the experimental work carried out in this study only yielded values for compressive strength. whereas the FE model's failure load was most influenced by tensile strength. Therefore, a relationship between compressive and tensile strengths was assumed based on the literature and sensitivity analysis was carried out to find the best suited value of this parameter as explained in the section 5.4.2.

5.4.1 Effect of mesh size

To evaluate the effect of mesh size on the results of FE model, three different sizes of mesh were considered for unplastered FE model M1 - (U) and divided into two categorises with reference to proposed mesh (medium mesh 30 mm, 25 mm and 37.5 mm in x, y and z direction respectively) in section 5.2. One alternative is fine mesh, which employs elements half those of medium mesh with a size of 15 mm, 12.5 mm and 18.75 mm in x, y and z direction respectively. The second alternative is coarse mesh, with elements twice the size of the medium mesh, with a size of 60 mm, 50 mm and 75 mm in x, y and z, respectively. From the outcome of the sensitivity analysis, it was observed that the medium mesh best suits the experimental results for unplastered column whereas fine and coarse mesh overestimate the peak load and grossly overestimate the stiffness of the model. This is due to the fracture energy G_f as the

same values of fracture energy G_f are used for three types of mesh which is required to be adjusted with the size of mesh.

5.4.2 Tensile Strength effect

An extensive testing was carried out by Schubert (1988a) for the tensile strength of clay units and proposed a ratio between the tensile and compressive strength which ranges from 0.30 to 0.10. Similarly, for the plaster a ratio of 0.10 was considered in many studies (Lignola 2012 & Stratford 2004). Trial values of this ratio were tested to identify the best value of tensile strength of block and plaster. It was found that model with tensile strength equal to 10% compressive strength gave the best results comparable to experimental results.

5.4.3 Parametric study

The following sections details the parametric study of varying three main parameters namely the compressive strength of block, compressive strength of plaster and thickness of plaster. In order to investigate the effect of these parameters, only one parameter was varied at a time and the values of other parameters remained unchanged in the FE models. A similar method was adopted by other researchers like Qapo et. al (2014) and Qin (2016).

a. Strength of block

Three values of block compressive strength were considered for parametric study. The value of 0.83 MPa was considered from the experimental work of this study. The other two values of 2.5 MPa and 5.42 MPa were found in different research studies for stabilised soil blocks (Anand et al. 2000 and Fundi et al. 2018). The unplastered model (M1 - U) was used to identify the effect of block compressive strength and the outcome is shown in the Figure 5.9. It can be observed that load carrying capacity of the ISSB column was increased with increase in compressive strength. The failure load was increased to 83 N from 15 N with increase in compressive strength from 0.83 to 5.42 MPa.

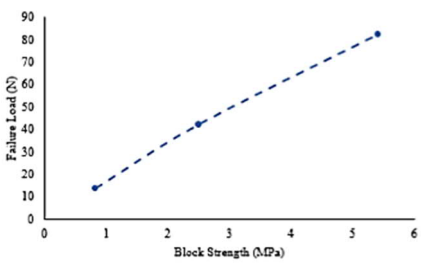

Figure 5.9: Effect of block strength on unplastered failure load (FE modelling)

b.Strength of plaster

Three values of compressive strength of plaster were considered for parametric study. The values of compressive strength of each cube sample (plain, rice straw and sisal fibrous plaster) evaluated from experimental work was chosen as the initial values for each model. The other two values were chosen from the literature review where most commonly the values of 29 MPa and 41MPa were found (Zych et al. 2012 & Lertwattanaruk et al. 2015). A total of 18 FE models were produced by keeping all other parameters constant except the compressive strength of plaster. The outcome of the parametric study is shown in the Figure 5.10. It can be observed that in almost all cases there is no change in the failure load with the increase in compressive strength of plaster. The reason for this as it was identified earlier in section 5.3.3, namely that the interface between the plaster and block was the governing failure mechanism. Therefore, increase in compressive strength of plaster did not result in increase in failure load.

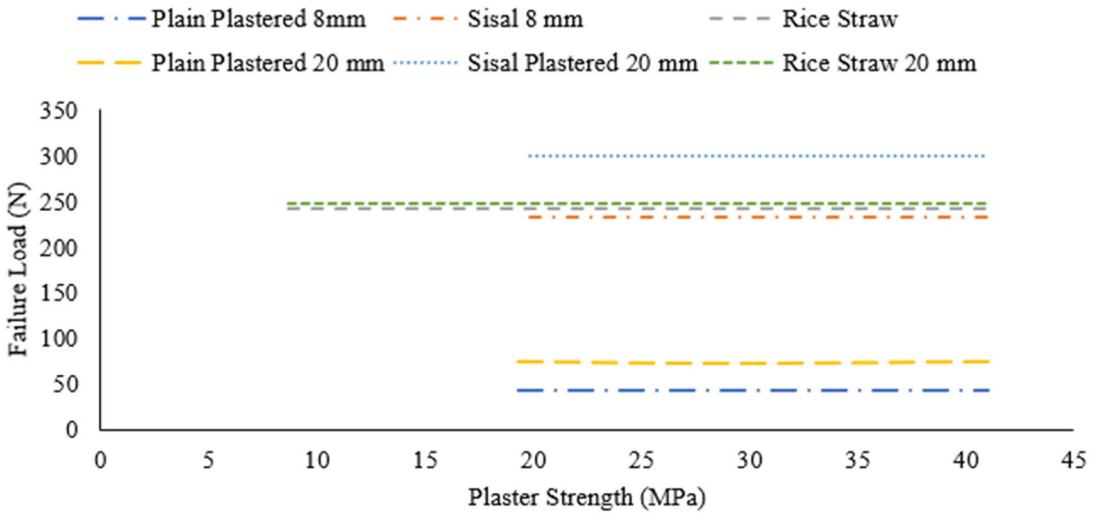

Figure 5.10: Effect of plaster strength on failure load graph

c.Thickness of plaster

Three values of thickness of plaster 8 mm, 12 mm and 20 mm were considered to observe the effect on failure load. In total nine FE model was produced by keeping all other parameters same except thickness of plaster. The results of parametric analysis are shown in the Figure 5.11.

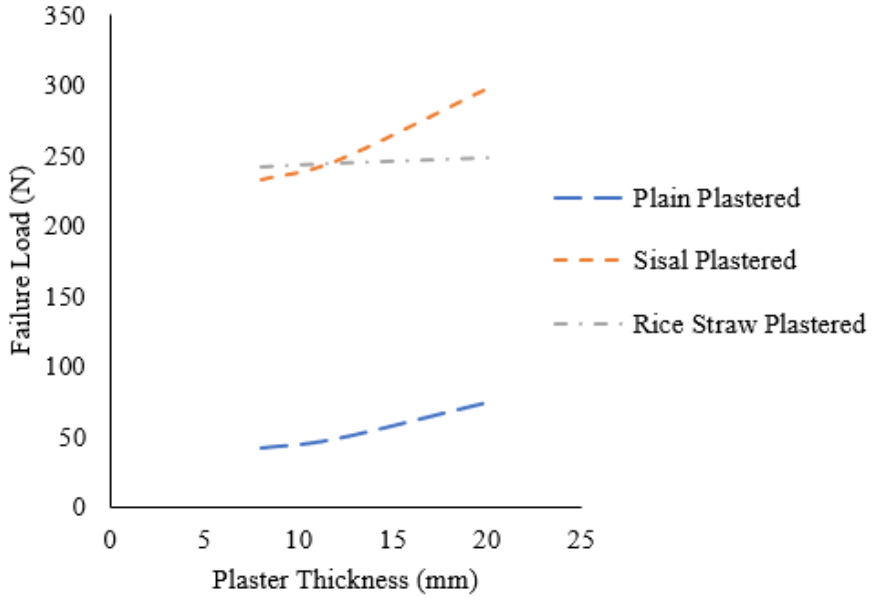

Figure 5.11: Effect of plaster thickness on failure load graph

It can be observed there is 77% increase in failure load for plain plastered column after increasing the thickness of plaster by factor of 2.5. For fibrous sample it was noted that a similar increase in thickness of plaster only gave 28% improvement in failure load.

5.4.4 Cost analysis

From experimental and numerical analysis, it was found that addition of fibrous plastering to the tension face of column enhanced the peak lateral load and other mechanical properties such as elastic stiffness, pre- and post-crack energy absorption and toughness. However, addition of plaster and fibres to one face will increase the overall construction cost. In order to reduce the construction cost of the wall, the thickness of the wall (i.e. thickness of blocks) could be reduced. Finite element sensitivity analysis was carried out to find the equivalent thickness of fibrous plastered column to an unplastered column having similar or better lateral resistance. An unplastered unmortared column of 150 mm thickness was taken as datum. Plain and fibrous plastered walls with mortar and interlock were compared to find this equivalent thickness. The following variations were considered as detailed below:

A – (Datum) Unmortared, unplastered column of thickness 150mm.

B – Unmortared, plain-plastered column of block thickness x (plus 8 mm plaster)

C – Unmortared, fibrous- plastered column of block thickness y (plus 8 mm plaster)

D – Mortared, unplastered wall of block thickness z

a. Sensitivity Analysis and results

Sensitivity analysis was carried out using hit and trial method of reducing the block-thickness in the models B, C and D until their lateral resistance was equal to that of datum model A. Results are detailed in the Table 5.9 below: (25 mm was considered to be the minimum practical block thickness)

It can be observed from the results Table 5.9 that in both cases (B and C) of unmortared masonry column, a 25-mm thick column with 8 mm plaster gave better lateral resistance than the unmortared unplastered 150 mm datum.

Table 5.9: Failure load sensitivity analysis for equivalent thickness

Model	Fz (N) with 150 mm block thickness	Fz (N) with reduced block thickness	Reduced thickness of block
A – Unmortared unplastered (Datum)	27.36	-	-
B – Unmortared plain plastered	137.54	35.8	25 mm + 8 mm plaster
C – Unmortared fibrous plastered	167.7	45.4	25mm + 8 mm plaster
D – Unplastered but Mortared	208	-	-

b. Cost comparison

Based on the above results, cost of construction of 1 m² of walling was calculated for the various options. It can be observed that 67% cost saving could be achieved by reducing the wall thickness to 25 mm for the examples B and C. They will have better lateral resistance than datum A.

Table 5.10: Comparison of cost

Type	A – Datum	B – thickness 25 mm	C – thickness 25 mm	D – 150 mm thickness
Cost ($)/m^2	3.52	1.15	1.16	5.90
Normalized to unmortared unplastered wall (A)	1.00	0.33	0.33	1.68

5.5 Summary

The aim of this numerical work was to develop NLFE predictive tools to firstly identify a likely failure mechanism (e.g. bond failure) compatible with the experimental work and secondly to do parametric studies more cheaply than via constructing many walls. 3D nonlinear FE models of unplastered, plain plastered and fibrous plastered columns made of unmortared blocks were developed. The FE models were validated using the experimental results. The FE model represented the block and plaster with eight-node isoparametric solid brick elements. For the interface between block and plaster, eight-node interface elements were used. The bond-slip interfaces between blocks and the block to plaster interface were adequately modelled. The adopted geometrical and material properties were either obtained from the experimental work or calculated based on well-used models. The solution method was adopted based on an incremental iterative procedure using displacement increments of 0.1 mm for 20 steps. Failure behaviour was verified by comparing the FE models failure load, load displacement curves and crack patterns to the experimental results. Based on the comparative results between FE models and experimental results, the following conclusions were obtained.

1. Lateral failure load from FE models were in fair agreement with the experimental results. The average experimental and FE failure lateral load ratios obtained were 1.0,1.07,1.00 and 1.04 for unplastered, plain plastered, rice-straw reinforced plaster and sisal-plastered columns respectively.

2. The load displacement curves showed that the stiffness of the FE model was markedly higher than the experimental results for the first stage of crack formation. Once the crack forms, the failure load was comparable between the FE values and experimental results, because of the rotational smeared crack model.
3. The FE models crack patterns have a good agreement with the crack patterns observed in the experimental tests. e.g. the opening of joints for unplastered columns and cracking in the interface between plaster and block for plastered ones.
4. Parametric study of block strength has shown that the failure load is directly proportional to the compressive strength of masonry blocks.
5. Parametric studies suggest that increasing the strength of plaster does not change the failure load. This is because failure is initiated by cracks in the interface between plaster and block.
6. Parametric study for thickness of plaster showed that increase in thickness of plaster resulted in the increase of failure load but this increase is not linear with increase in thickness of plaster. e.g. a 150% increase in thickness of plaster only resulted in 28% increase in failure load.
7. Column thickness can be reduced to 25 mm of blocks with 8 mm of plaster and yet exceed the lateral strength of a 150 mm thick unplastered column.
8. Cost comparison showed that fibrous plastered with 25 mm thickness gave equivalent performance to the 150-mm thick unplastered column with 67% cost saving.

Non-linear finite element modelling of interlocked masonry column was carried and validated using the experimental results. Based on validated models, parametric study was carried out. Based on the outcome of interlocked columns experimental work and finite element modelling, experimental work would be extended to 2200 mm high walls connected with roof truss and 8 mm fibrous plaster to explore the overall performance of masonry walling in the following chapter.

Chapter 6. Improvement in lateral resistance of mortar-free interlocking wall with fibrous plaster

Related ISI Impact Factor Journal Paper:

Qamar, F., Thomas, T. & Ali, M. (2019). Improvement in lateral resistance of mortar-free interlocking wall with plaster having natural fibres. *Construction and Building Materials*,234 117387. Impact factor: 4.046

Related Conference Paper:

Qamar, F., Thomas, T. & Ali, M. (2019). Effect of natural fibrous plaster on lateral resistance of mortarless interlocking wall. *5th International Conference on Sustainable Construction Materials and Technologies (SCMT5). Kingston University* London, UK 14 – 17 July. Paper IDSCMT5149.

6.1 Background

In Chapter 3 it was concluded that the addition of 2% sisal fibre in plaster (i.e. reinforced coating) of interlocked masonry walling is likely to improve its performance, including raising the lateral resistance of low-cost masonry house walls. This contribution by addition of sisal and rice straw fibre in plaster applied to interlocked columns was confirmed by experimental work as explained in Chapter 4. This was also confirmed numerically by using finite-element analysis in Chapter 5. In this chapter extended research is presented to evaluate the performance of the fibrous plastered interlocked walling system with respect to out-of-plane resistance. The contribution of natural fibre such as rice straw and sisal (2% by cement mass) in plaster was explored for a variety of static and dynamic parameters, namely first-crack load, peak load, lateral stiffness, energy dissipation, toughness, frequency and dynamic stiffness of walls. Empirical and analytical models are also proposed. In this chapter four plastering variants are compared, all are applied to an unmortared interlocked stabilised-soil block walling system. The first variant, A, ‘unmortared unplastered’ is generally taken as a datum for performance comparison. The second variant, B, is a plain plastered walling system (hereinafter called ‘plain plastered’). The third variant, C, is a walling system rendered with a plaster reinforced with rice-straw (hereinafter called ‘straw plastered’). The fourth, D, is walling system rendered with a plaster reinforced with sisal fibre (hereinafter called ‘sisal plastered’).

6.1.1 Proposed house construction

Figure 3.1(a-c) showed the proposed plan, section and elevation of a typical low-cost house. The house plan was of an area 11000 x 22000 mm^2, consisting of ensuite single bedroom, kitchen, store, living room and hall way. The walls of the house would be made using mortar-free interlocked blocks strengthened with natural fibrous plaster. The roof could be of timber truss and covered with roof tiles. The roof trusses are assumed connected (pin joints) with mortar-free interlocked-block walls with steel ties through timber beam. Locally obtained timber would be used to form the roof truss as shown in Figure 3.1 (b).

The shape and dimensions of blocks was presented in Figure 4.2. The overall size of each block is 300 mm x 150 mm x 100 mm. The mix design ratio for the interlocking blocks was 1:12 (Cement: Soil) and made by manually pressed machine. The average compressive strength of the blocks was tested as 1.58 MPa as detailed in Table 3.7. For plain and fibrous plastering of walls a design mix of 1:3 cement and sand with 0.67 w/c ratio was used. Cube testing of the plaster samples was carried out and their compressive strengths found to be 19.3 MPa, 9 MPa and 19.8 MPa for plain, rice-straw reinforced and sisal reinforced cubes, respectively, as detailed in Table 3.5.

6.2 Experimental procedure

6.2.1 Considered plaster, fibres and block configuration

Table 3.4 details the mix proportion and compressive strengths of the plaster and block used. The cement: sand mix ratio for the plaster with fibre and the plain plaster was the same. However, more water was added to plaster with fibre for better application to walls. Two natural fibres, rice straw and sisal, were used. The length of the fibres was about 50 mm. The width of rice straw was about 7 mm and diameter of sisal fibres was reported as 100±30 µmm (Zhang, 2018 and Naveen, 2019).

2% fibre (rice straw and sisal) by weight of cement was added to fibrous plaster. Plain and fibrous plaster were mixed manually. Firstly, cement and sand were dry-mixed and then water was added to make a paste. For plaster with fibre, firstly sand and cement were dry mixed together; secondly fibre was spread over and finally water was added to make a paste. Figure 6.1(a-c) shows the microscopic images of fibrous plaster cube samples. These samples were produced from the cube samples after carrying out the compression testing. In figure 6.1a, a sample of sisal fibre plaster cube showed the

embedment of sisal fibre in cement paste without any gap or void, indicating a proper bond of fibre in the cement matrix. Figure 6.1b shows the rice straw samples which indicated the presence of micro cracks and voids in the cement paste and loose bond with rice straw.

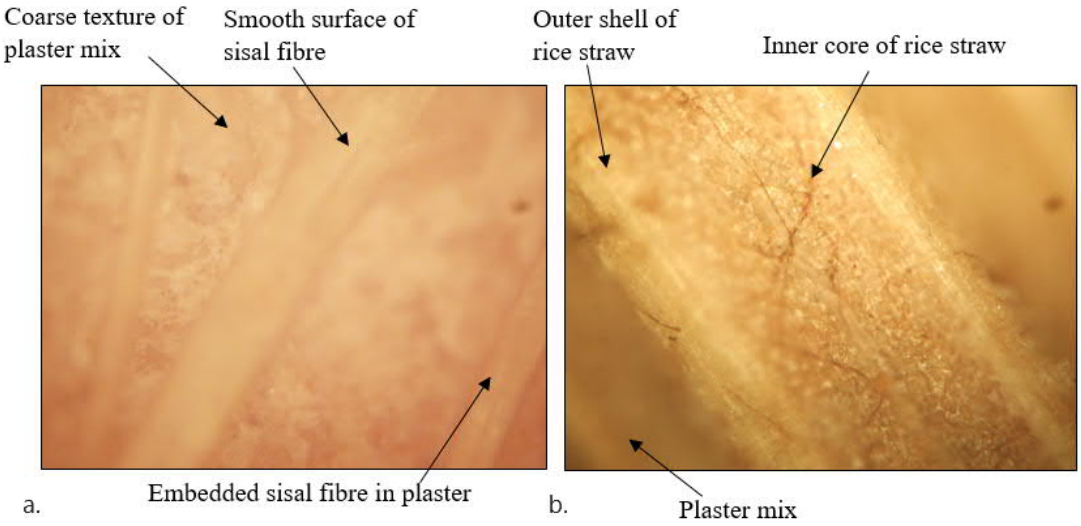

Figure 6.1: Microscopic images from plaster samples, a. Sisal fibre embedment in plaster, b. Rice straw embedment in plaster

6.2.2 Test specimens

In this experimental programme the Tanzanian interlocking-block system (TIB) was used to build the 2200 mm high walls of a typical low-cost house, as shown in Figure 3.1. Further details of wall preparation are included in Annex D. Figure 3.1a shows the plan of a typical house and the scaled part of the house is focused in this experimental work. A total of four walls having the geometric configuration of typical low-cost houses were constructed as shown in Figure 6.2 (a-c). Figure 6.2 (a-c) shows the geometry and dimensions of the tested walls. The wall panels were constructed on a plain concrete base. The overall dimensions of each panel were 900 mm length, 2200 mm high and 150 mm thick. The wall panel was covered with a timber roof truss and tiles which were connected to the top 3 courses of the wall with steel ties.

Table 6.1 details the variable values adopted for testing. Walls are designated as WA - WD and timber roof truss/diaphragm are designated as DA – DD. In order to differentiate between loaded and unloaded faces of the walls, letters “L” and “R” were used to represent the direction of applied lateral load. Three plaster configurations

were used: plain, rice straw and sisal plastered. Plaster was only applied to the tension face of the loaded wall as shown in the Figure 6.3.

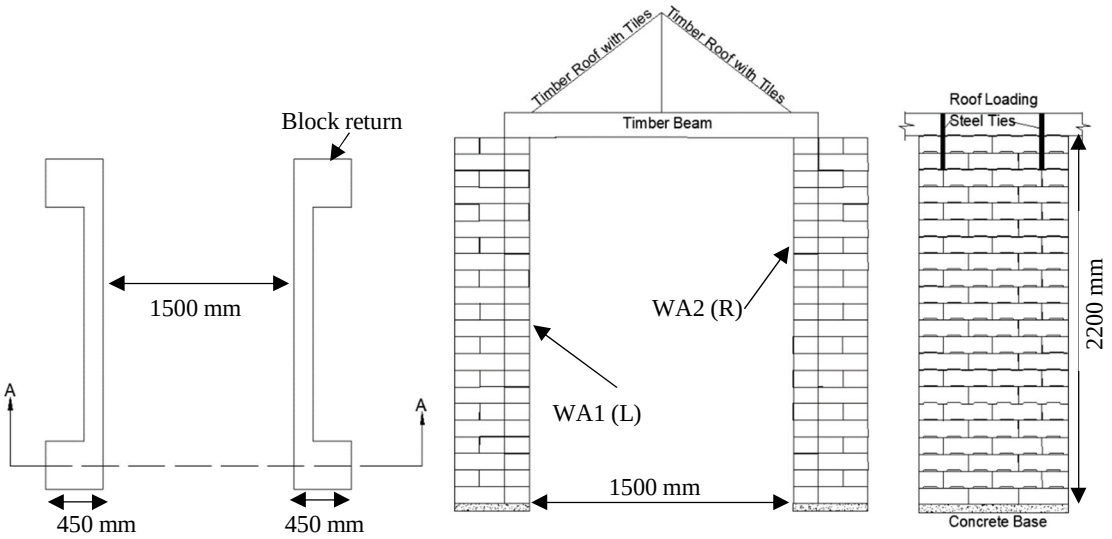

a. b. c.

Figure 6.2: Schematic diagram of walling system with diaphragm under consideration: a. Plan, b. Section A-A and c. Elevation

Table 6.1: Specimen labels

Specimen	Symbol
Unplastered wall	WA1 (L), WA2 (R)
Plain plastered wall	WB1 (L), WB2 (R)
Rice straw reinforced plastered wall	WC1 (L), WC2 (R)
Sisal fibre reinforced plastered wall	WD1 (L), WD2 (R)
Diaphragm over unplastered wall	DA
Diaphragm over Plain plastered wall	DB
Diaphragm over Rice straw reinforced plastered wall	DC
Diaphragm over Sisal fibre reinforced plastered wall	DD

Note: Left walls are loaded towards left side

6.2.3 Test setup and loading

a. Static lateral test

Figure 6.3a shows a schematic diagram representing the test setup. In small increments lateral load was applied with the help of a bespoke steel frame at a height of 2150 mm, as shown in Figure 6.3b. This steel loading frame was anchored in the concrete floor and extra load was placed on the bottom part of frame to resist the overturning/movement. Out of plane (lateral) load was applied by a pulley system attached to the frame. Lateral load is applied to only one of the two linked walls, and for only one of which is the plaster located where needed on the tension face as shown in Figure 6.3. The symmetry of the plastering meant that application of force to the right (on the left-hand wall) and to the left (on the right-hand wall) was expected to produce the same displacement and experimentally the sample size was effectively doubled. In order to measure the displacement dial gauges were attached to the independent frame at the top of both loaded and unloaded walls. Loading was restricted initially to that, giving a displacement of 1 mm. Loading was later increased, generally in steps of 160N, to find the start-of-cracking and the peak loads.

b. Snap-back Test

Figure 6.4a shows a schematic diagram representing the test setup. A Dytran accelerometer was attached to the top course of the wall and separately to the timber roof truss/diaphragm. This was connected to a digital processor to record the acceleration occurring during snap-back tests as shown in the Figure 6.4b. In the snap-back test walls were pulled 5 mm and then released suddenly to allow them to vibrate freely using the same loading frame as above. The acceleration of the walls during each snap-back test was recorded by an accelerometer using Lab View software and later data were imported in Seismograph software to plot the graphs.

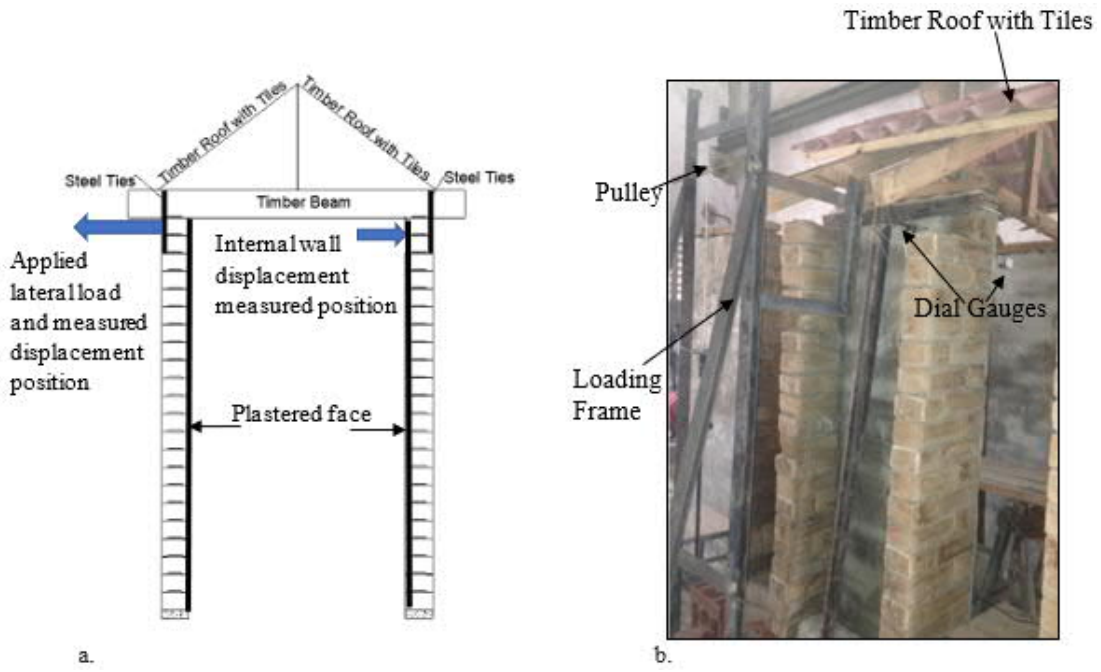

Figure 6.3: Test set-up for load displacement behaviour: a. Schematic sketch (section through single block width), and b. Experimental set up

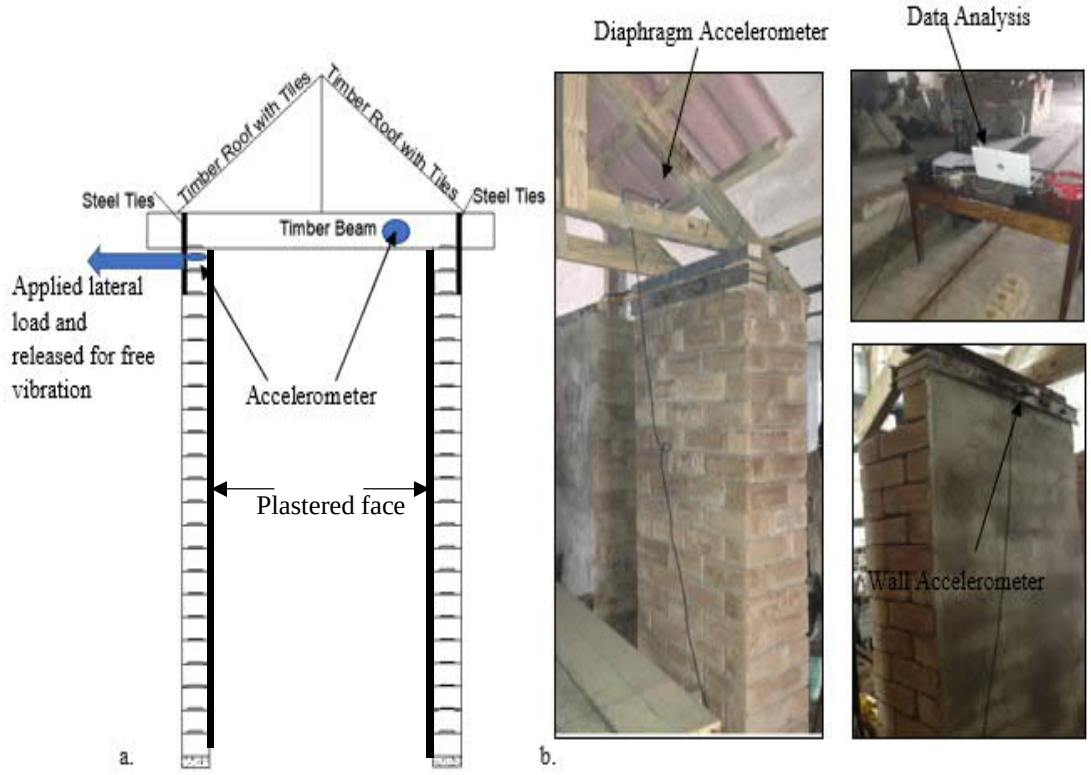

Figure 6.4: Snap-back test (5 mm displacement) set up: a. Schematic sketch (section through single block width), and b. Experimental set up side view

6.3 Walling behaviour

6.3.1 Lateral resistance

Load-displacement plots

The result of each loaded and unloaded wall in the form of a load-displacement plot is shown in Figure 6.5(a-d). Figure 6.5a shows the load displacement plot for unplastered loaded and unloaded wall. It can be observed that at same loading the displacement for unloaded wall was less than for loaded wall. This was due to the flexibility of the connection of walling system with timber diaphragm and due to this, less load was transferred to the unloaded wall. The peak load of 480 N was observed with a displacement of around 10-12 mm for the loaded wall and around 8 mm for the unloaded. These walls showed very low stiffness with a sort of brittle failure. This was expected as the interlocking walls resisted the lateral load due to self-weight and the interlocking mechanism. The imperfection of interlocking keys and the irregular surface of blocks also played a part in producing this poor resistance to lateral load. The addition of plastering does increase the stiffness and load-carrying capacity, as shown in Figure 6.5b. A peak load of 1570 N with a maximum displacement of 3 mm is observed. This showed a significant increase in stiffness and peak load as compared with an unplastered walling system. The first crack was observed around load of 1300 N with a displacement around 2 mm. Figures 6.5c and 6.5d show the behaviour of straw-plastered and sisal-plastered walling, respectively. It can be observed that the first crack load and the corresponding displacement in both cases showed similar behaviour to that of plain-plastered walling. However, peak load was increased from 1570 N to 1590 N and 1630 N for straw and sisal walling, respectively, with a maximum displacement of 5-6 mm in both cases. Thus the behaviour of fibrous-reinforced plastered walling was similar to that of plain-plastered walling but showed significant increase in peak load and stiffness as compared with unplastered walling system. However, fibrous-plastered walling showed lower stiffness than plain-plastered walling after the first-crack load. This showed that the effect of rice straw and sisal fibre after first-crack was to enhance the ductility behaviour.

a.

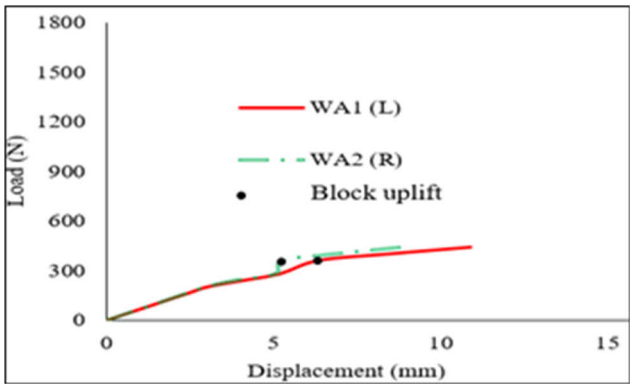

b.

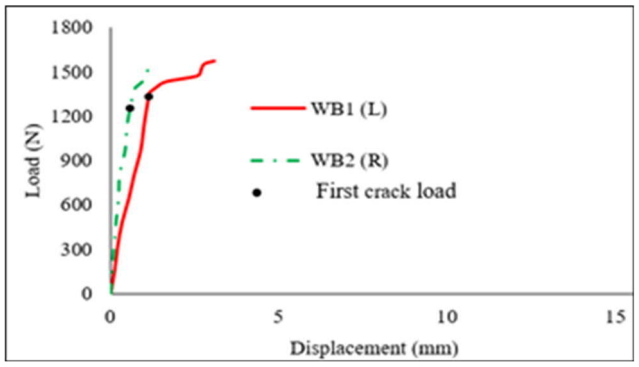

c.

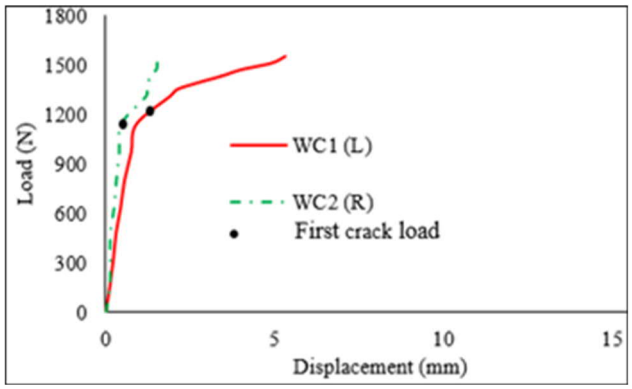

d.

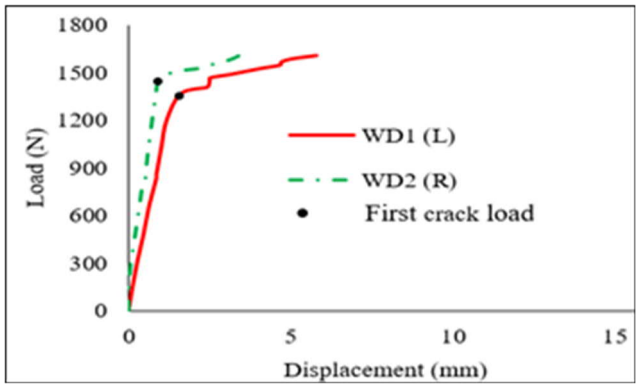

Figure 6.5: Load displacement behaviour (left loaded and right unloaded walls): a. Unplastered walling system, b. Plain plastered walling system, c. Rice-straw reinforced plastered walling system, and d. Sisal-fibre reinforced plastered walling system

Figure 6.6(a-d) shows images of first crack for unplastered, plain plastered, straw plastered and sisal plastered walling systems, respectively. For the unplastered walling system, before the peak load/failure load, opening of the block joint at tension face in the top course (opposite to applied lateral load) was observed, as shown in the Figure 6.6a. The opening of joint was observed at a load of 240 N, which was about 50% of peak load. For the plain plastered walling system, a hair-line crack was observed in the upper half of the wall, as shown in Figure 6.6b. The crack was observed at a load of 1350 N, which was about 85% of noted peak load. Crack initiation in the straw-plastered walling was observed near the base with thick crack around 300 mm long, as shown in Figure 6.6c. whereas in sisal-plastered walling cracking showed in the top course and very thin hair-line 100 mm long crack, as visible in Figure 6.6d. These were observed at loads of 1310 N and 1370 N in straw and sisal-plastered walling respectively. This is about 82% and 84% of their corresponding noted peak load. It should be noted that the plain-plastered and fibrous-plastered walling systems could not be tested to failure load due to experimental restrictions and therefore the noted peak load is not the true peak load. The latter was expected to be more than the load recorded. It can be observed that the peak load for plain plastered was significantly increased as compared to unplastered walling system. This showed an increase of about 2.25 times in peak load from unplastered to plain plastered walling system. The addition of fibres like rice straw and sisal in plaster increases the noted peak load by 2.4 and 3 times for straw plastered and sisal plastered walling respectively, as compared with plain plastered walling system. This indicates that the addition of plaster enhances the lateral resistance of unplastered walling system and addition of fibres in plaster further increased its lateral resistance.

Initiation of cracking in the walling system subjected to lateral load suggested that the point of failure was at the joint between block and plaster interface. Block joint opening was observed near the top course in unplastered walling system. Cracking was observed near the upper half of the wall in plain plastered and near the base in rice-straw reinforced plastered wall; whereas in the case of sisal-fibre reinforced plastered wall cracking was observed near the top course of wall.

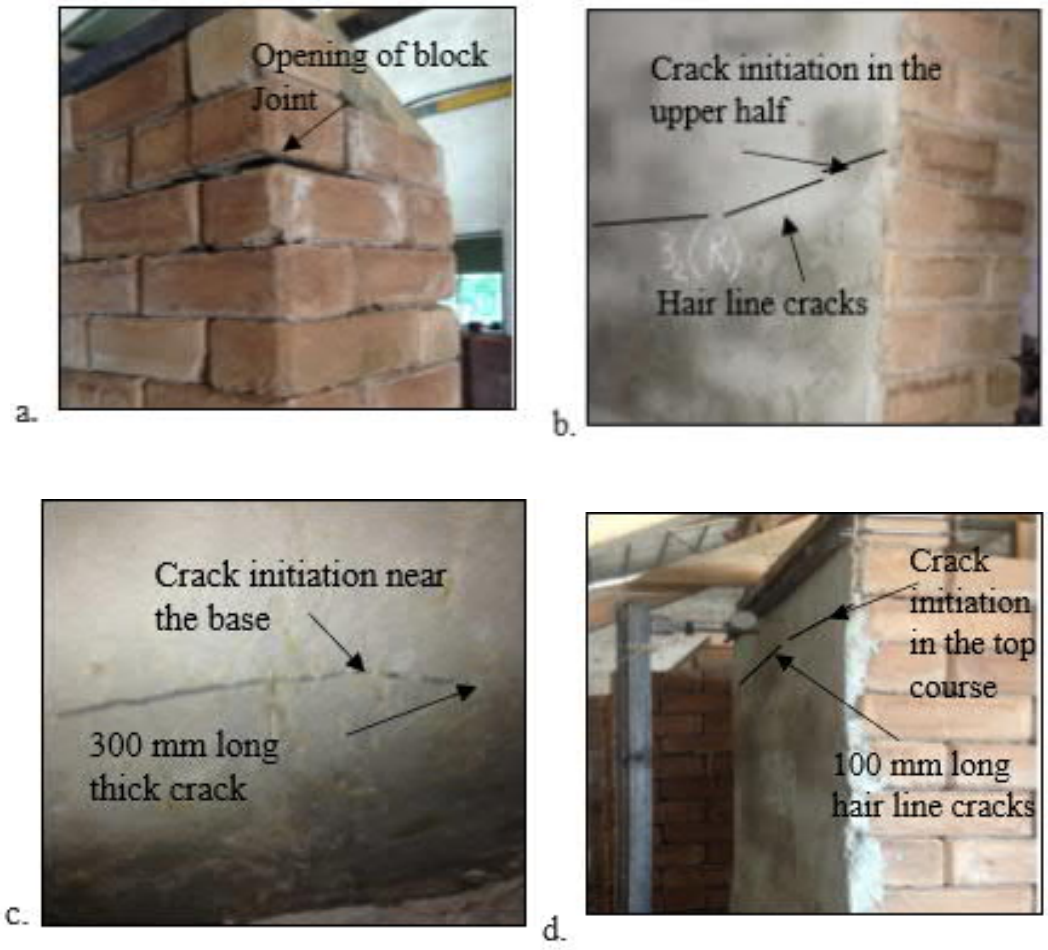

Figure 6.6: Failure mechanism of walling system: a. Unplastered walling system, b. Plain plastered walling system, c. Rice-straw reinforced plastered walling system, and d. Sisal-fibre reinforced plastered walling system

These cracking results showed flexural controlled failure mode for the fibrous plastered walling system. Failure mode in the masonry could be flexural or shear controlled and assessment of the resistance of these two failure modes is considered to be critical to estimating the strength of a walling system (Ismail et.al 2016).

6.3.2 Static mechanical properties of walling system

Table 6.2 details the calculated mechanical properties of unplastered, plain-plastered, straw-plastered and sisal-fibre plastered walling systems. These properties include initial elastic stiffness, energy absorbed (E1, E2, E) and toughness index (I). Elastic

stiffness was obtained from the first-crack slope of load-displacement plot of each walling system. First-crack energy absorbed E1 was calculated by summation of area under the load-displacement plot up to first-crack load. Peak load energy absorbed E2 was obtained by summing the area under the load-displacement plot up to peak load. The summation of E1 and E2 was considered to be total energy absorbed E. Toughness index I = E/E1 is the ratio of total energy absorbed and first-crack energy absorbed.

It can be observed that adding plain plaster increases the elastic stiffness of an unplastered from 64 N/mm to 1114 N/mm, a 17 times increase. The corresponding elastic stiffnesses for rice-straw and sisal-plastered walling were 980 N/mm and 893 N/mm, respectively. Thus the increase of elastic stiffness from unplastered walling was 15-fold for rice-straw and 14-fold for sisal-plastered walling. However, when compared with plain-plastered walling, rice-straw and sisal-plastered walling showed respectively 12% and 20% decrease in elastic stiffness. This was a function of the individual properties of fibre and addition of fibre in plaster which led to a reduction in stiffness which then in turn resulted in an increase in ductility. First-crack energy absorbed in the case of plain-plastered walling was increased to 766 J from 490 J with unplastered walling, which indicated a 1.5 times increase from unplastered to plain-plastered walling. Further increase was observed with the addition of fibre and values increased to 1170 J and 1272 J, which was about 1.52 and 1.66 times increase from plain-plastered to rice-straw and sisal-fibre plastered walling respectively. It was noted that peak load energy absorbed for unplastered, plain-plastered, rice-straw and sisal-fibre plastered walling was 791 J, 2858 J, 3290 J and 6298 J respectively, which showed significant increase of 61%, 273%, 180% and 395% respectively as compared with first-crack energy absorbed. This clearly indicates the contribution of plaster and fibre to enhancing the peak load energy absorbed. The greatest contribution was evident in the sisal-fibre plastered walling system. An increase of toughness index from unplastered to plain-plastered, rice-straw and sisal-fibre plastered walling system was noted as 55%, 58% and 127% respectively. This again indicates the contribution of fibre in plaster and its ability to take greater load after first crack.

Table 6.2: Static mechanical properties for interlocked loaded walls (unplastered, plain, straw-reinforced and sisal-reinforced plastered walling)

Specimen	First crack load	Max load	Elastic Stiffness	E1	E2	E	Toughness Index (I)
	N	N	N/mm	J	J	J	-
WA1 (L)	240	480	64.02	490	792	1281	2.61
WB1 (L)	1350	1570	1114	766	2239	3105	4.05
WC1 (L)	1310	1590	980	1171	3673	4844	4.13
WD1 (L)	1370	1630	893	1273	6298	7571	5.94

Table 6.3: Increase or decrease of static mechanical parameters from those of unplastered datum for plain, straw-reinforced and sisal-reinforced plastered walling

Specimen	First crack load	Max load	Elastic Stiffness	E1	E2	E	Toughness Index (I)
	N	N	N/mm	J	J	J	-
WB1 (L)	+460%	+227%	+1600%	+56%	+182%	+142%	+55%
WC1 (L)	+445%	+231%	+1400%	+138%	+364%	+278%	+58%
WD1 (L)	+470%	+240%	+1300%	+160%	+695%	+491%	+127%

Figure 6.7 displays, in bar-chart form, the data in Table 6.3. It is clear that sisal-reinforced plastering gives the best mechanical properties and is especially superior with respect to increasing 'post-crack energy absorption'.

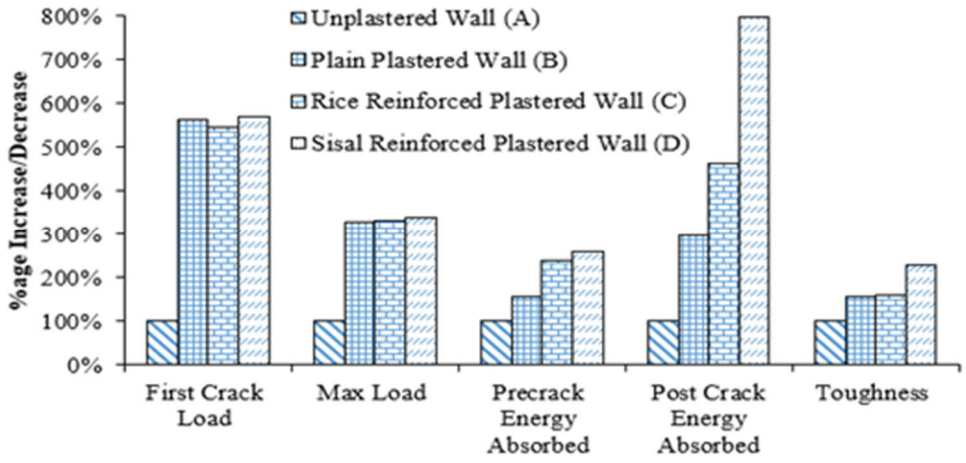

Figure 6.7: Comparison of static mechanical properties of walling systems

6.3.3 Dynamic properties of walling systems

Table 6.4 details the dynamic properties (i.e. frequency and dynamic stiffness) of unplastered, plain, rice-straw reinforced and sisal-fibre reinforced plastered walling systems which comprise two walls linked by a timber diaphragm. The values of frequency were obtained from snap-back test as described in section 6.2.3. Dynamic stiffness was derived from these frequencies by using the equation $K_d = f^2 * 4\pi^2 * m * f_d$. Where K_d, f, m and f_d are dynamic stiffness, frequency in Hz, mass in kg and dynamic factor, respectively. The values of dynamic stiffness obtained from this equation were 60 N/mm, 883 N/mm, 920 N/mm and 818 N/mm for unplastered, plain plastered, rice-straw and sisal-fibre walling system respectively.

Table 6.4: Dynamic properties of loaded walls and diaphragms

Specimen	Displacement (mm)	Frequency (Hz)	Dynamic Stiffness (N/mm)
WA1 (L)	5	1.13	60
WB1 (L)	1	1.19	883
WC1 (L)	1	1.22	920
WD1 (L)	1	1.15	818
DA	5	1.05	-
DB	1	1.15	-
DC	1	1.85	-
DD	1	1.12	-

Figure 6.8 shows the comparison of dynamic properties of walling systems. It can be observed that the frequency of walls was increased by 6%, 8% and 2% for plain-plastered, rice-straw and sisal-fibre plastered walling, respectively, as compared with unplastered walling. Similar behaviour was recorded for the linking diaphragms of each walling with 10%, 76% and 7% increase respectively, as compared with the diaphragm of unplastered walling. The increase in frequency of plastered and fibrous plastered walling system was indicated by tiny improvement in the dynamic stiffness. A significant increase in dynamic stiffness was observed in plain-plastered walling, showing 14 times increment over unplastered walling. The addition of fibre in plaster showed similar behaviour as compared with plain-plastered with a marginal decrease of 7% for sisal-fibre plastered walling. Plastering increased the stiffness of the walls

and the walls were also connected with each other through timber diaphragm. This connection may have prevented the walls from vibrating freely during snap back test. This resulted in reduced dynamic stiffness in the fibrous plastered walling system.

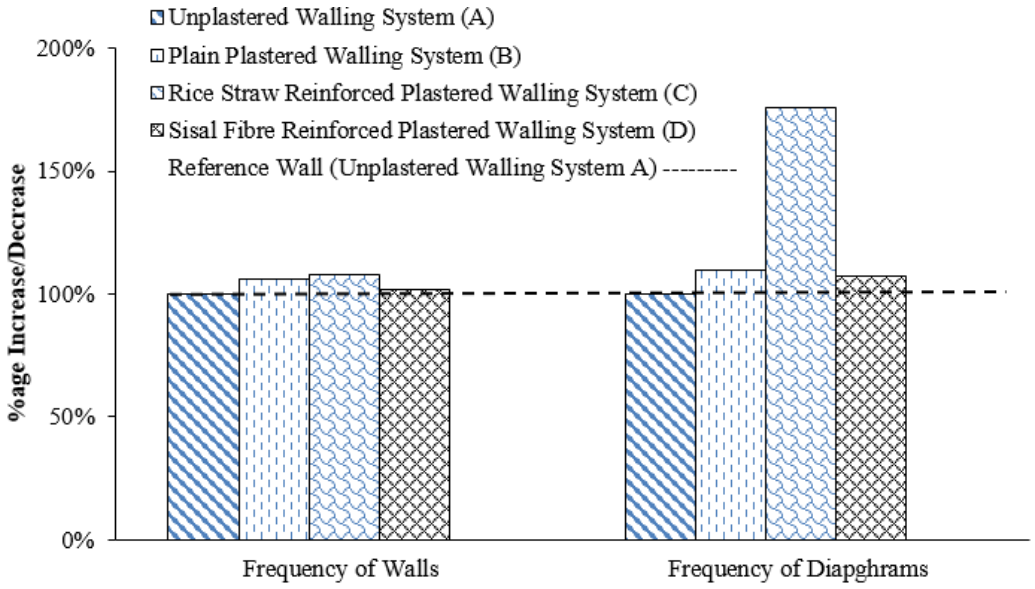

a.

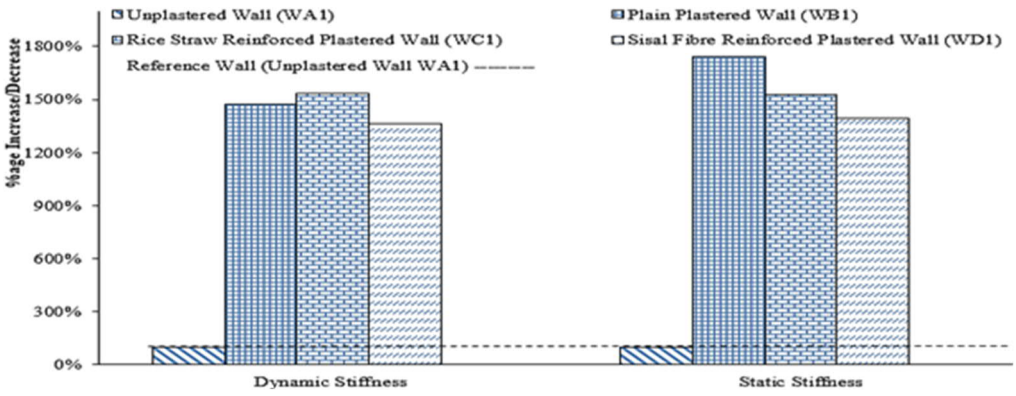

b.

Figure 6.8: Normalised dynamic properties of walling system, using the unplastered wall as a datum; a. Frequency of loaded walls and diaphragms and b. Dynamic and static stiffness of loaded walls

6.3.4 Empirical and analytical modelling

a. Empirical modelling

Table 6.5 details the comparison of experimental and theoretical values of lateral peak load. Theoretical values of lateral peak load were calculated by equating equations 1 and 2 below and solved for lateral peak load:

$M_D = \frac{\gamma f}{8} * P * L$……. Equation (1)

$M_R = E_{fk} * \frac{Z}{\gamma m}$…… Equation (2)

Where M_D, γ_f, P and L are design moment, safety factor for loads, applied lateral peak load and length of wall respectively in Equation 1. M_R, E_{fk}, Z and γ_m are design resistance, effective flexural strength factor, section modulus and material factor respectively in Equation 2. γ_f = 1.5, L = 2200 mm, Z= 3375000 mm^3 and γ_m = 2.7. E_{fk} = 0.175, 0.55 and 0.575 for unplastered, plain-plastered and fibrous-reinforced plastered wall, respectively.

The values obtained for lateral peak load from these equations were 530 N, 1667 N, 1750 N and 1750 N respectively, for unplastered, plain-plastered, rice-straw reinforced and sisal-fibre reinforced walling systems. This was in good agreement with experimental values with a maximum error of 10%, as shown in Table 6.5.

Table 6.5: Comparison of experimental and empirical results of static testing

Specimen	Lateral Peak Load (N)		
	Experimental	Theoretical*	Error (%age)
WA1(L)	480	530	10%
WB1(L)	1570	1667	6%
WC1(L)	1590	1750	10%
WD1(L)	1630	1750	7%

*Note: $M_D = \frac{\gamma f}{8} * P * L$ ……. *Equation (1)*

$M_R = Efk * \frac{Z}{\gamma m}$ …… *Equation (2)*

Where M_D, γf, P and L are design moment, safety factor for loads, applied lateral load and length of panel, respectively, in Equation 1.

And M_R, Efk, Z and γm are design resistance, effective flexural strength factor, section modulus and material factor, respectively, in Equation 2.

γf= 1.5 and L = 2200 mm. Efk = 0.175, 0.55 and 0.575 for unplastered, plain plastered and fibrous reinforced plastered wall, respectively, Z= 3375000 mm^3 and γm = 2.7

Table 6.6 details the comparison of static, empirical and dynamic stiffness for walling systems. Static and dynamic stiffness are explained in section 6.3.3. Empirical stiffness is derived based on an empirical equation. The empirical equation $Ke = \mu G$ and $\mu = x^2 + Ax - B$ is derived from the experimental data. K_e is empirical stiffness and G is geometrical stiffness. And G= 284 N/mm, x = 1, 2, 3 and 4 for unplastered, plain- plastered, rice-straw reinforced plastered and sisal-fibre reinforced plastered wall, respectively, A = 5.95 and B = 4.7. Static stiffness obtained from the experimental work was compared with empirical and dynamic stiffness. It can be observed that empirical and dynamic stiffness agreed well with the experimental values with a maximum error of 20% with empirical stiffness and 21% with dynamic stiffness.

Table 6.6: Comparison of static, empirical and dynamic stiffness

Specimen	**Static stiffness from load-displacement test N/mm**	**Empirical stiffness* N/mm**	**Error %**	**Dynamic stiffness** from snap back test N/mm**	**Error %**
WA1 (L)	64	71.0	-11%	60	+6%
WB1 (L)	1114	908.8	18%	883	+21%
WC1 (L)	980	1178.6	-20%	920	+6%
WD1 (L)	892	880.4	1%	818	+8%

**Note 1: $K_e = \mu G$ and $\mu = x^2 + Ax - B$*

Where K_e is empirical stiffness and G is geometrical stiffness. And G= 284 N/mm, x = 1, 2, 3 and 4 for unplastered, plain plastered, rice straw reinforced plastered and sisal fibre reinforced plastered wall, respectively, A = 5.95 and B = 4.7.

***Note 2: $K_d = F^2 * 4\pi^2 * m * Fd$*

Where K_d, F, m and $F_{d\ are}$ dynamic stiffness, frequency in Hz, mass in kg and dynamic factor, respectively.

And F = 1.06,1.19,1.22 and 1.15 for unplastered, plain plastered, rice straw reinforced plastered, sisal fibre reinforced plastered walls, respectively, m = 594 and 630 kg for unplastered and plastered walls, respectively, and F_d = 25.

b. Analytical modelling

Analytical modelling is carried out for this developed technology keeping in mind the previous analytical approaches adopted by other researchers for their devised mechanism in brick masonry (Laursen, 2015 and Padalu, 2018). The proposed procedure for the evaluation of out-of-plane lateral resistance of walling system is detailed in Figure 6.9 below.

When plain and fibrous-plastered walling systems were subjected to lateral load, the plastering on the tension face of the wall was considered to resist the crack opening and thus contributed to wall strength. Using beam theory (Padalu et al., 2018) the out-of-plane peak strength of masonry walling system was obtained using the equation. $Mn = \alpha\beta f_m * N_a \left(\frac{t}{2} - \frac{\beta N_a}{2}\right) + T_p * A_p * F_{fe} * \frac{t}{2}$.

where $\alpha\ and\ \beta$ are equivalent stress block parameter, f_m = wall compressive strength, N_a = depth to neutral axis for lateral loading, t = thickness of wall,T_p = thickness of plaster, A_p = area of plaster, F_{fe} = effective stress. The governing failure mode assumption made to develop the relationship was checked using equation $\varepsilon_m = \varepsilon_d * (N_a/(t - N_a)$<0.0035. In order to ensure that the plastered walling system has enough resistance to cracking, moment to initiate cracking was calculated using the equation $M_{cr} = (f_t * f_a) * S$, where M_{cr} = cracking moment, f_t = tensile strength of plastered walling system, f_a= axial stress and S = section modulus and limitation of lateral resistance $M_n > 1.3M_{cr}$ was applied.

Table 6.7 details the comparison of out-of-plane lateral resistance of unplastered, plain plastered, rice-straw reinforced and sisal-fibre reinforced walling systems, calculated by the equations explained in Figure 6.9 with the experimental applied moment. Out-of-plane lateral resistance moment was obtained 0.906 kN-m, 2.796 kN-m, 3.126 kN-m and 3.360 kN-m for unplastered, plain-plastered, rice-straw reinforced and sisal-fibre reinforced walling systems respectively. It can be observed that the experimental values agreed well with analytical procedure for all walling systems and maximum error found was only 23.51% for plain plastered walling system.

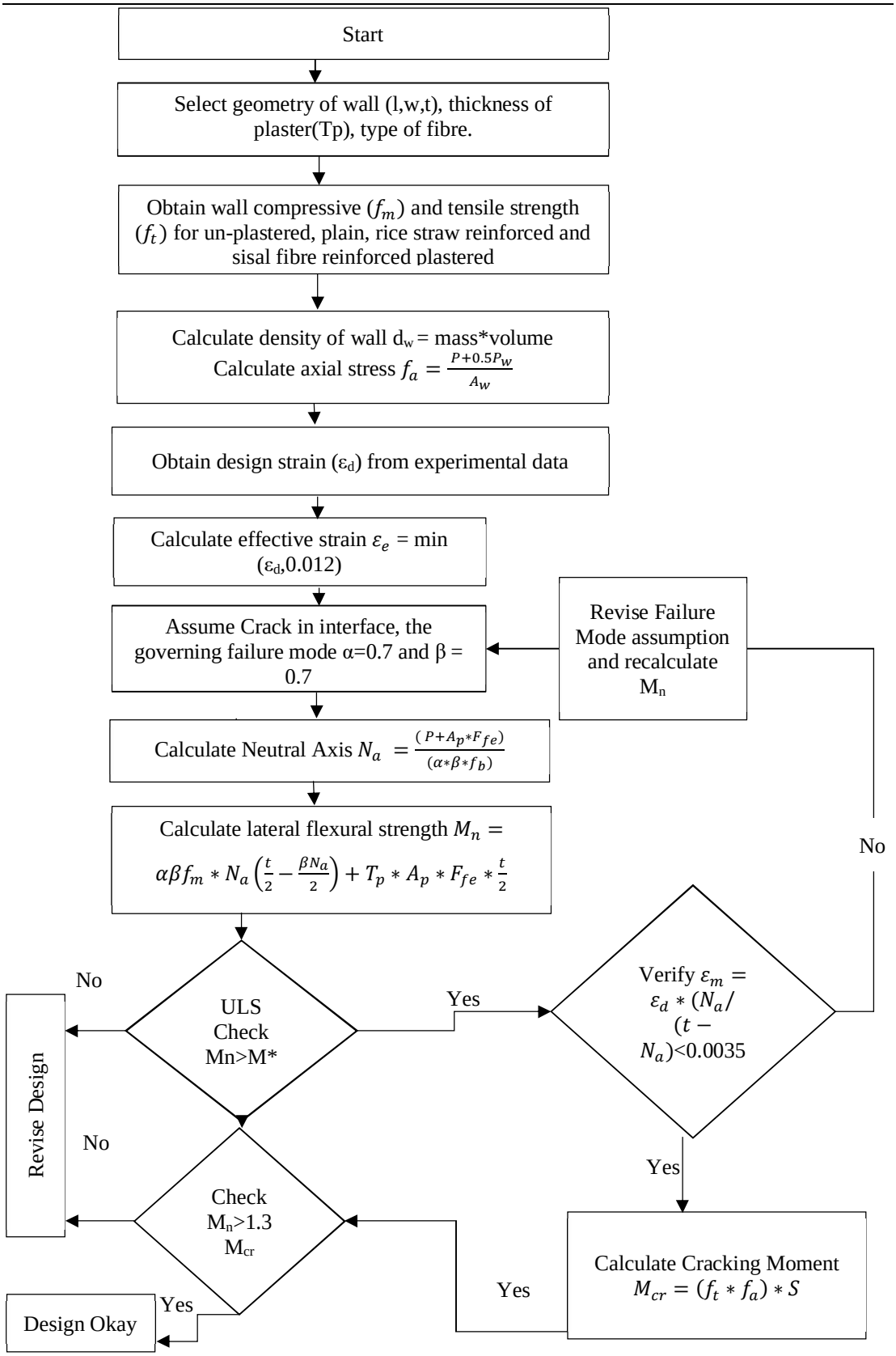

Figure 6.9: Design flow chart for fibrous and plain plastered interlocking wall lateral flexural resistance

Table 6.7: Comparison of experimental and design flexural resistance of walling system

Specimen	**Density of wall d_w**	**Design strain for fibrous plaster ε_d**	**Effective strain ε_e**	**Modulus of Elasticity E_p**	**Effective stress F_{fe}**	**first Moment of area S**	**Wall Self Weight P_w**	**Axial stress at wall mid-height, f_a**	**Neutral Axis N_a**	**Out of Plane Flexural Strength (M_n)**	**Cracking Moment M_{cr}**	**Applied Moment M***	**Difference Percentage**
	kg/m^3	**-**	**-**	**MPa**	**MPa**	**m^3**	**kN**	**MPa**	**m**	**kN-m**	**kN-m**	**kN-m**	**%**
WA1 (L)	1580	-	-	-	-	0.0123	4.60	0.071	0.017	**0.906**	0.880	**1.056**	**16.48%**
WB1 (L)	2239	0.0035	0.0035	2990	10.46	0.0118	7.39	0.078	0.018	**2.796**	1.242	**3.454**	**23.51%**
WC1 (L)	2262	0.002	0.002	2050	4.1	0.0118	7.46	0.072	0.018	**3.127**	1.290	**3.498**	**11.85%**
WD1 (L)	2489	0.0174	0.012	7170	86.04	0.0118	8.21	0.074	0.019	**3.360**	1.320	**3.586**	**6.70%**

Note 1: Length of wall (l) = 900 mm; Height of wall (h) = 2200 mm; Thickness of wall (t) = 150 mm; Thickness of plaster (Tp) = 20 mm; Wall compressive strength fm = 1.5 MPa, 4 MPa and 4.5 MPa for unplastered, plain and fibrous plastered, respectively; Wall tensile strength ft=0, 0.028 MPa, 0.032 MPa for unplastered, plain and fibrous plastered wall; Wall axial load fa = 7.3 kN; Failure mode α =0.7, β=0.7; compressive strength of ISSB = 0.83 MPa.

Note 2: For formulas, refer to Figure 6.9.

6.3.5 Discussion

The out-of-plane lateral resistance of a mortarless interlocked masonry walling system is a primary concern. Masonry walling acts as a cantilever for out-of-plane loads in the absence of adequate wall-diaphragm restraint and can result in sudden failure, whereas a masonry walling system with adequate restraint like a diaphragm and projections behaves differently (Ismail et.al 2016). In either case it required improvement in the out-of-plane lateral resistance. To evaluate the enhancement of lateral resistance by the addition of natural fibrous plastering experimental work was carried out for an interlocked walling system. Static mechanical properties were measured which include first-crack load, peak load, elastic stiffness, energy absorbed and toughness. Initiation of cracks and failure mode were observed for unplastered, plain-plastered and fibrous plastered walling systems. The addition of plaster has increased the inertia which has resulted in increased loading and stiffness for plastered walling systems. Figure 6.7 compared static mechanical properties obtained from experimental work. It can be observed that all properties are increased by the addition of plaster and further increase can be attained by the addition of fibre. Enhancement due to addition of fibre was not significant in the case of first-crack load. This might be because the fibre contribution or bridging phenomenon started after the initiation of cracks. Moreover, first crack observed for fibrous plastered walling was very minor as compared with that of the plain-plastered walling system. It was expected that ultimate lateral resistance in the fibrous-plastered walling system would be much higher than in plain-plastered. However, this could not be recorded due to the limitation of loading assembly. Other properties like energy absorption and toughness showed significant increase due to the addition of fibre. Dynamic properties (frequency and dynamic stiffness) were also measured by snap-back test. Figure 6.8 shows the comparison of dynamic properties of walling systems. It can be observed that there was an increase in frequency and dynamic stiffness obtained by the addition of plaster as compared with unplastered walling system. However, further addition of natural fibre did not enhance the frequency and dynamic stiffness. This might be due to the connection/tying of walls with a diaphragm that did not allow the wall to vibrate freely during snap back test. Empirical and analytical modelling was carried out for lateral load and stiffness of the walling system. This was compared with the

experimental work and agreed well, with a maximum error of 23.51%. A design flow chart was developed based on analytical modelling. This will enable development of the design guideline for the out-of-plane lateral resistance of mortarless interlocked walling system.

6.4 Implementation in real life

From the experimental and analytical modelling work, it has been established that low lateral resistance of interlocked masonry walls can be improved by the addition of plaster on the tension face of the wall. Further improvement in the ductility of the plastering could be achieved by the addition of cheap natural fibres like rice straw and sisal. It was observed that a walling system reinforced with sisal plaster performed better than others. For the practical application of building a low-cost house using interlocked blocks, the following points need to be considered:

- Good seismic design, beyond the scope of this thesis imposes limits on the proportions and shape of buildings. Interlocked block house plan should be symmetrical in both plan and elevation, as shown in the Figure 6.2. The height of house should not exceed twice the least horizontal dimension which is 2000 mm for hall way in Figure 6.2, for better lateral stability.
- Stabilised-soil interlocking blocks could be manufactured by cheap manually pressed machine requiring less skilled labour. The design mix ratio for soil and cement was recommended to be 12:1. However, blocks need to be kept moist to attain compressive strength of 1.5 MPa or above.
- During the building of a wall with interlocking blocks special consideration should be given to the geometry and contact area of the blocks. Any unevenness in the surface of the block could lead to increased out-of-plumbness of wall and reduced lateral resistance. Better contact area could be achieved by reversing the sides of the blocks.
- Thin fibrous plastering of 8 to 10 mm thickness should be considered for better performance and low cost. 2% fibre by weight of cement should be added in plaster with a w/c ratio of 0.67.
- Single-storey structures with timber roof trusses and beams, require special consideration be given to the joints between the timber beam and interlocked

walls, as this can affect the load distribution between laterally loaded and unloaded walls.

- Fibrous plastering of external walls subjected to weathering (action) could be re-applied in layers maintaining structural integrity.

6.5 Summary

Experimental work was performed to estimate the improvement in wall performance against out-of-plane loading following the addition of fibrous plastering. Rice-straw and sisal fibres were used. Mechanical and dynamic properties like elastic stiffness, energy absorbed, toughness index, frequency and dynamic stiffness were determined. Conclusions are listed below:

1. Lateral peak load was noted to increase by 2.25 times from unplastered to plain plastered walling system.
    - Further addition of fibre to the plaster can realistically increase lateral strength by 3 times for sisal fibre and 2.4 times for rice straw.
2. Static mechanical properties were significantly increased from unplastered (datum) to plain plastered, rice-straw reinforced plastered and sisal-fibre reinforced plastered, namely:
    - Elastic stiffness was increased by factors of 17, 15 and 14 from datum respectively. However, it reduced by 12% and 20% for straw and sisal-fibre as compared with plain plastered walling. This was accompanied by increase in ductility of fibrous plastered walling system.
    - First-crack energy absorbed was increased 1.5 fold by progressing from unplastered to plain plastered. The further increase from the addition of fibres was 1.52 and 1.66 fold for straw and sisal fibre plastered walling system, respectively.
    - The peak-load energy absorbed showed significant increases of 273%, 180% and 395% respectively as compared with first crack energy absorbed.
    - The increase in toughness index was respectively by 55%, 58% and 127% above datum values for plain, straw and sisal-plastered walling.

3. Significant increase was noted in the dynamic properties of walls with plain, straw and sisal-fibre plastered walling systems, respectively, as compared with the unplastered walling system (datum).
    - The natural frequency of walls was increased slightly by 6%, 8% and 2% respectively, as compared with datum.
    - Dynamic stiffness for plain plastered walling was 14-fold greater than for unplastered walling. The addition of fibres in plaster did not significantly further increase dynamic stiffness.
4. An empirical equation was developed for dynamic stiffness based on experimental data and the outcome agreed well with the experimental dynamic stiffness.
5. An analytical procedure was developed for estimating the lateral resistance of a walling system which compared well with the experimental outcome. The maximum error was found to be only 23%.

From the experimental results it became clear that mechanical and dynamic properties of ISSB walling systems were improved by using fibrous plastering. This will enhance the lateral resistance of ISSB walls by the addition of the plaster and further improvement could be achieved by the addition of natural fibre in the plaster. The behaviour of walls connected with a diaphragm was also explored proving this to be beneficial for internal fibrous plastering for both inward and outward lateral resistance.

Chapter 7. Conclusions and recommendations for future work

7.1 Conclusions

The objective of this doctoral study is to determine what improvement to the lateral resistance of unmortared walls of low-cost housing can be achieved through the addition of natural fibrous plaster. Two fibres were considered: rice straw because it is very cheap and sisal because it is known to have superior properties. Measurement of the mechanical properties of blocks and fibrous plaster is required to evaluate the overall performance of masonry walls. The properties of cementitious materials, strengthened with the fibres listed above, were examined and their characterisation as reported in the literature was extended. Lateral strength and stiffness of masonry single-block ISSB columns was experimentally evaluated at the National Housing and Building Research Agency (NHBRA) in Dar es Salam with different variations of 8 mm thin and 20 mm thick plastering. Mortared columns with 8 mm thin sisal plaster were also tested at Warwick University UK. Numerical modelling of experimental work related to ISSB columns was carried out. The aim of this numerical work was to develop Non-Linear Finite Element (NLFE) models compatible with the experimental findings to explore the likely failure mechanism (e.g. plaster-to-block bond failure) and to conduct parametric studies more cheaply than by constructing many walls. The extended research was carried out to evaluate the performance of the fibrous plastered interlocked walling system for out-of-plane resistance. The conclusions from this study are listed below:

- Ability adequately to resist lateral loads mainly determines the design thickness of masonry walls.
    - For cheap mortarless ISSB walling, the lateral resistance is poor and fails to offer significant resistance to earthquakes.
    - Use of fibres in plaster is a better technique for enhancing the strength of masonry structure than adding fibres to either block or mortar. Moreover, the addition of fibres to plaster is easier than adding them to block or mortar.
- The failure modes of the fibrous-plaster samples were characterised by a bridging phenomenon due to presence of fibres as compared to unlike crushing failure of plain-plaster samples.

- Microscopic images of sisal fibrous samples showed the embedment of sisal fibre in cement paste without any gap or void, indicating a proper bond of fibre to the cement matrix. This resulted in better mechanical properties than samples containing rice straw.

- Plastering increased the lateral elastic **stiffness** by 4 times for ISSB columns, and a further increase of 2.6 times was observed following the addition of sisal fibres to the plaster.
  - Addition of plaster substantially improved the lateral out-of-plane **strength** of an ISSB column - by 2.2 times as compared with an unplastered ISSB column. Further addition of fibres to the plaster can realistically increase lateral strength by 3 times for sisal fibres and 2.4 times for rice straw.
  - Sisal fibres in the plaster increases pre- and post-crack **energy absorption** by factors of 6 and 10 times respectively, whereas for rice straw the factors were less, namely 2.5 and 3.5 times.
  - Fibres enhance the **toughness** of plastered columns by a factor of 1.49 for sisal and 1.09 times for rice straw.
  - Addition of sisal fibres in the mortar of mortared masonry columns did not enhance their performance.
- Finite-element parametric study suggested that increasing the strength of plaster will not increase the lateral failure load for ISSB column.
  - The increase in lateral strength following inclusion of fibres in plaster may allow a reduction in the thickness of the blocks used in walling. Analysis showed that fibrous plaster applied to a wall of only 25 mm thickness would give a lateral performance equal to that of a 150-mm thick unplastered wall. This yielded a 67% cost saving.
  - Parametric study for plaster strength suggested that increasing the strength of plaster will not change the failure load. This is because failure occurs at the interface between plaster and block.
  - Parametric study for the thickness of applied plaster showed that increase in the thickness results in some increase of failure load. However, this

increase is not linear: for example, a 150% increase in thickness only resulted in a 28% increase in lateral failure load.

- Elastic **stiffness** was increased for the plain plastered walling system by 14 times whereas for sisal and rice straw plastered walling system this increase was 11 and 12 times respectively than unplastered walling system.
  - Lateral out-of-plane **strength** was increased by 2.2 times for plain plastered and 2.4 and 2.3 times, for sisal and rice straw reinforced plastered walling system, respectively.
  - Total **energy absorbed** for the plain plastered walling system was increased by 142% as compared with unplastered wall; whereas further increases of 144% and 56% were observed for sisal plastered and rice straw plastered walling system respectively.
  - Plastering increased the **toughness** index of ISSB walls by 55%, whereas a further 47% increase was observed for sisal plastered walls and a small increase of 2% increase was observed for rice straw plastered walls.
  - Natural fibres will decay in wet conditions and is therefore more suitable for internal, not external plaster. The inclusion of fibres only on internal faces of a wall means its resistance to outward is higher than to inwards forces. To achieve bi-directional strengthening facing walls need to be connected with a diaphragm and act as a portal frame.

From the experimental results it became clear that the lateral resistance of interlocked walls was enhanced by the addition of plaster and further improvement could be achieved by the addition of natural fibres in the plaster. It can therefore be concluded that addition of fibrous plaster could lead to masonry interlocking wall with better out-of-plane performance.

Finite element analysis parametric study revealed that lateral strength of an interlocked wall will not be increased by increasing the strength and thickness of plaster. It was found that the interface between block and plaster governs failure mode in such construction. It was also found from analysis that a 67% cost saving could be achieved by reducing the thickness of blocks.

7.2 Recommendations

7.2.1 For future researcher

Following are the recommendations for the future work:

- Evaluations of long-term durability of fibrous external plastering
- Experimental investigation of interface between block/block and block plaster.
- Out-of-plane testing of roof connections under seismic loading
- In-plane testing of wall assembly and connections
- Full-scale testing of interlocked wall housing under 3D seismic loading.
- Finite element modelling of walls with validated interface properties
- Development of complete design guidelines for fibrous plastered interlocked walling system

7.2.2 For housing industry

From the experimental and analytical modelling work, it has been established that low lateral resistance of interlocked masonry walls can be improved by the addition of the plaster on the tension face of the wall. Further improvement in the ductility of the plastering could be achieved by the addition of cheap natural fibres like rice straw and sisal. It was observed that the walling system reinforced with sisal plaster performed better than the rice-straw reinforced plaster. For the practical application of building a low-cost house using interlocked blocks the following points should be considered:

- Soil-stabilised interlocking blocks could be manufactured using a cheap manual press and unskilled labour. The recommended design mix ratio of soil and cement was 12:1. However, blocks need to be kept moist during curing to attain compressive strength of 1.5 MPa or above.
- Plastering of a wall on the tension face should be considered for improved lateral resistance. Further improvement can be achieved by the addition of locally available natural fibres like sisal having good tensile strength. 2% fibres by weight of cement should be added in plaster with a W/C ratio of 0.67. Thin fibrous plastering of 8 to 10 mm thickness should be considered for better performance and low cost.

- In the case of single storey structure with timber roof truss and timber beam, special consideration should be given to the joint between timber beam and interlocked wall for bi-directional strengthening. This will enable application of fibrous plaster only on internal faces of walls.
- Fibrous plastering of external walls subject to weathering could be periodically re-applied in layers to maintain structural integrity.

References

Aggarwal, L. K. (1992) Studies on cement-bonded coir fibre boards. *Cement and Concrete Composites,* 14 (1): 63-69.

Agopyan, V., Savastano Jr, H., John, V. M. & Cincotto, M. A. (2005) Developments on vegetable fibre-cement based materials in São Paulo, Brazil: An overview. *Cement and Concrete Composites,* 27 (5): 527-536.

Albahttiti, M. T., Rasheed, H. A., Peric, D. & Davis, L. (2013) Assessment of wheat fibre reinforced cementitious matrix. *IES Journal Part A: Civil & Structural Engineering,* 6 (3): 211-221.

Alecci, V., Fagone, M., Rotunno, T. & De Stefano, M. (2013) Shear strength of brick masonry walls assembled with different types of mortar. *Construction and Building Materials,* 40 1038-1045.

Ali, M., Liu, A., Sou, H. & Chouw, N. (2012) Mechanical and dynamic properties of coconut fibre reinforced concrete. *Construction and Building Materials,* 30 814-825.

Ali, M., Liu, A., Gultom, R. & Chouw, N. (2012) Capacity of innovative interlocking blocks under monotonic loading. *Construction and Building Materials,* 37 812-821.

Ali, Q. & Naeem, A. (2007) Seismic resistance evaluation of unreinforced masonry buildings. *Journal of Earthquake Engineering,* 11 (2): 133-146.

Amin Al-Fakih, Bashar, S. M. & Mohd. S. L. (2018) Behavior of the Dry Bed Joint in the Mortarless Interlocking Masonry System: an Overview. *Civil Eng Research Journal,* 4 (3): 1-5.

Anand, K. B. & Ramamurthy, K. (2000) Development and performance evaluation of interlocking-block masonry. *Journal of Architectural Engineering,* 6 (2): 45-50.

Asadi, A., Baaij, F., Mainka, H., Rademacher, M., Thompson, J. & Kalaitzidou, K. (2017) Basalt fibers as a sustainable and cost-effective alternative to glass fibers in sheet molding compound (SMC). *Composites Part B: Engineering,* 123 210-218.

Asasutjarit, C., Charoenvai, S., Hirunlabh, J. & Khedari, J. (2009) Materials and mechanical properties of pretreated coir-based green composites. *Composites Part B: Engineering,* 40 (7): 633-637.

Asasutjarit, C., Hirunlabh, J., Khedari, J., Charoenvai, S., Zeghmati, B. & Shin, U. C. (2007) Development of coconut coir-based lightweight cement board. *Construction and Building Materials,* 21 (2): 277-288.

Balsamo, A., Di Ludovico, M., Prota, A. & Manfredi, G. (2011a) Masonry walls strengthened with innovative composites. *Am. Concr. Inst.* 275 769–786.

Basili, M., Marcari, G. & Vestroni, F. (2016) Nonlinear analysis of masonry panels strengthened with textile reinforced mortar. *Engineering Structures,* 113 245-258.

Bejarano-Urrego, L., Verstrynge, E., Giardina, G. & Van Balen, K. (2018) Crack growth in masonry: Numerical analysis and sensitivity study for discrete and smeared crack modelling. *Engineering Structures,* 165 471-485.

Bernat, E., Gil, L., Roca, P. & Sandoval, C. (2013) Experimental and numerical analysis of bending-buckling mixed failure of brickwork walls. *Construction and Building Materials,* 43 1-13.

Bosiljkov, V. Z., Totoev, Y. Z. & Nichols, J. M. (2005) Shear modulus and stiffness of brickwork masonry: An experimental perspective. *Structural Engineering and Mechanics,* 20 (1): 21-43.

Bouhicha, M., Aouissi, F. & Kenai, S. (2005a) Performance of composite soil reinforced with barley straw. *Cement and Concrete Composites,* 27 (5): 617-621.

BS EN 1015-11:1999 Methods of test for mortar for masonry. Determination of flexural and compressive strength of hardened mortar. *British Standards Institution*.

BS EN 1052-1:1999 Methods of test for masonry. Determination of compressive strength. *British Standards Institution*.

Chewe Ngapeya, G. G., Waldmann, D. & Scholzen, F. (2018) Impact of the height imperfections of masonry blocks on the load bearing capacity of dry-stack masonry walls. *Construction and Building Materials*, 165 898-913.

Curtin, W. G., Shaw, G., Beck, J., Bray, W. A. & Easterbrook, D. (2006) *Structural Masonry Designer's Manual*. Chichester, United Kingdom: John Wiley & Sons, Incorporated.

Danso, H., Martinson, B., Ali, M. & Mant, C. (2015a) Performance characteristics of enhanced soil blocks: A quantitative review. *Building Research & Information*, 43 (2): 253-262.

De Felice, G., Aiello, M. A., Bellini, A., Ceroni, F., De Santis, S., Garbin, E., Leone, M., Lignola, G. P., Malena, M., Mazzotti, C., Panizza, M. & Valluzzi, M. R. (2016) Experimental characterization of composite-to-brick masonry shear bond. *Materials and Structures/Materiaux et Constructions*, 49 (7): 2581-2596.

De Risi, M. T., Furtado, A., Rodrigues, H., Melo, J., Verderame, G. M., António, A., Varum, H. & Manfredi, G. (2020) Experimental analysis of strengthening solutions for the out-of-plane collapse of masonry infills in RC structures through textile reinforced mortars. *Engineering Structures*, 207 110203.

Dehghan, S. M., Najafgholipour, M. A., Baneshi, V. & Rowshanzamir, M. (2018) Mechanical and bond properties of solid clay brick masonry with different sand grading. *Construction and Building Materials*, 174 1-10.

Di Bella, G., Fiore, V., Galtieri, G., Borsellino, C. & Valenza, A. (2014) Effects of natural fibres reinforcement in lime plasters (kenaf and sisal vs. Polypropylene). *Construction and Building Materials*, 58 159-165.

Dirar, S., Lees, J. & Morley, C. (2012) Precracked Reinforced Concrete T-Beams Repaired in Shear with Bonded Carbon Fiber-Reinforced Polymer Sheets. *Aci Structural Journal*, 109 (2): 215-223.

Dirar, S., Lees, J. M. & Morley, C. T. (2013) Precracked Reinforced Concrete T-Beams Repaired in Shear with Prestressed Carbon Fiber-Reinforced Polymer Straps. *Aci Structural Journal*, 110 (5): 855-865.

Dizhur, D., Griffith, M. & Ingham, J. (2014) Out-of-plane strengthening of unreinforced masonry walls using near surface mounted fibre reinforced polymer strips. *Engineering Structures*, 59 330-343.

Ehsani, M. R., Saadatmanesh, H. & Al-Saidy, A. (1997) Shear behavior of URM retrofitted with FRP overlays. *Journal of Composites for Construction*, 1 (1): 17-25.

Emami, A., Fehling, E. & Schlimmer, M. (2011a) External strengthening of masonry structures with natural fibers. *International Journal for Housing Science and Its Applications*, 35 (2): 125-135.

EN 1996-1-1:2005 Eurocode 6: design of masonry structures-part 1-1: common rules for reinforced and unreinforced masonry structures. *Brussels.*

Figueiredo, A., Varum, H., Costa, A., Silveira, D. & Oliveira, C. (2013) Seismic retrofitting solution of an adobe masonry wall. *Materials and Structures*, 46 (1-2): 203-219.

Fundi, S. I., Kaluli, J. W. & Kinuthia, J. (2018) Performance of interlocking laterite soil block walls under static loading. *Construction and Building Materials*, 171 75-82.

Gassan, J., Chate, A. & Bledzki, A. K. (2001) Calculation of elastic properties of natural fibers. *Journal of Materials Science*, 36 (15): 3715-3720.

Gattesco, N. & Boem, I. (2015) Experimental and analytical study to evaluate the effectiveness of an in-plane reinforcement for masonry walls using GFRP meshes. *Construction and Building Materials*, 88 94-104.

Giamundo, V., Lignola, G. P., Prota, A. & Manfredi, G. (2014a) Nonlinear analyses of adobe masonry walls reinforced with fiberglass mesh. *Polymers*, 6 (2): 464-478.

Graham, R. K., Baoshan, H., Xiang, S. & Burdette, E. G. (2013) Laboratory evaluation of tensile strength and energy absorbing properties of cement mortar reinforced with micro- and meso-sized carbon fibers. *Construction and Building Materials*, 44 751-756.

Guerreiro, J., Proença, J., Ferreira, J. G. & Gago, A. (2018) Experimental characterization of in-plane behaviour of old masonry walls strengthened through the addition of CFRP reinforced render. *Composites Part B: Engineering*, 148 14-26.

Gupta, R. (2014) Characterizing material properties of cement-stabilized rammed earth to construct sustainable insulated walls. *Case Studies in Construction Materials*, 1 60-68.

Hee, S.C. & Jefferson, A.D. (2008) A new model for simulating cracks in cementitious composites. *Proceedings of the Institution of Civil Engineers – Engineering and Computational Mechanics*, 161(1): 3-16.

Ismail, N. & Ingham, J. M. (2016) In-plane and out-of-plane testing of unreinforced masonry walls strengthened using polymer textile reinforced mortar. *Engineering Structures*, 118 167-177.

Jaafar, M. S., Thanoon, W. A., Najm, A. M. S., Abdulkadir, M. R. & Ali, A. A. A. (2006) Strength correlation between individual block, prism and basic wall panel

for load bearing interlocking mortarless hollow block masonry. *Construction and Building Materials*, 20 (7): 492-498.

John, V. M., Cincotto, M. A., Sjostrom, C., Agopyan, V. & Oliveira, C. T. A. (2005) Durability of slag mortar reinforced with coconut fibre. *Cement & Concrete Composites*, 27 (5): 565-574.

Juarez, C., Guevara, B., Valdez, P. & Duran-Herrera, A. (2010) Mechanical properties of natural fibers reinforced sustainable masonry. *Construction and Building Materials*, 24 (8): 1536-1541.

Kalali, A. & Kabir, M. Z. (2012a) Experimental response of double-wythe masonry panels strengthened with glass fiber reinforced polymers subjected to diagonal compression tests. *Engineering Structures*, 39 24-37.

Kennedy, N. E. (2013). Seismic design manual for interlocking compressed earth blocks. *Master of Science Thesis*. California Polytechnic State University.

Khonsari, S. V., Eslami, E. & Anvari, A. (2018) Fibrous and non-fibrous Perlite concretes–experimental and SEM studies. *European Journal of Environmental and Civil Engineering*, 22 (2): 138-164.

King, C., Richardson, M., McEniry, J. & O'Kiely, P. (2013a) Potential use of fibrous grass silage press-cake to minimise shrinkage cracking in low-strength building materials. *Biosystems Engineering*, 115 (2): 203-210.

Kintingu, S. H. (2009). Design of interlocking bricks for enhanced wall construction, flexibility, alignment accuracy and load bearing. *PhD Thesis*, University of Warwick, UK.

Kohail, M., Elshafie, H., Rashad, A. & Okail, H. (2019) Behavior of post-tensioned dry-stack interlocking masonry shear walls under cyclic in-plane loading. *Construction and Building Materials*, 196 539-554.

Laursen, P. T., Herskedal, N. A., Jansen, D. C. & Qu, B. (2015) Out-of-plane structural response of interlocking compressed earth block walls. *Materials and Structures/Materiaux et Constructions,* 48 (1-2): 321-336.

Lee, Y. H., Shek, P. N. & Mohammad, S. (2017) Structural performance of reinforced interlocking blocks column. *Construction and Building Materials,* 142 469-481.

Lertwattanaruk, P. & Suntijitto, A. (2015) Properties of natural fiber cement materials containing coconut coir and oil palm fibers for residential building applications. *Construction and Building Materials,* 94 664-669.

Li, Z. J., Wang, X. G. & Wang, L. J. (2006) Properties of hemp fibre reinforced concrete composites. *Composites Part a-Applied Science and Manufacturing,* 37 (3): 497-505.

Lignola, G. P., Prota, A. & Manfredi, G. (2009) Nonlinear analyses of tuff masonry walls strengthened with cementitious matrix-grid composites. *Journal of Composites for Construction*, 13 (4): 243-251.

Lignola, G. P., Prota, A. & Manfredi, G. (2012) Numerical investigation on the influence of frp retrofit layout and geometry on the in-plane behavior of masonry walls. *Journal of Composites for Construction*, 16 (6): 712-723.

Lilholt, H. & Lawther, J. M. (2000) 1.10 - Natural Organic Fibers. In: Kelly, A. & Zweben, C., eds. *Comprehensive Composite Materials*. Oxford: Pergamon: 303-325.

Macabuag, J. Guragain, R. & Bhattacharya, S. (2012) Seismic retrofitting of non-engineered masonry in rural Nepal. *Proceedings of the Institution of Civil Engineers-Structures and Buildings,* 165 (6): 273-286.

Magenes, G. & Calvi, G. (1997) In-plane seismic response of brick masonry walls. *Earthquake Engineering & Structural Dynamics,* 26 (11): 1091-1112.

Mahmood, H. & Ingham, J. M. (2011) Diagonal compression testing of FRP-retrofitted unreinforced clay brick masonry wallettes. *Journal of Composites for Construction*, 15 (5): 810-820.

Marcari, G., Manfredi, G., Prota, A. & Pecce, M. (2007) In-plane shear performance of masonry panels strengthened with FRP. *Composites Part B: Engineering*, 38 (7-8): 887-901.

Martínez, M. & Atamturktur, S. (2019) Experimental and numerical evaluation of reinforced dry-stacked concrete masonry walls. *Journal of Building Engineering*, 22 181-191.

Menna, C., Asprone, D., Durante, M., Zinno, A., Balsamo, A. & Prota, A. (2015) Structural behaviour of masonry panels strengthened with an innovative hemp fibre composite grid. *Construction and Building Materials*, 100 111-121.

Mesbah, A., Morel, J. C., Walker, P. & Ghavami, K. (2004) Development of a direct tensile test for compacted earth blocks reinforced with natural fibers. *Journal of Materials in Civil Engineering*, 16 (1): 95-98.

Millogo, Y., Morel, J. C., Aubert, J. E. & Ghavami, K. (2014) Experimental analysis of Pressed Adobe Blocks reinforced with Hibiscus cannabinus fibers. *Construction and Building Materials*, 52 71-78.

Mohamad, G., Lourenco, P. B. & Roman, H. R. (2007) Mechanics of hollow concrete block masonry prisms under compression: Review and prospects. *Cement & Concrete Composites*, 29 (3): 181-192.

Mohanty, A. K., Misra, M., Drzal, L. T., Selke, S. E., Harte, B. R. & Hinrichsen, G. (2005) Natural fibers, biopolymers, and biocomposites: An introduction. In: *Natural Fibers, Biopolymers, and Biocomposites*. 1-36.

Naveen, J., Jawaid, M., Amuthakkannan, P. & Chandrasekar, M. (2019) 21 - Mechanical and physical properties of sisal and hybrid sisal fiber-reinforced polymer composites. In: Jawaid, M., Thariq, M. & Saba, N., eds. *Mechanical and*

Physical Testing of Biocomposites, Fibre-Reinforced Composites and Hybrid Composites. Woodhead Publishing: 427-440.

Ngowi, H. C. U. a. J. V. (2003) Structural Behaviour of Dry-stack Interlocking Block Walling Systems Subject to In-plane Loading. *Concrete Beton*, 103 9-13.

Odogherty, M. J., Huber, J. A., Dyson, J. & Marshall, C. J. (1995) A study of the physical and mechanical-properties of wheat-straw. *Journal of Agricultural Engineering Research*, 62 (2): 133-142.

Padalu, P. K. V. R., Singh, Y. & Das, S. (2018) Efficacy of basalt fibre reinforced cement mortar composite for out-of-plane strengthening of unreinforced masonry. *Construction and Building Materials*, 191 1172-1190.

Paramasivam, P., Nathan, G. K. & Das Gupta, N. C. (1984) Coconut fibre reinforced corrugated slabs. *International Journal of Cement Composites and Lightweight Concrete*, 6 (1): 19-27.

Parisi, F., Iovinella, I., Balsamo, A., Augenti, N. & Prota, A. (2013) In-plane behaviour of tuff masonry strengthened with inorganic matrix-grid composites. *Composites Part B: Engineering*, 45 (1): 1657-1666.

Parisi, F., Lignola, G. P., Augenti, N., Prota, A. & Manfredi, G. (2011) Nonlinear behavior of a masonry subassemblage before and after strengthening with inorganic matrix-grid composites. *Journal of Composites for Construction*, 15 (5): 821-832.

Park, s. (1991) Experimental-study on the engineering properties of carbon-fiber reinforced cement composites. *Cement and Concrete Research*, 21 (4): 589-600.

Pereira, M., Fujiyama, R., Darwish, F. & Alves, G. (2015a) On the Strengthening of Cement Mortar by Natural Fibers. *Materials Research-Ibero-American Journal of Materials*, 18 (1): 177-183.

Phillips, D. V. & Zhang, B. S. (1993) Direct tension tests on notched and un-notched plain concrete specimens. *Magazine of Concrete Research*, 45 (162): 25-35.

Prota, A., Marcari, G., Fabbrocino, G., Manfredi, G. & Aldea, C. (2006) Experimental in-plane behavior of tuff masonry strengthened with cementitious matrix-grid composites. *Journal of Composites for Construction*, 10 (3): 223-233.

Qapo, M., Dirar, S., Yang, J. & Elshafie, M. (2015) Nonlinear finite element modelling and parametric study of CFRP shear-strengthened prestressed concrete girders. *Construction and Building Materials*, 76 245-255.

Qin, S. (2016). Shear behaviour of corroded reinforced concrete t-beams repaired with fibre reinforced polymer systems. *PhD Thesis*, University of Birmingham, UK

Qu, B., Stirling, B. J., Jansen, D. C., Bland, D. W. & Laursen, P. T. (2015a) Testing of flexure-dominated interlocking compressed earth block walls. *Construction and Building Materials*, 83 34-43.

Ramakrishna, G. & Sundararajan, T. (2005a) Impact strength of a few natural fibre reinforced cement mortar slabs: A comparative study. *Cement and Concrete Composites*, 27 (5): 547-553.

Ramakrishna, G. & Sundararajan, T. (2005b) Studies on the durability of natural fibres and the effect of corroded fibres on the strength of mortar. *Cement and Concrete Composites*, 27 (5): 575-582.

Ramamoorthy, S. K., Skrifvars, M. & Persson, A. (2015) A Review of Natural Fibers Used in Biocomposites: Plant, Animal and Regenerated Cellulose Fibers. *Polymer Reviews*, 55 (1): 107-162.

Ramamurthy, K. & Anand, K. B. (2001) Influence of construction method on the behaviour of interlocking block masonry. *Journal of the Institution of Engineers (India): Civil Engineering Division*, 81 (4): 167-173.

Reis, J. M. L. (2006) Fracture and flexural characterization of natural fiber-reinforced polymer concrete. *Construction and Building Materials*, 20 (9): 673-678.

Rots, J. G. & Blaauwendraad, J. (1989) Crack models for concrete: discrete or smeared? Fixed multi-directional or rotatin? *Heron*, 34 (1): 3-59.

Safiee, N., Jaafar, M., Alwathaf, A., Noorzaei, J. & Abdulkadir, M. (2011) Structural behavior of mortarless interlocking load bearing hollow block wall panel under out-of-plane loading. *Advances in Structural Engineering*, 14 (6): 1185-1196.

Sandoval, C., Roca, P., Bernat, E. & Gil, L. (2011) Testing and numerical modelling of buckling failure of masonry walls. *Construction and Building Materials*, 25 (12): 4394-4402.

Sarhosis, V., Garrity, S. W. & Sheng, Y. (2015) Influence of brick-mortar interface on the mechanical behaviour of low bond strength masonry brickwork lintels. *Engineering Structures*, 88 1-11.

Sato, Y. & Vecchio, F. J. (2003) Tension stiffening and crack formation in reinforced concrete members with fiber-reinforced polymer sheets. *Journal of Structural Engineering-Asce*, 129 (6): 717-724.

Satyanarayana, K. G., Sukumaran, K., Mukherjee, P. S. & Pillai, S. G. K. (1986) Materials science of some lignocellulosic fibers. *Metallography*, 19 (4): 389-400.

Savastano, H., Santos, S. F., Radonjic, M. & Soboyejo, W. O. (2009) Fracture and fatigue of natural fiber-reinforced cementitious composites. *Cement & Concrete Composites*, 31 (4): 232-243.

Savastano, H., Warden, P. G. & Coutts, R. S. P. (2003) Potential of alternative fibre cements as building materials for developing areas. *Cement & Concrete Composites*, 25 (6): 585-592.

Schubert, P. (1988) The influence of mortar on the strength of masonry. *Brick and Block Masonry, Vols 1-3*, 162-174.

Scordelis, A.C. & Ngo, D. (1967). Finite element analysis of reinforced concrete beams. *J. Am. Concrete Inst*., 64 (14): 152-163.

Silva, F. d. A., Chawla, N. & Filho, R. D. d. T. (2008) Tensile behavior of high performance natural (sisal) fibers. *Composites Science and Technology*, 68 (15-16): 3438-3443.

Sivaraja, M., Kandasamy, Velmani, N. & Pillai, M. S. (2010) Study on durability of natural fibre concrete composites using mechanical strength and microstructural properties. *Bulletin of Materials Science*, 33 (6): 719-729.

Sorrentino, L., Masiani, R., Benedetti, S., Santini, A. & Moraci, N. (2008) Experimental estimation of energy damping during free rocking of unreinforced masonry walls. First results. *2008 Seismic Engineering Conference Commemorating the 1908 Messina and Reggio Calabria Earthquake, Pts 1 and 2*, 1020 1888-1895.

Soto Izquierdo, I., Soto Izquierdo, O., Ramalho, M. A. & Taliercio, A. (2017a) Sisal fiber reinforced hollow concrete blocks for structural applications: Testing and modeling. *Construction and Building Materials*, 151 98-112.

Stratford, T., Pascale, G., Manfroni, O. & Bonfiglioli, B. (2004) Shear strengthening masonry panels with sheet glass-fiber reinforced polymer. *Journal of Composites for Construction*, 8 (5): 434-443.

Sturm, T., Ramos, L. F. & Lourenço, P. B. (2015) Characterization of dry-stack interlocking compressed earth blocks. *Materials and Structures/Materiaux et Constructions*, 48 (9): 3059-3074.

Tavakoli, M., Tavakoli, H., Azizi, M. H. & Haghayegh, G. H. (2010) Comparison of mechanical properties between two varieties of rice straw. *Advance Journal of Food Science and Technology*, 2 (1): 50-54.

Thanoon, W. A., Jaafar, M. S., Kadir, M. R. A., Ali, A. A. A., Trikha, D. N. & Najm, A. M. S. (2004) Development of an innovative interlocking load bearing hollow block system in Malaysia. *Construction and Building Materials,* 18 (6): 445-454.

Thanoon, W. A., Jaafar, M. S., Noorzaei, J., A. Kadir, M. R. & Fares, S. (2007) Structural behaviour of mortar-less interlocking masonry system under eccentric compressive loads. *Advances in Structural Engineering,* 10 (1): 11-24.

Toihidul Islam, M. & Bindiganavile, V. (2011) The impact resistance of masonry units bound with fibre reinforced mortars. *Construction and Building Materials,* 25 (6): 2851-2859.

Toledo, R. D., Ghavami, K., Sanjuan, M. A. & England, G. L. (2005) Free, restrained and drying shrinkage of cement mortar composites reinforced with vegetable fibres. *Cement & Concrete Composites,* 27 (5): 537-546.

Toledo Filho, R. D., Silva, F. (2009) Durability of compression molded sisal fiber reinforced mortar laminates. *Construction and Building Materials,* 23: 2409-2420.

Tomazevic, M. (2009) Shear resistance of masonry walls and Eurocode 6: shear versus tensile strength of masonry. *Materials and Structures,* 42 (7): 889-907.

Tripura, D. D. & Singh, K. D. (2018) Mechanical behaviour of rammed earth column: A comparison between unreinforced, steel and bamboo reinforced columns. *Materiales De Construccion,* 68 (332): 11.

Uzoegbo, H. C. (2001) - Lateral Loading Tests on Dry-Stack Interlocking Block Walls. In: Zingoni, A., ed. *Structural Engineering, Mechanics and Computation*. Oxford: Elsevier Science: 427-436.

Vaculik, J., Griffith, M. C. & Magenes, G. (2014) Dry stone masonry walls in bending-Part II: Analysis. *International Journal of Architectural Heritage,* 8 (1): 29-48.

Valluzzi, M. R., da Porto, F., Garbin, E. & Panizza, M. (2014) Out-of-plane behaviour of infill masonry panels strengthened with composite materials. *Materials and Structures/Materiaux et Constructions*, 47 (12): 2131-2145.

Vargas, H. G. (1988) Mortarless Masonry: The Mecano System. *International Journal for Housing Science and Its Applications*, 12 (2): 145-157.

Velazquez-Dimas, J. I. & Ehsani, M. R. (2000) Modeling out-of-plane behavior of URM walls retrofitted with fiber composites. *Journal of Composites for Construction*, 4 (4): 172-180.

Wang, C. L., Forth, J. P., Nikitas, N. & Sarhosis, V. (2016) Retrofitting of masonry walls by using a mortar joint technique; experiments and numerical validation. *Engineering Structures*, 117 58-70.

Wei, J. Q., Ma, S. W. & Thomas, D. G. (2016) Correlation between hydration of cement and durability of natural fiber-reinforced cement composites. *Corrosion Science*, 106 1-15.

Zhang, K., Wang, F. X., Liang, W. Y., Wang, Z. Q., Duan, Z. W. & Yang, B. (2018) Thermal and Mechanical Properties of Bamboo Fiber Reinforced Epoxy Composites. *Polymers*, 10 (6): 18.

Zhu, M. & Chung, D. (1997) Improving brick-to-mortar bond strength by the addition of carbon fibers to the mortar. *Cement and Concrete Research*, 27 (12): 1829-1839.

Zia, A. & Ali, M. (2017) Behavior of fiber reinforced concrete for controlling the rate of cracking in canal-lining. *Construction and Building Materials*, 155 726-739.

Zych, T. & Wojciech, K. (2012) Study on the properties of cement mortars with basalt fibres. In: Brandt, A. M., Olek, J., Glinicki, M. A. & Leung, C. K. Y., eds. *Brittle Matrix Composites 10*. Woodhead Publishing: 155-166.

Çaktı, E., Saygılı, Ö., Lemos, J. V. & Oliveira, C. S. (2016) Discrete element modeling of a scaled masonry structure and its validation. *Engineering Structures,* 126 224-236.

Annex A Natural fibres classification, properties and applications

A1- Natural fibres

Researchers have identified natural fibres as a possible substitute for steel or artificial fibres in composites such as cement paste, mortar and concrete (Ramaswamy et al., 1983; Paramasivam et al., 1984; Aggarwal, 1992; Agopyan et al., 2005; John et al., 2005; Ramakrishna and Sundararajan, 2005a and 2005b; Toledo et al., 2005; Li et al., 2006; Asasutjarit et al., 2007; Reis, 2007). These natural fibres include sisal, coconut, jute, hibiscus cannabinus, eucalyptus grandis pulp, malva, ramie bast, pineapple leaf, kenaf bast, sansevieria leaf, abaca leaf, vakka, date, bamboo, palm, banana, hemp, flax, cotton and sugarcane fibres. Natural fibres are much cheaper than synthetic fibres (Paramasivam et al. 1984) and are locally available in many countries. At fibre contents below 5% the cost of using of natural fibres for improving the properties of composite is only a fraction of the total cost of composites. They are also easier to handle than steel fibres because of their higher flexibility, especially when the fibre fraction is high. However, in this case, a new casting methodology needs to be developed. In different studies, terminologies such as ‘volume fraction’ and ‘fibre content’ are used for expressing the quantities of fibres (Asasutjarit et al., 2007). The ‘volume fraction’ of fibres is the percentage of fibres by volume of composite materials or of any of its ingredients, e.g. 1% fibre mortar. Similarly, ‘fibre content’ is the percentage of fibres *by mass* of composite materials or any of its ingredients, e.g. 5% fibres in a fibre-reinforced cement (‘frc’) mix. Researchers have sought to identify the quantity and length of fibres needed to obtain maximum strength of the composite, as any deviation in volume fraction about the optimum level may be detrimental for strength properties or for economy.

A2- Classification and properties of natural fibres

Plant cells are protected by a rigid cell wall which doesn't exist in cells from animals. These rigid walls give plants superior mechanical properties such as rigidity. The dimensions of these fibres vary between different plants but their overall shape is elongated with lengths in the range 1-35mm and diameters in the range 15-30µm. Natural plant fibres are sometimes classified according to origin into 'wood' and 'non-wood' species. Figure A2.1 below details the classification of natural fibres based on their origin.

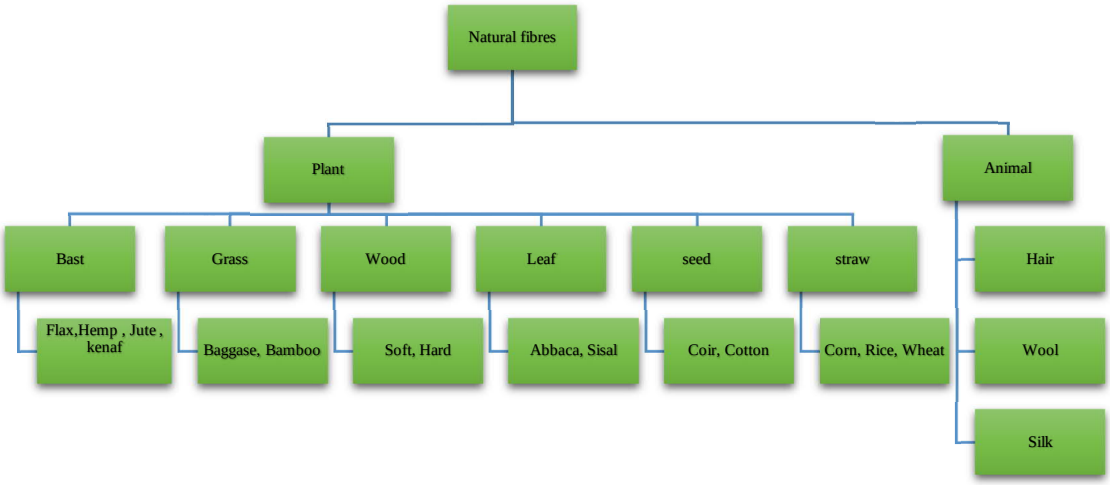

Figure A2.1: Classification of natural fibres

Plant fibres are basically comprise a matrix of (rigid crystalline) cellulose, lignin and hemicellulose. The major part is cellulose which represents 40-50% of plant solids.. The structure, cell dimensions and chemical composition of plant fibres are the most important variables determining their overall properties. (Mukherjee and Satyanarayana, 1986). Physical properties like structure, density and microfibrillar angle (MFA) also have impact on the mechanical properties of fibres. It is reported by

Mohanty et al. (2005a, b) that both higher fibre content and lower MFA map onto higher ultimate tensile strength. Table A1 below summarise some physical and mechanical properties of common vegetable found fibres. Based on this data fibres can be classed as 'high strength' like sisal, hemp, flax and coir and 'low strength' like wheat and rice straw. This research will examine use of both high and low strength fibres and their impact on the strength of masonry wall composites when fibres are utilised in plastering and mortar.

Table A1: Physical and mechanical properties of natural fibres

	Physical Properties			**Mechanical Properties**			
Fibre	Density (kg/m^3)	Cellulose content (%)	Microfibrillar angle (MFA) (degrees)	Tensile strength (MPa)	Young's Modulus (GPa)	Ultimate stress (MPa)	Reference
Wheat straw	1600	-	-	273	4.76-6.58	-	O'Dogherty et al. (1995)
Rice straw	1650	-	-	449	1.21-1.25	-	Tavakoli et al. (2010)
Sisal	1200	66-78	10-25	507-885	9.4-22	100-800	Mohanty et al. (2005a, b), Gassan et al. (2001), Lilholt and Lawther (2000)
Hemp	1350	70-74	6	580-1110	70	300-800	Mohanty et al. (2005a, b), Gassan et al. (2001), Lilholt and Lawther (2000)
Flax	1380	64-71	6-10	343-1035	27.6	500-900	Mohanty et al. (2005a, b), Gassan et al. (2001), Lilholt and Lawther (2000)
Coir	1200	32-43	30-49	175	4-6	-	Mohanty et al. (2005a, b), Gassan et al. (2001), Lilholt and Lawther (2000)

A3 - Application of natural fibres reinforced composites in civil engineering

Most researchers have examined coir and sisal fibres due to their good mechanical properties like high tensile strength etc. Table A2 lists examples of applications of fibre-reinforced composites.

Table A2: Examples of application of fibre reinforced composites in civil engineering

Type of Fibre	Application	Reference
Coir	Corrugated slab	Paramasivam et al. (1984)
Sisal& Coir	Impact resistance of slabs	Ramakrishna and Sundararajan (2005b)
Sisal & Coir	Roofing tiles	Agopyan et al. (2005)
Coir	Wall panels/boards	Asasutjarit et al. (2007)

A4 - Durability of natural fibres

The durability of natural fibres remains a topic of interest for many researchers. Table A3 presents a summary of research into the durability of natural fibres in isolation and when incorporated in frcs.

Table A3: Literature review of durability of natural fibres

Fibres used	Variables investigated	Durability test	Main findings	Reference
coconut, sisal, jute and hibiscus cannabinus	Variation in chemical composition & tensile strength	Alternate wetting & drying & continuous immersion for 60 days in water, saturated lime and sodium hydroxide	Chemical composition of all fibres changed and loss in tensile strength was observed, however sisal and coir retained over 75% of their initial tensile strength	Ramakrishna and Sundararajan (2005)
sisal and coconut	Flexural strength and toughness	Fibres stored in tap water of pH 8.3; a solution of calcium hydroxide of pH 12; and a solution of sodium hydroxide of pH 11.	After 420 days, sisal and coconut fibres retained, respectively, 83% and 77% of their original strength when conditioned in tap water of pH 8.3.	Toledo.et.al. (2005)
sisal and coconut	Durability of flexural strength of frc.	Controlled cycles of wetting and drying. Carbonation of matrix in CO_2-rich environments, in silica fume slurry, and replacement of portland cement by silica fume.	Samples in a CO_2-rich environment retained 70-93.5% of their flexural strength and toughness Immersion of fibres in silica fume increased their flexural strength and toughness by 50% and 38% respectively (after 180 days when compared to sample at 28 days).	Toledo.et.al. (2005)

coir-mesh frc	Four-point bending test	Alkaline treated fibres	frc reinforced with treated fibres had greater toughness (44%) and ductility (73%) than that reinforced with untreated fibres.	Li et al. (2006)
coir and sugarcane frc	Mass loss	300 cycles of freezing and thawing	Concrete mass loss was 16.5% & 15.6% for coir and sugarcane frc respectively as compared to 14% for unreinforced concrete.	Sivaraja et al. (2010)
sisal	Fibre degradation and mechanism responsible for fibre composite degradation	5,10,15 and 20 cycles of wetting and drying	Two fibre degradation mechanism were observed in frcs, fibre mineralization and degradation of cellulose & lignin due to adsorption of calcium and hydroxyl ions.	Toledo Filho et al. (2009)
sisal	Degradation of sisal fibre in frc	Seven aggressive conditions including repeated wetting and drying; static environments with various temperature and humidities	Cyclic changes of humidity at relative high temperature accelerate the degradation of sisal in frc more effectively than do static aggressive conditions	Jianqing Wei et.al (2016)
sisal	influence of cement hydration on durability of sisal fibres	5, 30 and 50 wetting and drying cycles	Four supplementary cementitious materials (SCMs) in frc mixes slowed down both mineralization and alkaline hydrolysis by promoting the hydration of cement. Degradation of sisal fibre was significantly mitigated and durability of the frc improved.	Jianqing Wei et.al (2016)

The different studies listed in the table above suggest that sisal and coconut fibres have better resistance to severe conditions than the other fibres as they retained about 70% of their initial mechanical strengths.

The study by Toledo Filho et al. (2009) examined different approaches to improving the durability of natural-fibre-reinforced composites. These consisted of;

- Carbonation of the matrix in a CO_2-rich environment

- The immersion of fibres in slurried silica fume (SF) prior to incorporation in the Ordinary Portland Cement (OPC) matrix; and
- Partial replacement of OPC by undensified SF or blast furnace slag.

The study by Jianqing Wei et al. (2016) suggested that durability of sisal fibre within a cement matrix can be enhanced by addition of supplementary cementitious material like metakaolin (MK) at about 30% wt. of cement. This can be employed for external walling subjected to extreme weather.

A5 - Effect of natural fibres on seismic parameters

Earthquakes are natural hazards which can lead to a catastrophic failure of structures and the loss of human lives. It has been observed through a number of studies that non-engineered structures, including low-cost houses of unreinforced brick masonry or mud suffer most from earthquake damage (M. Ehsani 1996). It is reported by Figueiredo. A (2013) that earthquake in 2001 in the region of Peru, resulted in destruction of 36,000 houses, out of which 25,000 were composed of adobe. Therefore, there is a great need to understand the parameter of earthquake loading and develop techniques to increase the resistance of these structures. Broadly, methods for strengthening masonry can be divided into two general categories Firstly one can add significant extra structural elements within an existing structure which result in changes of load path. Secondly one can enhance the strength and ductility of walling of masonry by adding of various ‘coatings’. This research will mainly focus on the second technique.

Seismic parameters Masonry is a typical composite construction material which is suitable to carry compressive loads but whose capacity to carry tension and shear is low. During earthquakes, structures are subjected to lateral loads which lead to in-plane shear and out-of-plane flexural stresses. Many studies have been carried out to evaluate the seismic resistance of masonry structures. Some of these are summarised in the Table A4 below;

Table A4: Literature review of seismic resistance of masonry structures

Reference	Type of Study	Application	Variable investigated	Main Findings
Figueiredo. A, 2013	Behaviour of adobe construction under large cyclic loads	Masonry houses with and without seismic retrofitting	Stiffness, energy dissipation and shear capacity of walls	Walls were subjected to cyclic tests. After the first cycle of loading, wall strength decreased with a notable reduction in stiffness, resulting in a fragile-failure mode under the dynamic loading. After the first cycle, some walls were repaired with hydraulic lime gum and strengthened with synthetic mesh and testing again for cyclic loading. Repair and strengthening increased the wall's maximum resistance or shear capacity by 23%, maximum drift (ratio of displacement by wall height) by 220% and significant improved energy dissipation. In addition, no fragile ruptures were observed.
Sorrentino.L, 2008	Estimation of energy damping	Unreinforced masonry walls unconstrained ('two-sided rocking') or constrained on one side only ('one-sided rocking')	Impact energy dissipation	Damage reduces both displacement capacity and energy damping. Much faster energy damping for one sided rocking wall (adjacent to two transverse walls) was found as compared to two-sided rocking wall. More energy damping means motion will stop quickly. Transition from two sides rocking to one side rocking accompanied by marked increase in energy dissipation.
Macabuag, 2012	Upgrading of masonry structure to reduce the damage using polypropylene meshing	Low cost traditional masonry houses	Behaviour of masonry structure under static and dynamic loading with and without upgrading	Masonry shear resistance to in-plane lateral load was obtained by testing strengthened and non-strengthened prisms. It was found that strengthened model continued to carry load

				after initial failure. Under dynamic testing it was found that strengthening with polypropylene mesh enhanced the seismic resistance of the masonry model significantly.
Ehsani, 1996	Retrofitting technique to enhance the lateral load carrying capacity of masonry structure	Unreinforced masonry walls	In-plane shear and out of plane flexural capacity	It was found that plastering an unreinforced masonry wall with a composite fabric of glass and carbon fibres embedded in epoxy resin) is a very effective technique for increasing the flexural & shear strength and ductility of these elements.
Ali, 2007	Seismic resistance evaluation	Unreinforced masonry building	Dynamic field test	Peak acceleration of ground motion was found to be the main parameter affecting the damage potential of ground motion on single-story masonry building. Single-storey masonry buildings exhibit very low natural period. Unreinforced masonry could tolerate ground acceleration of 0.5g without collapse [Gulkan 1979] Bond strength and coefficient of friction of brick to mortar, were considered as governing factors to resist shear damage and minimum value given for these parameters are 0.09MPa and 1.0 respectively. The walling around openings was found vulnerable to cracking.
Tomazevic, 2009	Shear resistance of masonry walls and Euro code 6	Masonry walls	Shear and tensile strengths	According to Euro code 6, the critical mechanism for shear failure of structural walls is considered to be sliding shear. However, for masonry structures subjected to seismic actions, wall failure mechanisms is characterised by the formation of diagonal cracks

It has been observed throughout the literature review; important parameters in seismic design of masonry structure include the following;

- Building material properties
- Unit weight (density)
- Bond strength between bricks and mortar and coefficient of sliding friction
- Dynamic characteristics of the building system including periods and damping
- Failure mechanism under dynamic loading

Three types of principal failure mechanisms of masonry walls when subjected to seismic actions were analysed by (Magenes & Calvi, 1997). These were:

- **Rocking failure:** This failure is initiated due to increase in horizontal load.-As a result, bed-joints crack in tension and shear is carried by the compressed masonry. Final failure is caused by overturning of the wall and simultaneous crushing of the compressed corner.
- **Shear cracking:** This failure is due to the formation and development of inclined diagonal cracks which may follow the path of bed- and head-joints or may pass through bricks depending on the relative strength of mortar joints, the brick –mortar interface and the bricks.
- **Sliding:** This failure can occur due to the formation of tensile horizontal cracks in the bed joints

According to the best knowledge of the author after reviewing the literature it is found that behaviour of masonry structure under seismic loading is well understood. Retrofitting techniques were also suggested by few researchers. However the utilisation of natural fibres to increase the seismic resistance of masonry not been much considered This technique is the main aim of this study and can result in an economical solution of enhancing the strength of masonry under dynamic effects.

Annex B Preparation of plaster cubes

B1 – Mix Ratio

Table B1: Mix ratio for different samples of plain and fibrous plaster cubes

Preparation of Plain Plaster Cubes (100 mm x 100 mm x100 mm)		
Ingredients	**Weight (Kg)**	**No of Samples**
Weight of cement	6.5kg	**3 (A1, A2, A3)**
Weight of Sand	20kg	
Weight of Water	3.25kg	

Preparation of 2% Rice Straw Plaster Cubes (100 mm x 100 mm x100 mm)		
Ingredients	**Weight (Kg)**	**No of Samples**
Weight of cement	6.5kg	**3 (B1, B2, B3)**
Weight of Sand	20kg	
Weight of Water	5.0kg	
Weight of Rice Straw	0.13kg	

Preparation of 2% Sisal Plaster Cubes (100 mm x 100 mm x100 mm)		
Ingredients	**Weight (Kg)**	**No of Samples**
Weight of cement	6.5kg	**3 (C1, C2, C3)**
Weight of Sand	20kg	
Weight of Water	5.0kg	
Weight of Sisal	0.13kg	

Preparation of 5% Rice Straw Plaster Cubes (100 mm x 100 mm x100 mm)		
Ingredients	**Weight (Kg)**	**No of Samples**
Weight of cement	6.5kg	**3 (D1, D2, D3)**
Weight of Sand	20kg	
Weight of Water	5.0kg	
Weight of Rice Straw	0.32kg	

Preparation of 5% Sisal Plaster Cubes (100 mm x 100 mm x100 mm)		
Ingredients	**Weight (Kg)**	**No of Samples**
Weight of cement	6.5kg	**3 (E1, E2, E3)**
Weight of Sand	20kg	
Weight of Water	5.0kg	
Weight of Sisal	0.32kg	

B2 – Photographs

Figure B2.1: Pouring of cubes

Figure B2.2: Curing and demoulding of cubes

Figure B2.3: Testing Equipment and loading of cubes

Annex C Preparation of ISSB and SSB columns

C1 – Preparation of ISSB

Figure C1.1: Pressed machine for ISSB preparation

Figure C1.2: ISSB

C2 – Slump test

Figure C2.1: Slump test for plain and fibrous plaster

Table C1: Slump results of different samples

Mix Ratio of Sample	W/C ratio	Slump Value	Type of Sample
1:3	0.69	40mm	20mm plaster with Rice fibres
1:3	0.69	120mm	20mm plaster with sisal fibres
1:3	0.67	90mm	8mm plaster with sisal fibres
1:3	0.69	100mm	20mm with no fibre
1:3	0.67	140mm	8mm with no fibre

C3 - Preparation of SSB

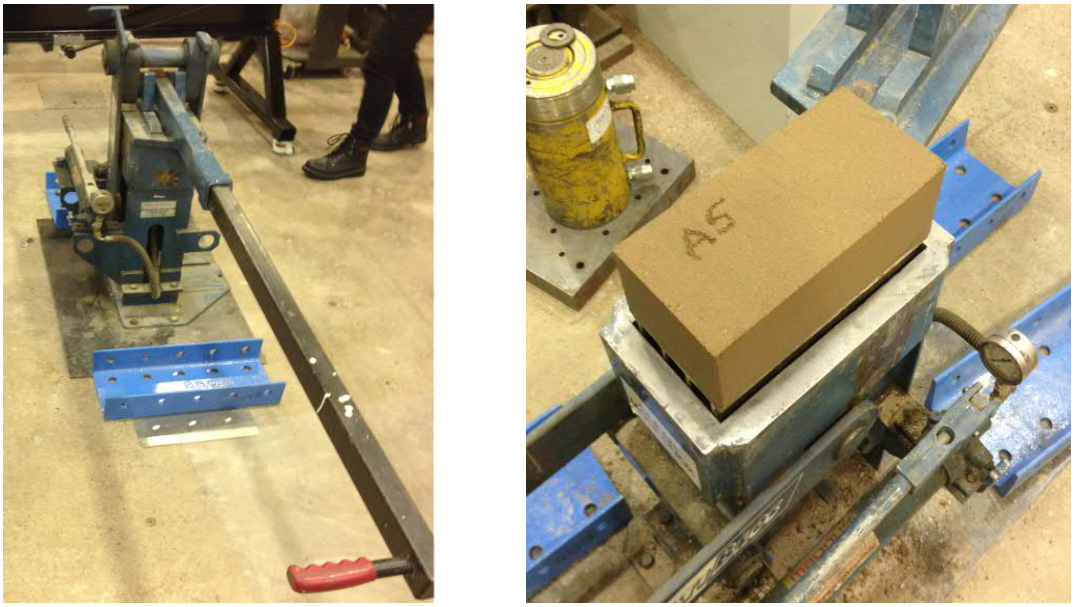

Figure C3.1: Pressed machine for SSB preparation

Figure C3.2: 1500 mm high SSB columns

Annex D Interlocking wall experimental work

D1 – Preparation of roof truss and loading assembly

Figure D1.1: Preparation of timber roof truss

Figure D1.2: Preparation of loading frame

Figure D1.3: Erection of roof truss at interlocking walls

Figure D1.4: setting up of lateral load assembly

D2 – Setting up of accelerometer test

Figure D2.1: Attachment of accelerometer with wall

Figure D2.2: Set up for data recording